

Supporting information

for

On the effect of conformational isomerism on the optical properties of bis(8-oxyquinolato) diboron complexes with 2,2'-biphenyl backbone

Mateusz Urban,^a Patrycja Górká,^a Krzysztof Nawara,^b Krzysztof Woźniak,^c Krzysztof Durka,^{a*}
Sergiusz Luliński^{a*}

^aFaculty of Chemistry, Warsaw University of Technology, Noakowskiego 3, 00-664 Warsaw,
Poland.

^bFaculty of Mathematics and Science, Cardinal Stefan Wyszyński University, Dewajtis 5, 01-815
Warsaw, Poland

^cBiological and Chemical Research Centre, Department of Chemistry, University of Warsaw,
Żwirki i Wigury 101, 02-089 Warsaw, Poland.

Corresponding authors:

Krzysztof Durka: kdurka@ch.pw.edu.pl

Sergiusz Luliński: serek@ch.pw.edu.pl

Table of contents

1	X-ray crystallography – additional information	2
2	Optical properties – additional information	5
3	Hydrolytic stability.....	6
4	Theoretical calculations	8
5	NMR studies.....	20

1 X-ray crystallography – additional information

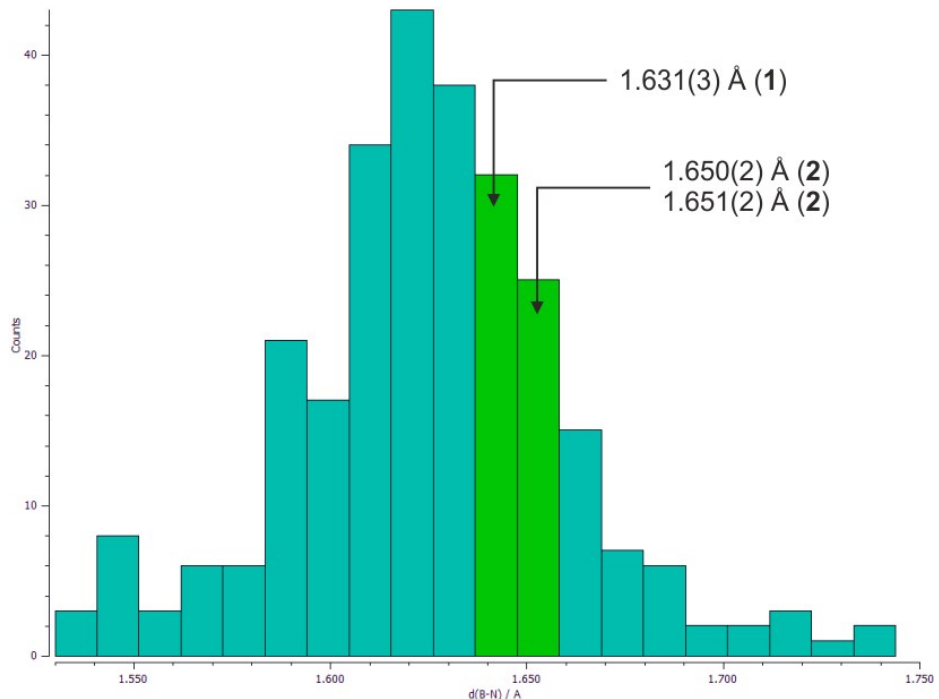


Figure S1. Histogram showing the distribution of B-N distances (single/dative bonds) within a group of 227 tetracoordinated organoboron (N,O) chelate complexes.

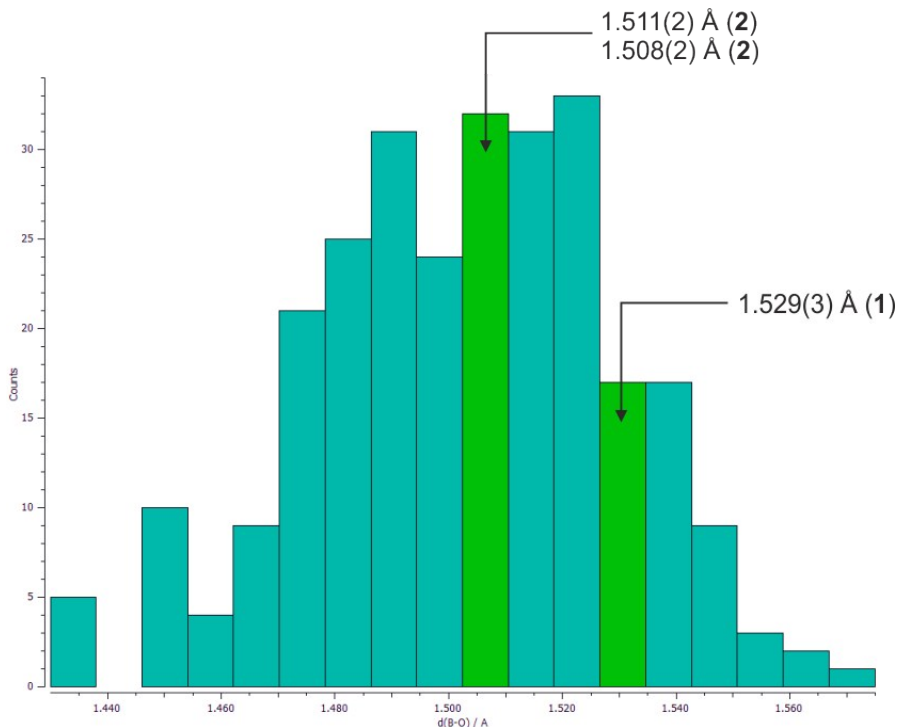


Figure S2. Histogram showing the distribution of B-O distances within a group of 227 tetracoordinated organoboron (N,O) chelate complexes.

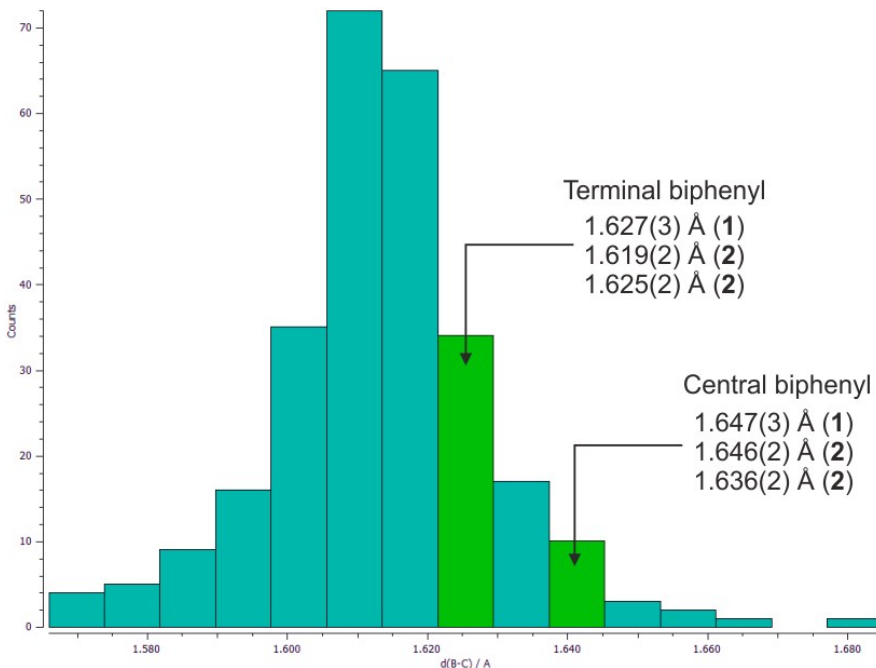


Figure S3. Histogram showing the distribution of B-C distances within a group of 227 tetracoordinated organoboron (N,O) chelate complexes.

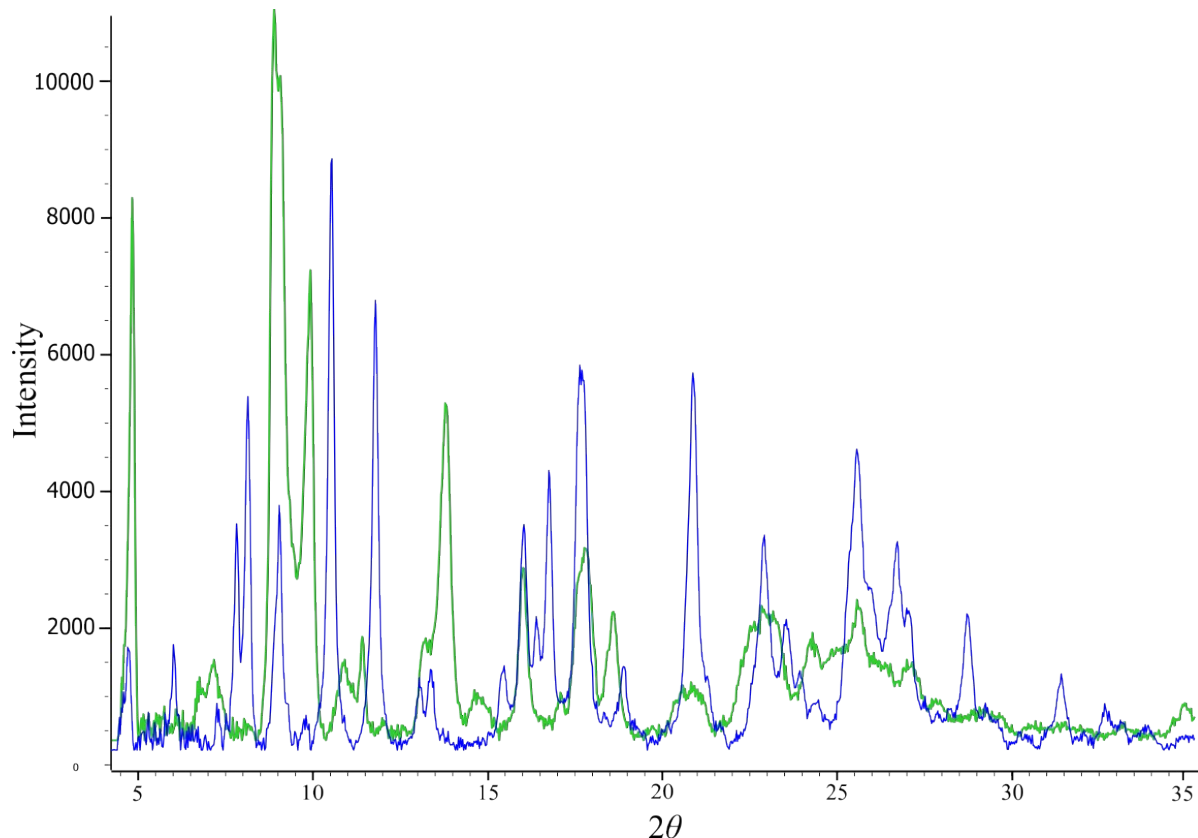


Figure S4. Overlay of the PXRD patterns of samples of **2** obtained by crystallization from benzene (blue) and acetone (green).

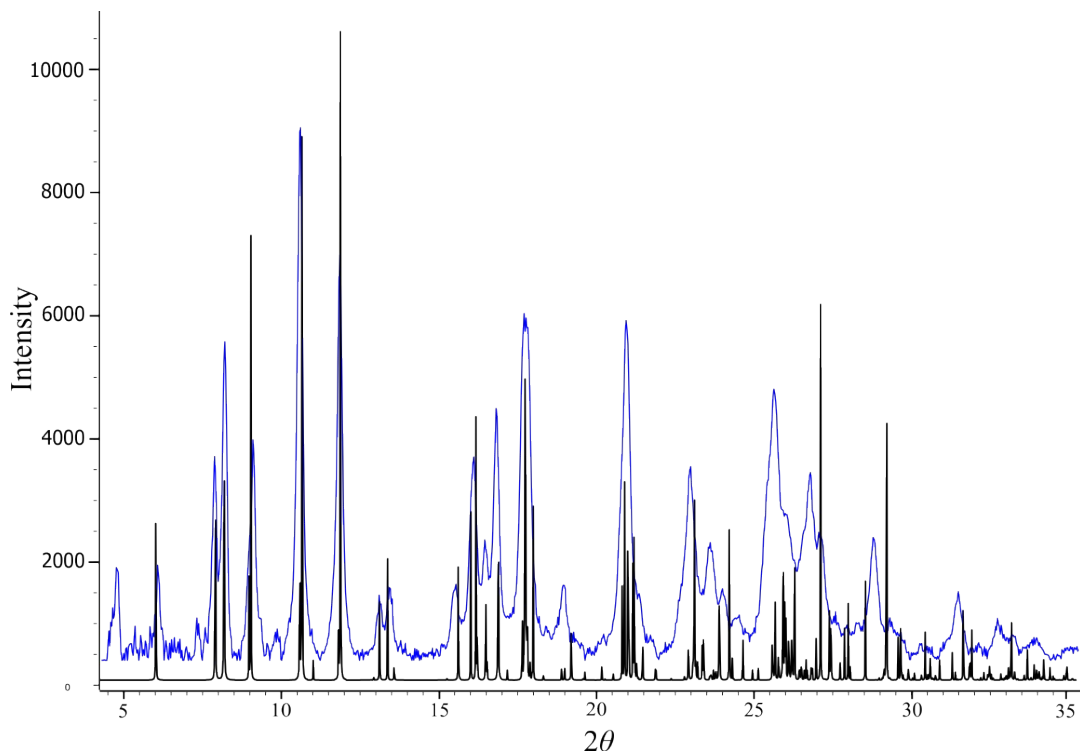


Figure S5. PXRD pattern of **2** (blue) obtained by crystallization from benzene together with the pattern simulated from single-crystal X-ray structure of **2** (black).

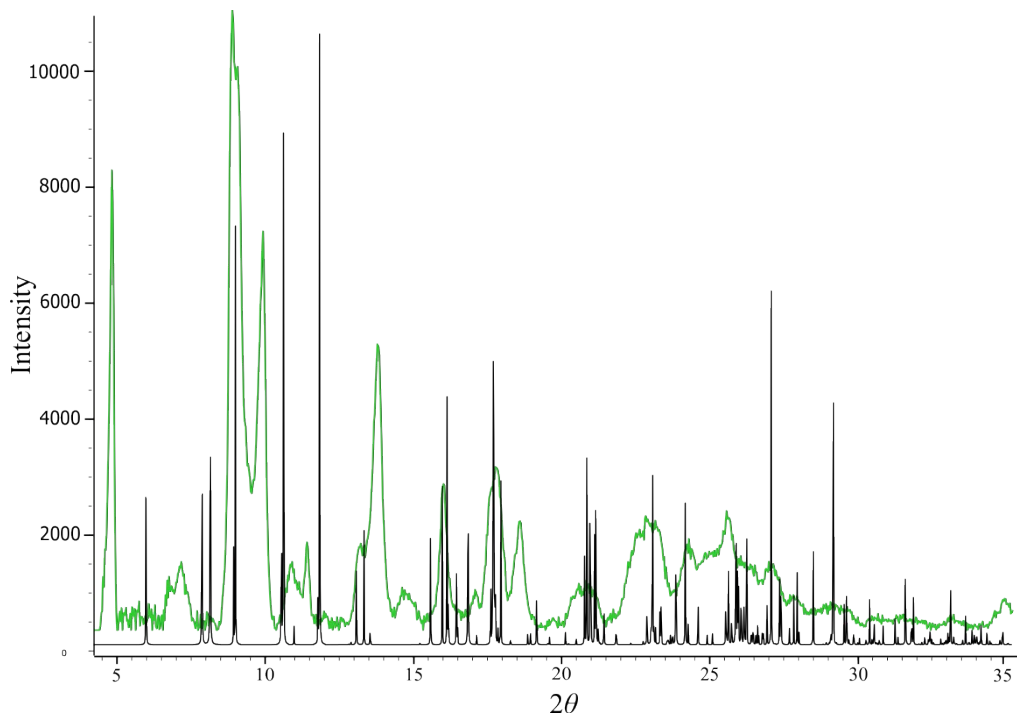


Figure S6. PXRD pattern of **2** (green) obtained by crystallization from acetone together with the pattern generated from single-crystal X-ray structure of **2** (black).

2 Optical properties – additional information

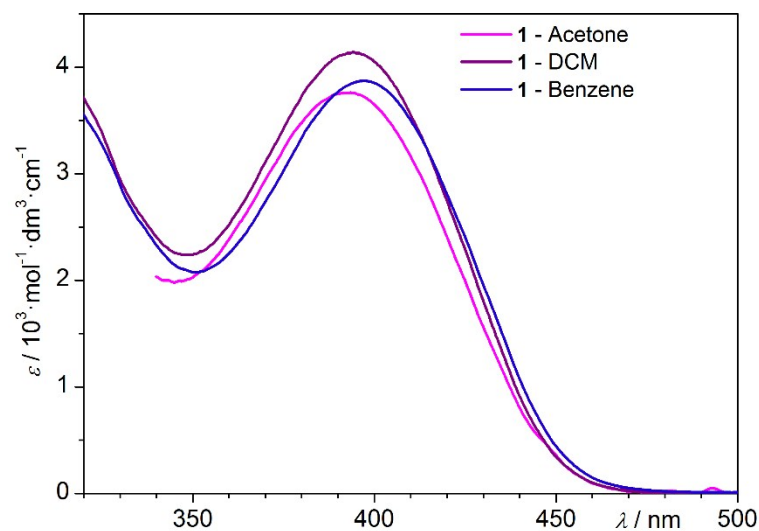


Figure S7. UV-Vis absorption spectra of **1** in various solvents

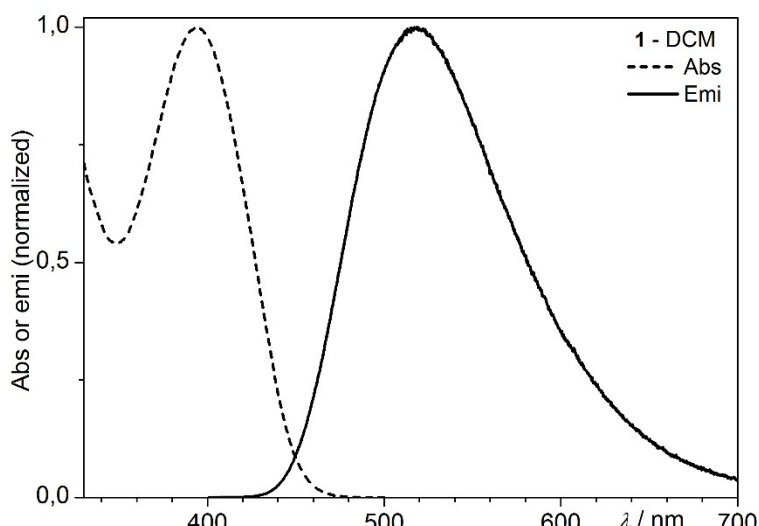


Figure S8. Overlay of normalized UV-Vis absorption and emission spectra of **1** in DCM.

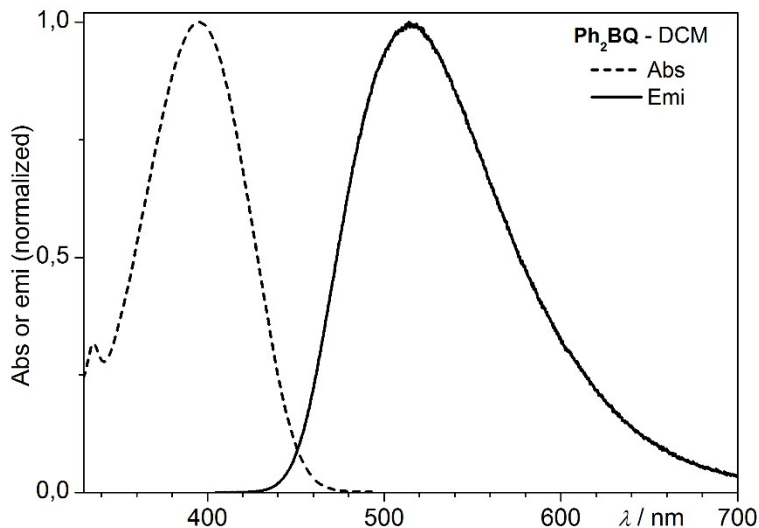


Figure S9. Overlay of normalized UV-Vis absorption and emission spectra of Ph_2BQ in DCM

3 Hydrolytic stability

Method: The analysis was performed by repetitive measurements of UV-Vis spectra of diluted solutions of complexes over a long period of time. Complexes were dissolved in CH_2Cl_2 ($c = 8 \cdot 10^{-5} \text{ mol} \cdot \text{dm}^{-3}$), which was not dried before use. The first measurement was performed immediately after dissolution, the consecutive measurements were performed after time stated on the diagrams (up to 3 days). The spectrum of a free ligand 8-hydroxyquinoline (pink dashed line) is overlaid for comparison.

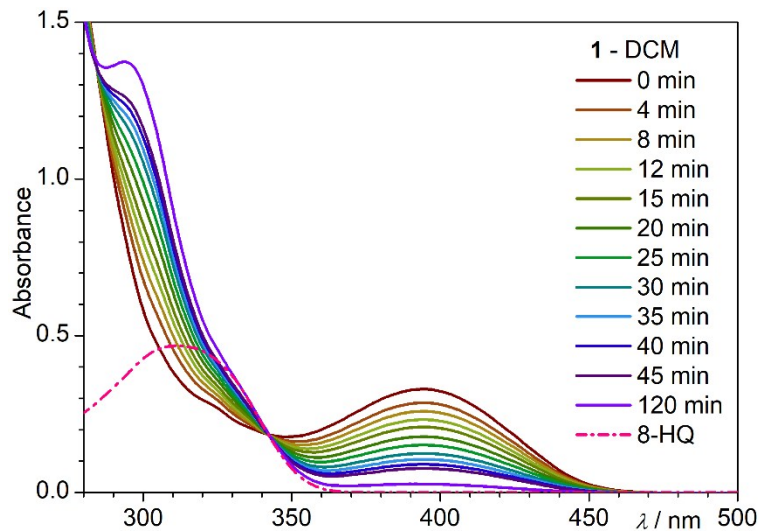


Figure S10. Overlay of UV-Vis spectra of compound **1** in CH_2Cl_2 (measured over 2 hours) and free 8-hydroxyquinoline .

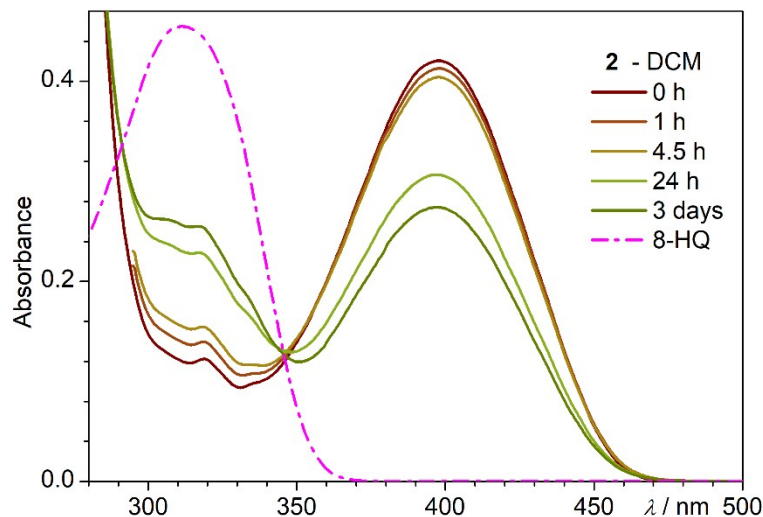


Figure S11. Overlay of UV-Vis spectra of compound **1** in CH_2Cl_2 measured over 2 hours and free 8-hydroxyquinoline.

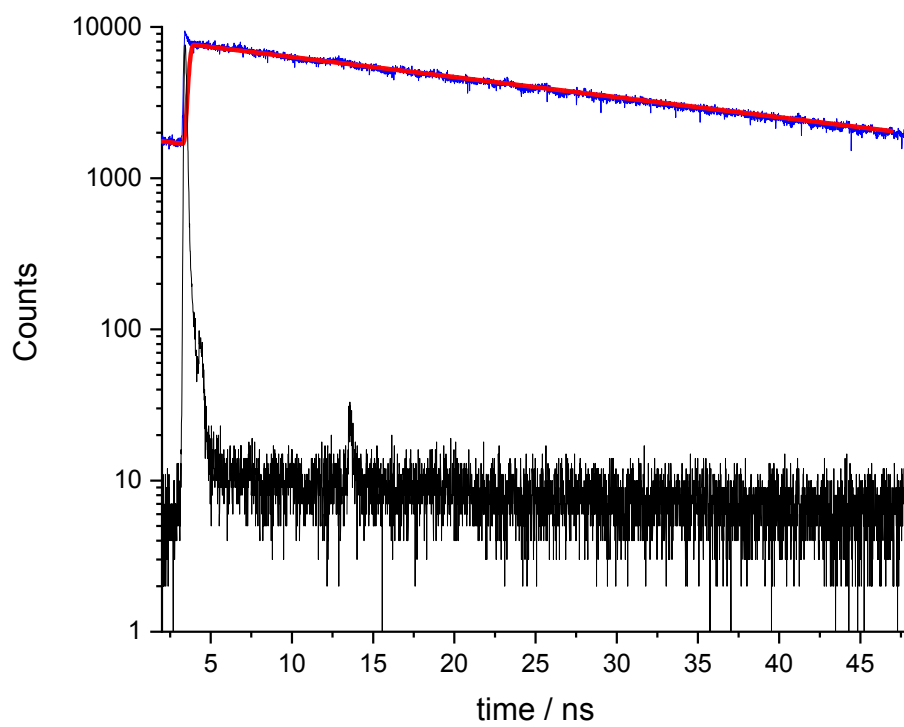


Figure S12. TCSPC data for compound **2** in acetonitrile: IRF curve in black, experimental fluorescence decay at 515 nm (channels width 12.5 nm) in blue, and modelled curve in red.

4 Theoretical calculations

4.1 Conformation.

Table S1. The comparison of molecular energy of isomers related to the most stable form in the series calculated on different levels of theory. All ΔE values are given in kJmol^{-1} .

	<i>syn</i> -(bphR)		<i>anti</i> -(bphS)			
	(1BR, 2BR)	<i>meso</i>	(1BS, 2BS)	(1BR, 2BR)	<i>meso</i>	(1BS, 2BS)
M06-2X/6-311++g(d,p)						
1	0.0	25.5	59.4	107.4	81.4	57.8
2	51.2	36.3	9.9	63.3	41.5	0.0
PBE0/6-311++g(d,p)						
1	0.0	27.0	53.0	104.6	76.2	52.2
2	65.5	47.7	12.4	71.8	42.6	0.0
B3PW91/6-311++g(d,p)						
1	0.0	26.5	54.5	98.2	81.1	56.1
2	55.7	41.7	10.6	64.7	40.2	0.0

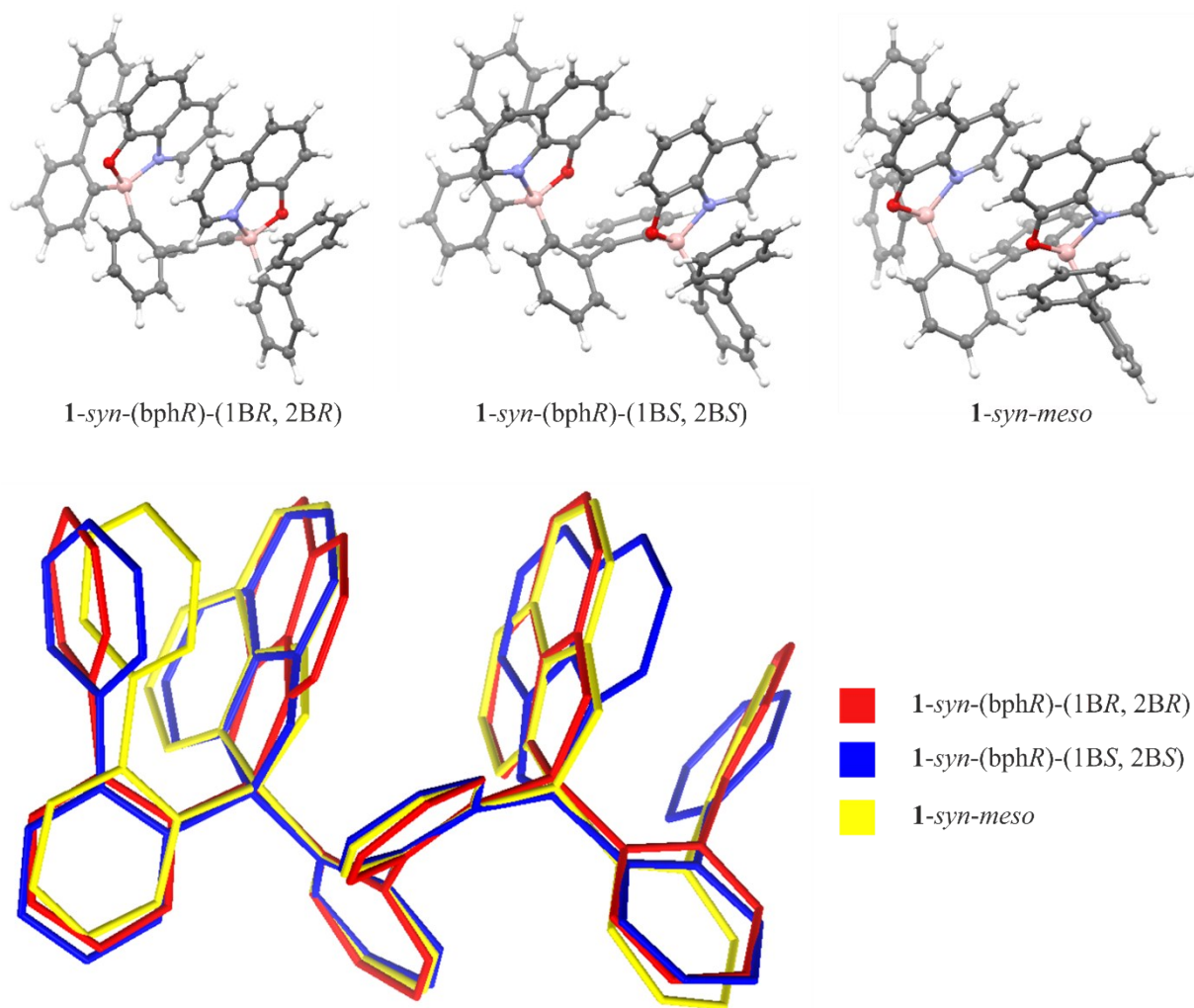


Figure S13. Molecular geometries of **1-syn** conformers obtained from DFT (PBE0/6-311++g(d,p)) calculations together with the overlay of molecules.

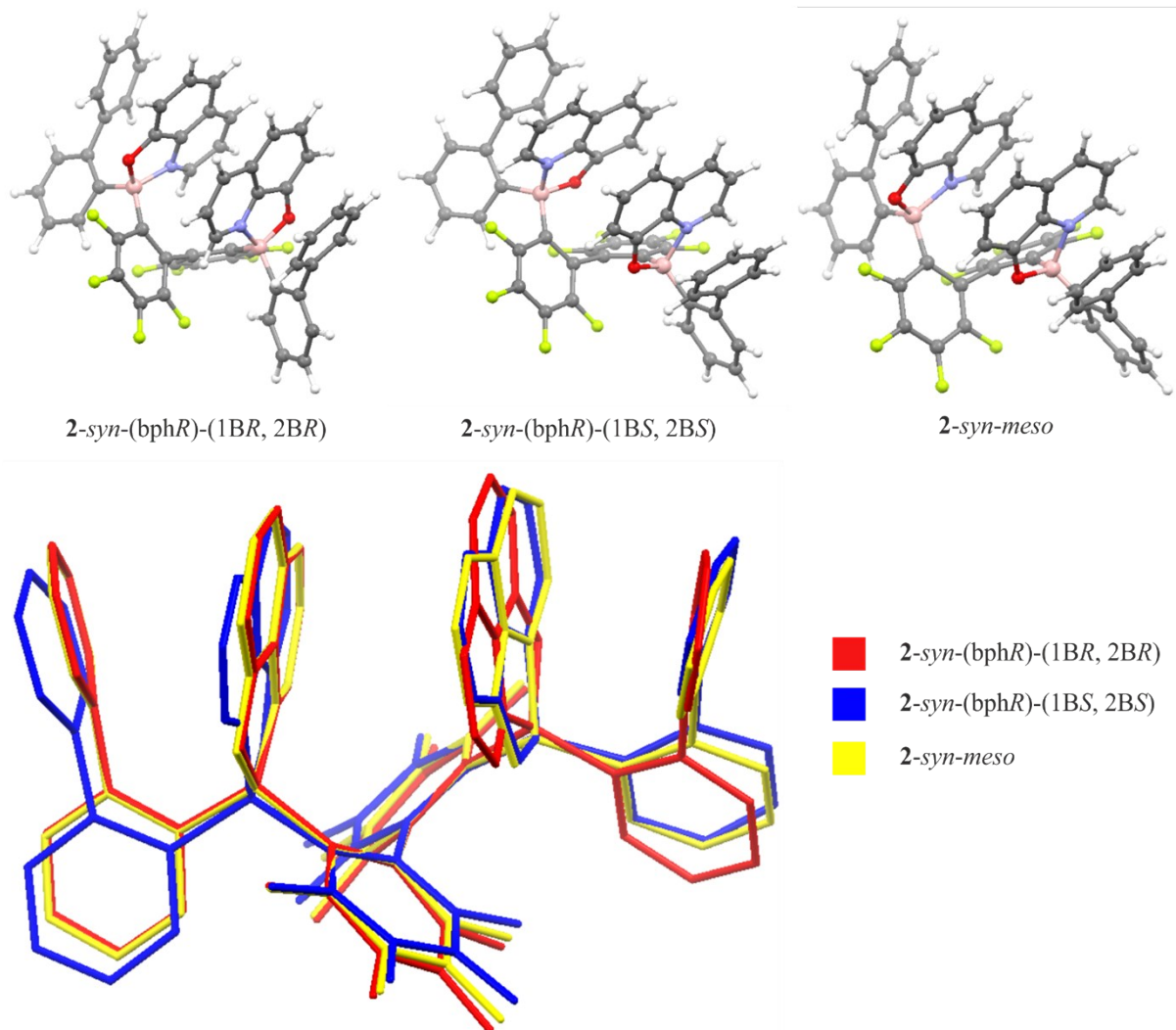


Figure S14. Molecular geometries of **2-syn** conformers obtained from DFT (PBE0/6-311++g(d,p)) calculations together with the overlay of molecules.

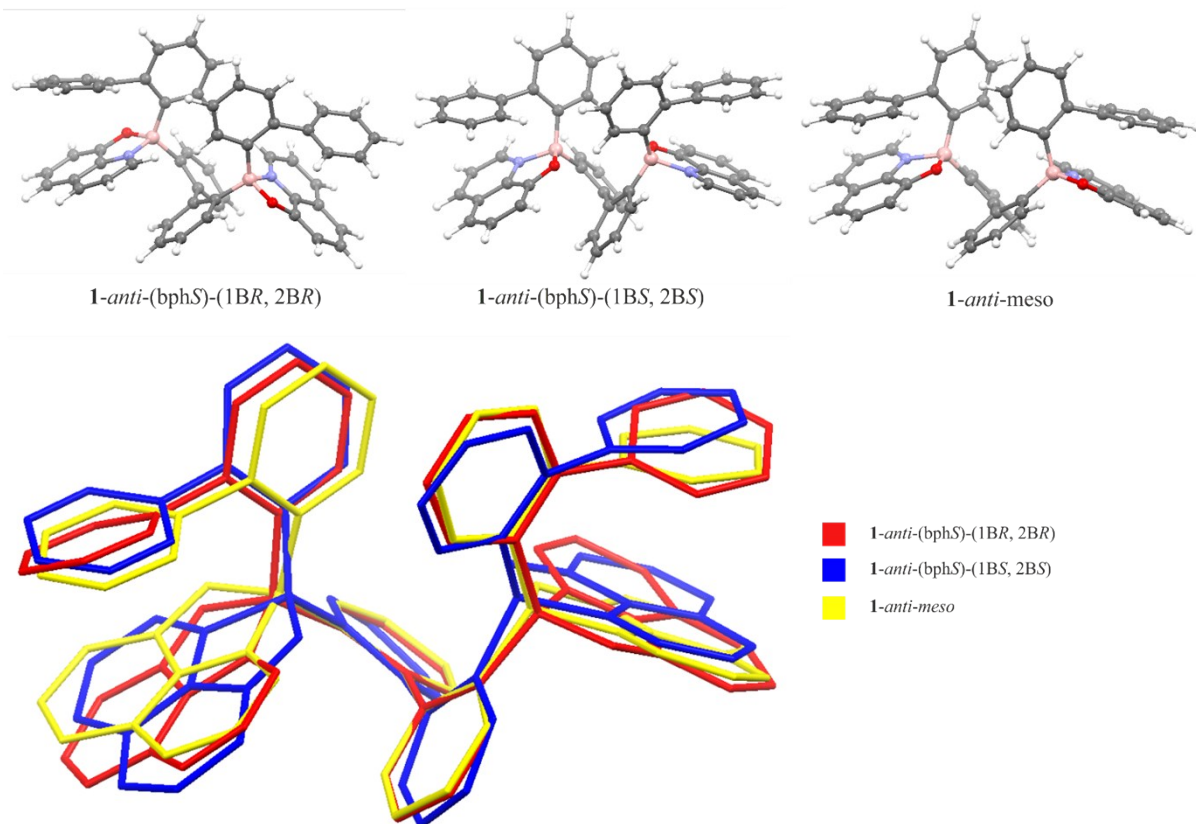


Figure S15. Molecular geometries of **1-anti** conformers obtained from DFT (PBE0/6-311++g(d,p)) calculations together with the overlay of molecules.

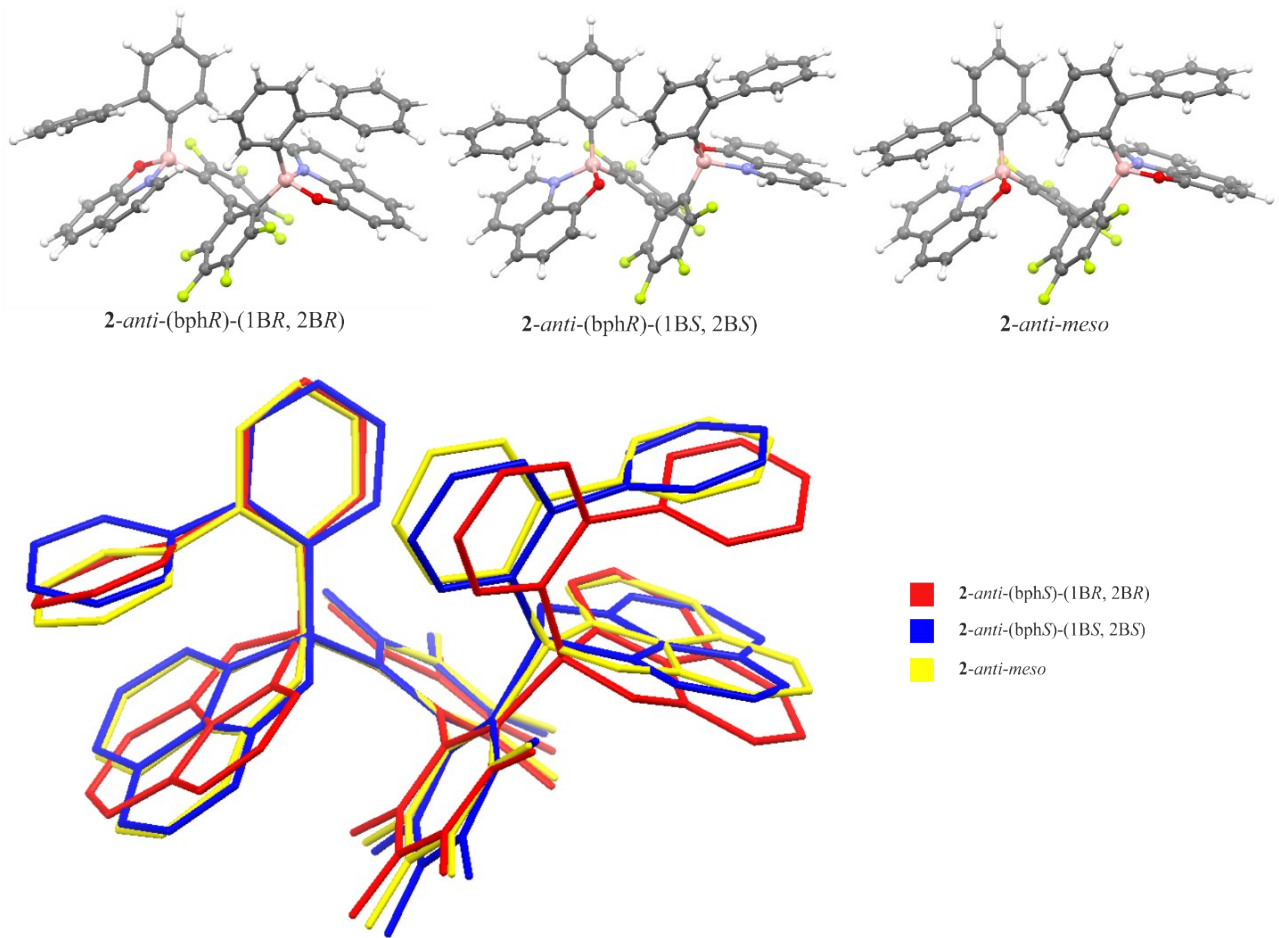


Figure S16. Molecular geometries of **2-anti** conformers obtained from DFT (PBE0/6-311++g(d,p)) calculations together with the overlay of molecules.

4.2. Dipole moment and electrostatic potential

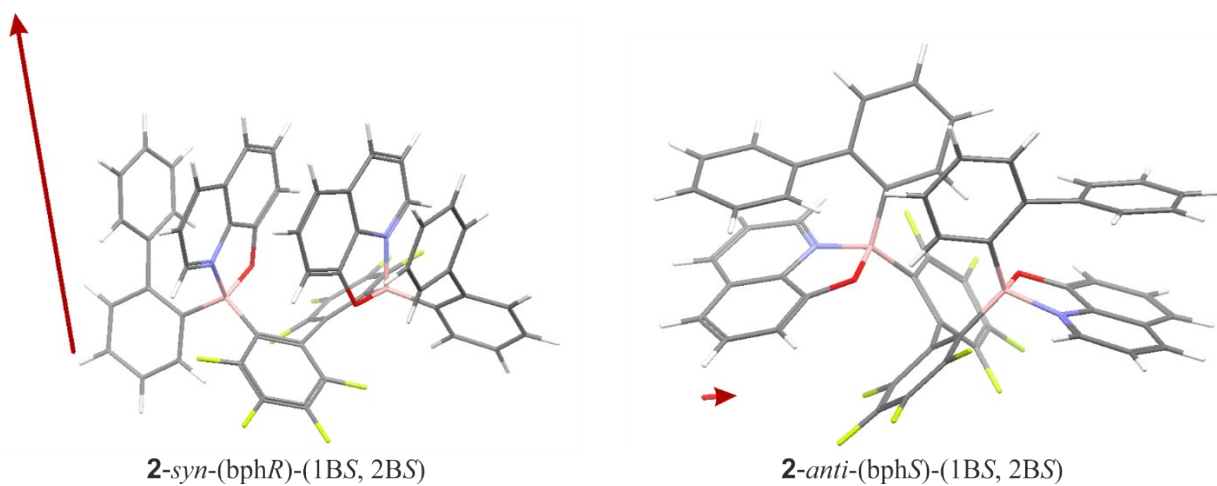


Figure S17. Visualization of the calculated dipole moment vector in the rotamers **2-syn** and **2-anti**. Level of theory: PBE0/6-311++g(d,p).

Table S2. The comparison of dipole moments (D) of various forms of **1** and **2** calculated at 3 different levels of DFT theory.

	<i>syn</i> -(bphR) (1BR, 2BR)			<i>anti</i> -(bphS) (1BR, 2BR)		
	<i>meso</i>	(1BS, 2BS)	<i>meso</i>	(1BS, 2BS)		
M06-2X/6-311++g(d,p)						
1	5.91	8.93	9.11	3.84	7.10	2.46
2	8.26	12.20	11.76	1.58	5.98	0.33
PBE0/6-311++g(d,p)						
1	6.14	9.38	7.75	2.55	6.70	3.67
2	8.78	11.81	12.19	1.30	5.93	0.23
B3PW91/6-311++g(d,p)						
1	6.08	9.31	7.69	2.54	6.66	3.64
2	8.65	11.70	12.08	1.26	5.91	0.25

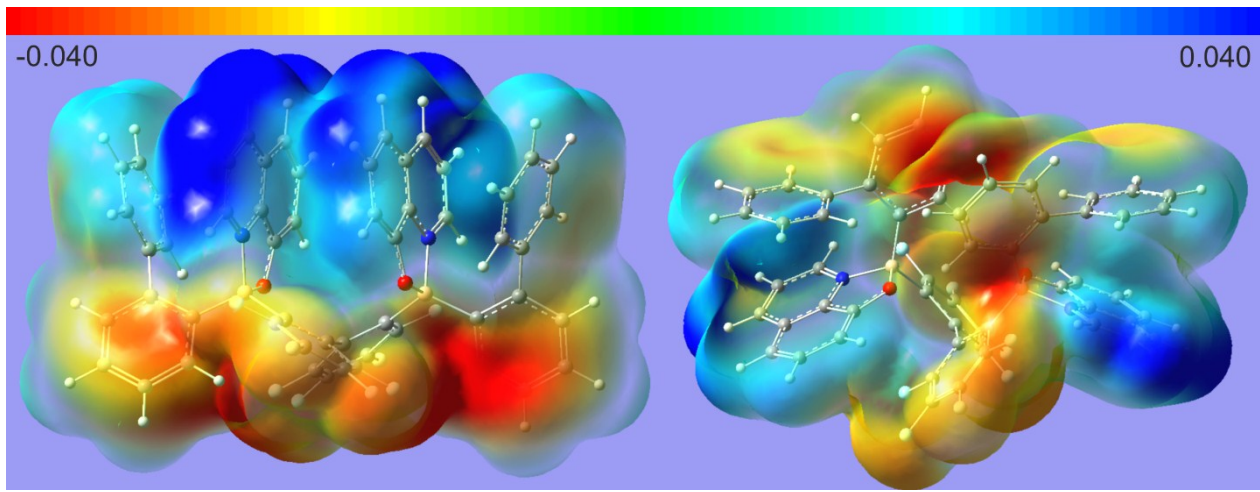


Figure S18. Electrostatic potential mapped onto electron density surface ($\rho = 0.0064 \text{ e}\text{\AA}^{-3}$) generated for *syn* and *anti* rotamers of **2**.

4.3. Periodic calculations.

The periodic DFT calculations were performed using *CRYSTAL09*. The evaluation of Coulomb and exchange series was controlled by five thresholds, set arbitrary to values of 10^{-7} , 10^{-7} , 10^{-7} , 10^{-7} , 10^{-25} . The condition for the SCF convergence was set to 10^{-7} on the energy difference between two subsequent cycles. Shrinking factor was equal to 4, which refers to 30-36 k-points (depending on space group symmetry) in the irreducible Brillouin zone in the case of the studied systems and assures the full convergence of the total energy.

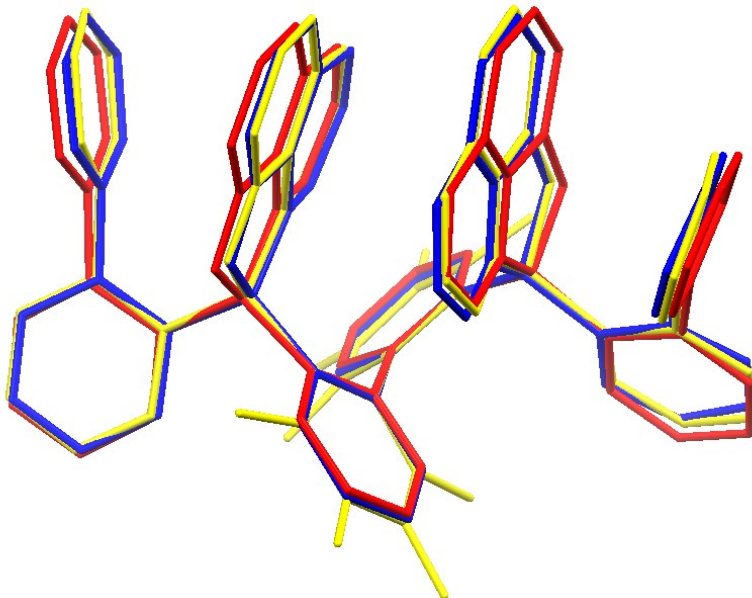


Figure S19. Overlay of experimental **1-syn** (red), theoretical **1-syn** (blue) and theoretical **2-syn** (yellow) molecular geometries derived from periodic DFT optimisation in *Crystal09*.

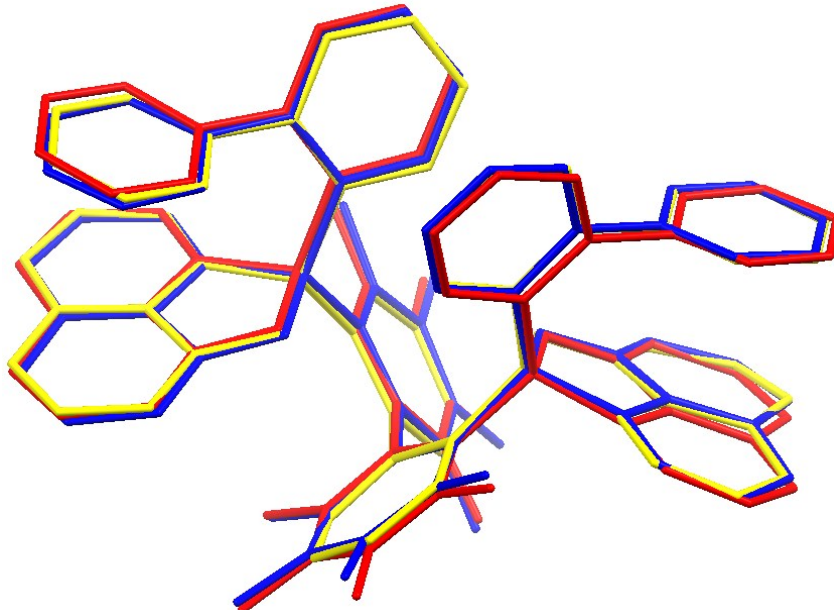


Figure S20. Overlay of experimental **2-anti** (red), theoretical **2-anti** (blue) and theoretical **1-anti** (yellow) molecular geometries derived from periodic DFT optimisation in Crystal09.

Table S3. Crystal09 optimised atom-site fractional coordinates for **1-syn** and **2-syn**.

1-syn				2-syn			
Monoclinic, $C\ 2/c$				Monoclinic, $C\ 2/c$			
$a = 20.6482\ \text{\AA}, b = 11.1806\ \text{\AA}, c = 17.8790\ \text{\AA}, \beta = 117.64^\circ$				$a = 20.6482\ \text{\AA}, b = 10.9106\ \text{\AA}, c = 17.4408\ \text{\AA}, \beta = 116.97^\circ$			
atom	<i>x</i>	<i>y</i>	<i>z</i>	atom	<i>x</i>	<i>y</i>	<i>z</i>
O	0.007032	-0.436777	0.422125	O	0.008516	-0.442472	0.420352
N	0.083449	-0.414013	0.351305	N	0.080772	-0.420045	0.353429
C	0.064993	0.466568	0.354593	C	0.060357	0.461680	0.353124
C	0.131962	-0.389217	0.322067	C	0.128997	-0.396749	0.328368
H	0.150993	-0.296038	0.327603	H	0.148795	-0.304547	0.335453
C	0.021018	0.454435	0.396941	C	0.017798	0.449975	0.392212
C	0.000266	0.339049	0.408734	C	-0.005306	0.336535	0.400504
H	-0.033067	0.325309	0.441399	H	-0.037547	0.324057	0.431015
C	-0.256369	0.068447	-0.482975	C	-0.256341	0.072907	-0.486401
H	-0.241012	0.147364	0.491330	H	-0.240619	0.153536	0.492324
C	-0.088323	-0.233000	0.347646	C	-0.082573	-0.234412	0.344714
H	0.413861	0.217374	0.402417	F	0.417708	0.216262	0.413928
C	-0.149151	-0.085064	0.233768	C	-0.138300	-0.083292	0.239224
H	-0.195312	-0.024612	0.196727	F	-0.190337	-0.000051	0.200150
C	-0.310407	0.078490	-0.454820	C	-0.310195	0.078417	-0.463452
C	0.089740	0.367808	0.323392	C	0.084166	0.362850	0.324393
C	0.157298	-0.481865	0.286528	C	0.151113	-0.488461	0.292508
H	0.193114	-0.455887	0.258727	H	0.186626	-0.463854	0.267852
C	0.135080	0.398852	0.284354	C	0.129169	0.392722	0.289821

H	0.152731	0.328443	0.254029	H	0.147445	0.322125	0.262826
C	-0.029087	-0.246816	0.327559	C	-0.026024	-0.253771	0.327905
C	-0.220546	-0.042085	-0.476839	C	-0.221165	-0.036214	-0.480998
H	-0.178504	-0.048263	-0.498744	H	-0.178359	-0.038600	-0.497285
C	-0.235870	-0.141773	-0.438641	C	-0.238135	-0.139329	-0.450161
H	-0.205944	-0.226374	-0.430807	H	-0.208603	-0.222795	-0.441980
C	-0.147067	-0.153352	0.302097	C	-0.138164	-0.152633	0.301992
H	0.308987	0.359538	0.320680	F	0.306424	0.355577	0.317747
C	0.067236	0.249752	0.335624	C	0.060900	0.246370	0.334803
H	0.082778	0.170024	0.310875	H	0.077573	0.165287	0.315676
C	-0.031109	-0.173544	0.261007	C	-0.028731	-0.184799	0.262116
C	0.024425	0.238362	0.377605	C	0.017603	0.236047	0.371309
H	0.005987	0.148356	0.385903	H	-0.000816	0.146398	0.378034
C	-0.290578	-0.133197	-0.412036	C	-0.294402	-0.136474	-0.432221
H	-0.302182	-0.210994	-0.382133	H	-0.308481	-0.218270	-0.410378
C	-0.090902	-0.095613	0.213570	C	-0.082870	-0.099096	0.220793
H	-0.092594	-0.045504	0.159235	F	-0.081404	-0.026695	0.162170
C	0.094988	-0.250367	0.475771	C	0.093365	-0.256685	0.474511
C	-0.328613	-0.024113	-0.420924	C	-0.329940	-0.027534	-0.437876
H	-0.371367	-0.017090	-0.400118	H	-0.373461	-0.023884	-0.422829
C	0.071858	-0.133558	0.486760	C	0.070124	-0.143087	0.487450
H	0.025508	-0.090760	0.432525	H	0.021167	-0.103481	0.438343
B	0.040048	-0.331185	0.392816	B	0.040738	-0.338631	0.394700
C	0.103480	-0.072770	-0.434775	C	0.106365	-0.079183	-0.438345
H	0.082335	0.015774	-0.428800	H	0.085224	0.007722	-0.431689
C	-0.338375	0.372526	-0.363822	C	-0.331474	0.372203	-0.373522
H	-0.315164	0.414965	-0.300813	H	-0.302419	0.419751	-0.314808
C	-0.343268	0.199443	-0.452724	C	-0.342764	0.196741	-0.459363
C	-0.310996	0.260962	-0.373650	C	-0.306398	0.261460	-0.384787
H	-0.264382	0.219680	-0.319092	H	-0.257963	0.222580	-0.334439

Table S4. Crystal09 optimised atom-site fractional coordinates for **1-anti** and **2-anti**.

1-anti			2-anti			
Triclinic, $P\ -1$			Triclinic, $C\ 2/c$			
$a = 10.7065\ \text{\AA}, b = 11.0425\ \text{\AA}, c = 15.1342\ \text{\AA}, \alpha = 78.57^\circ, \beta = 75.23^\circ, \gamma = 81.99^\circ$			$a = 11.0384\ \text{\AA}, b = 11.2823\ \text{\AA}, c = 15.3884\ \text{\AA}, \alpha = 77.79^\circ, \beta = 75.49^\circ, \gamma = 81.67^\circ$			
atom	x	y	z	atom	x	
H	-0.093380	0.405905	0.371108	F	-0.098979	0.420843
H	-0.28573	0.169752	0.270313	F	-0.27343	0.159241
H	-0.282775	0.366994	0.322172	F	-0.286213	0.372720
H	-0.09524	0.010777	0.271996	F	-0.06134	-0.00166
H	0.252205	-0.229851	0.427975	F	0.253653	-0.241766
H	0.05807	-0.0791	0.436403	F	0.046854	-0.0802
H	0.416368	-0.037884	0.159424	F	0.437129	-0.029104
H	0.433563	-0.20382	0.285127	F	0.452593	-0.20752
O	0.247455	0.162873	0.373899	O	0.246327	0.171395
O	0.097855	0.224828	0.134099	O	0.104195	0.231905
N	0.233937	0.087293	0.038309	N	0.232787	0.097398
N	0.107077	0.283233	0.480388	N	0.111147	0.284909
C	0.125479	0.024929	0.300953	C	0.136941	0.035402
					0.300038	

C	0.015995	0.231454	0.347809	C	0.02092	0.232483	0.347106
C	-0.201687	0.296871	0.322859	C	-0.186763	0.288625	0.313148
C	0.188091	0.199336	-0.47834	C	0.192262	0.201754	-0.4828
C	0.012708	0.120798	0.316573	C	0.024560	0.124718	0.315060
C	0.343694	-0.14398	0.2903	C	0.345043	-0.13173	0.291046
C	0.040410	0.203395	0.070866	C	0.044710	0.210447	0.077568
C	0.1458	0.447053	0.228319	C	0.139712	0.449733	0.227697
H	0.077280	0.398383	0.211017	H	0.071903	0.402962	0.211465
C	0.351103	0.230959	0.108277	C	0.349144	0.241673	0.105845
C	0.264372	0.124336	0.459433	C	0.265942	0.130725	0.455110
C	-0.09438	0.316859	0.351294	C	-0.08817	0.310124	0.346203
C	-0.203444	0.186220	0.293746	C	-0.180945	0.180748	0.283041
C	0.332607	-0.049	0.217151	C	0.334278	-0.03612	0.220135
C	0.196895	0.394563	0.304988	C	0.190820	0.398325	0.303203
C	0.351682	0.416857	0.402318	C	0.344481	0.418115	0.396349
C	0.019766	0.354276	-0.469110	C	0.024750	0.350146	-0.470332
H	-0.04419	0.418495	0.495379	H	-0.03931	0.413697	0.496353
C	0.134872	-0.073567	0.373588	C	0.143150	-0.064315	0.369055
C	0.224012	0.03737	0.21903	C	0.232267	0.050055	0.219808
C	0.365023	0.436297	-0.444519	C	0.360184	0.437493	-0.453928
H	0.330904	0.479678	-0.38378	H	0.329235	0.481635	-0.39538
C	0.099392	0.263856	-0.333484	C	0.105283	0.256055	-0.337966
H	0.093101	0.257601	-0.26044	H	0.099285	0.244965	-0.26554
C	0.294269	0.102285	-0.358497	C	0.290931	0.094782	-0.363767
H	0.311228	0.093675	-0.28988	H	0.304349	0.080953	-0.29506
C	0.243563	-0.158115	0.368881	C	0.246913	-0.148379	0.366481
C	0.455084	0.325116	0.399973	C	0.442779	0.325803	0.394818
H	0.487503	0.281204	0.339589	H	0.474057	0.282834	0.335714
C	0.323031	0.016149	-0.01104	C	0.317803	0.027794	-0.00579
H	0.412240	-0.012446	0.010668	H	0.405577	0.000218	0.014247
C	-0.03154	0.146687	-0.08283	C	-0.03241	0.153513	-0.06863
H	-0.063953	0.122406	-0.138698	H	-0.064880	0.132795	-0.124011
C	0.309369	0.473941	0.480161	C	0.304885	0.474241	0.472226
H	0.233278	-0.450621	0.480526	H	0.230654	-0.452237	0.472356
C	0.132338	0.446546	-0.10102	C	0.12452	0.445549	-0.09676
H	0.045224	-0.490470	-0.088565	H	0.037635	-0.496485	-0.082576
C	0.012664	0.344404	-0.3747	C	0.018051	0.334728	-0.37687
H	-0.062769	0.400236	-0.335045	H	-0.054902	0.388024	-0.336646
C	0.290463	0.458695	0.322179	C	0.282847	0.460652	0.31829
C	0.318460	0.333542	-0.050336	C	0.311021	0.340368	-0.050441
C	-0.09785	0.098438	0.293315	C	-0.07547	0.100333	0.285862
C	0.203543	0.411013	-0.034247	C	0.198946	0.415442	-0.033481
H	0.172494	0.442635	0.031549	H	0.171291	0.447688	0.030646
C	0.342440	0.026629	0.492468	C	0.343734	0.034268	0.485965
H	0.393261	-0.04047	0.449289	H	0.397671	-0.02646	0.441571
C	0.195205	0.189191	-0.386101	C	0.198855	0.186040	-0.391606
C	-0.48659	0.289698	0.474024	C	0.499984	0.290443	0.467897
H	-0.402094	0.223253	0.468964	H	-0.420599	0.221743	0.464718
C	0.421237	0.228677	0.175141	C	0.420291	0.239672	0.169568
H	0.388705	0.176544	0.243657	H	0.391334	0.189207	0.238038
C	-0.08036	0.245366	0.056025	C	-0.07375	0.251718	0.065236
H	-0.147217	0.300681	0.101779	H	-0.136664	0.309228	0.108322
C	0.092587	0.100788	-0.06788	C	0.089891	0.108894	-0.05626
C	0.122386	0.128973	0.010387	C	0.121623	0.136116	0.019145
C	-0.47068	0.294293	0.156434	C	-0.47212	0.300024	0.147379
H	-0.420622	0.294768	0.210082	H	-0.423084	0.303196	0.199281

C	0.302824	-0.01639	-0.09054	C	0.293675	-0.00585	-0.08142
H	0.376425	-0.078002	-0.126944	H	0.363715	-0.066178	-0.117745
C	-0.48939	0.359122	-1.9E-06	C	-0.49606	0.361285	-0.00615
H	-0.455829	0.411155	-0.068483	H	-0.465414	0.411681	-0.074541
C	0.262708	-0.37334	0.1972	C	0.256253	-0.37606	0.192521
H	0.283253	-0.280663	0.161019	H	0.278426	-0.286977	0.153068
C	-0.42297	0.356178	0.067786	C	-0.42723	0.356874	0.058363
H	-0.338501	0.406881	0.052629	H	-0.343799	0.404663	0.040629
C	0.395822	0.303164	0.020857	C	0.389902	0.310654	0.018011
C	0.468188	0.345282	-0.448307	C	0.458221	0.345895	-0.456464
H	-0.48566	0.318852	-0.39103	H	-0.4952	0.321421	-0.40087
C	0.175582	-0.438505	0.176208	C	0.169385	-0.438834	0.174093
H	0.124452	-0.39734	0.123	H	0.12147	-0.39959	0.120083
C	0.188574	0.023124	-0.117501	C	0.182322	0.034780	-0.106941
H	0.171751	-0.01005	-0.17512	H	0.164327	0.006323	-0.16427
C	-0.113571	0.214159	-0.020641	C	-0.110886	0.218735	-0.007153
H	-0.21102	0.243186	-0.02801	H	-0.20655	0.247798	-0.01338
C	0.360903	0.292564	-0.134820	C	0.348443	0.299183	-0.133102
H	0.450909	0.23376	-0.14741	H	0.435818	0.242118	-0.14661
C	0.323519	-0.428175	0.267534	C	0.315245	-0.428697	0.262729
H	0.39569	-0.38176	0.282695	H	0.388154	-0.38502	0.275735
C	0.358760	0.021312	-0.416963	C	0.355646	0.019708	-0.422905
H	0.425647	-0.05244	-0.39288	H	0.421338	-0.05351	-0.39975
C	0.175233	0.404621	-0.184859	C	0.162039	0.402747	-0.178502
H	0.120707	0.434654	-0.23745	H	0.104304	0.427485	-0.22803
B	0.228361	0.149141	0.131237	B	0.232359	0.160351	0.130981
B	0.142225	0.269572	0.370331	B	0.142712	0.275048	0.369697
C	0.289046	0.326619	-0.201262	C	0.274615	0.329953	-0.196769
H	0.322637	0.29475	-0.26684	H	0.305081	0.298775	-0.26143

Table S5. The comparison of molecular volumes (V) and surface area (S) derived from the Hirshfeld surface analysis for the Crystal09 optimised structures of crystallographic **1-syn** and **2-anti** forms as well as their corresponding calculated **1-anti** and **2-syn** rotamers.

	$V / \text{\AA}^3$	$S / \text{\AA}^2$
1-syn	840	597
1-anti	910	638
2-syn	835	591
2-anti	893	621

4.4 Molecular orbital and TD-DFT calculations

Table S6. The comparison of HOMO/LUMO orbital energies (eV). Level of theory: PBE0/6-311++g(d,p).

	HOMO	LUMO	Band gap
1-syn-(bphR)			
(1BR, 2BR)	-5.92	-2.38	3.54
<i>meso</i>	-5.83	-2.56	3.27
(1BS, 2BS)	-5.73	-2.40	3.34
1-anti-(bphS)			
(1BR, 2BR)	-5.88	-2.32	3.55
<i>meso</i>	-5.70	-2.47	3.23
(1BS, 2BS)	-5.74	-2.28	3.46
2-syn-(bphR)			
(1BR, 2BR)	-6.11	-2.77	3.34
<i>meso</i>	-6.14	-2.79	3.35
(1BS, 2BS)	-6.25	-2.73	3.52
2-anti-(bphS)			
(1BR, 2BR)	-6.13	-2.66	3.46
<i>meso</i>	-6.00	-2.67	3.33
(1BS, 2BS)	-6.14	-2.56	3.58

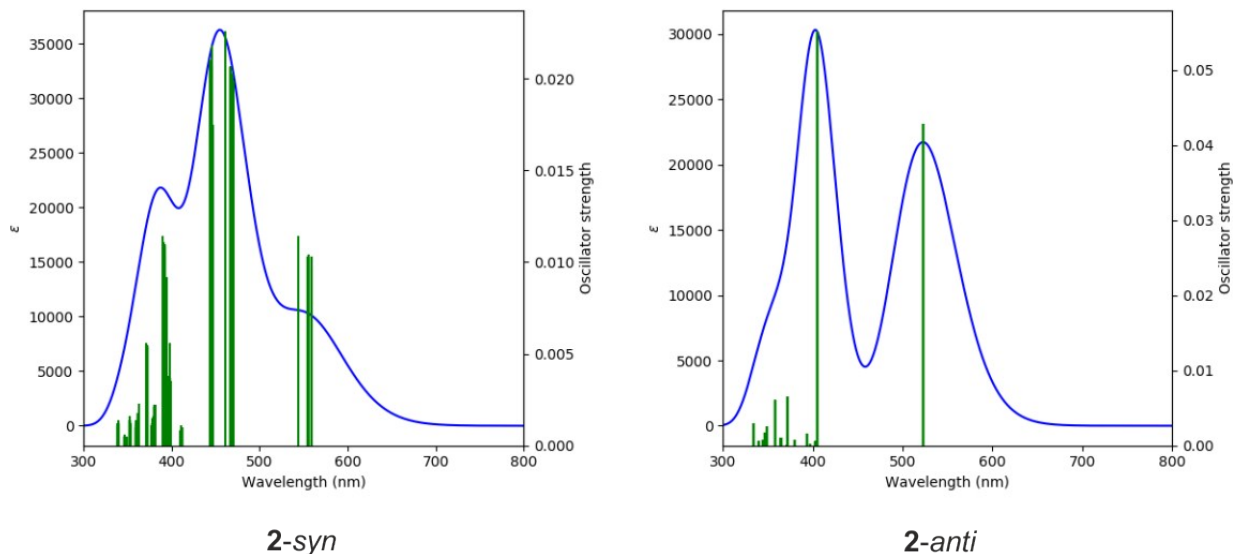


Figure S21. Emission spectra for the optimised molecular structures of rotamers **2-syn** and **2-anti** calculated at the PBE0/6-311++g(d,p) level of theory.

5 NMR studies

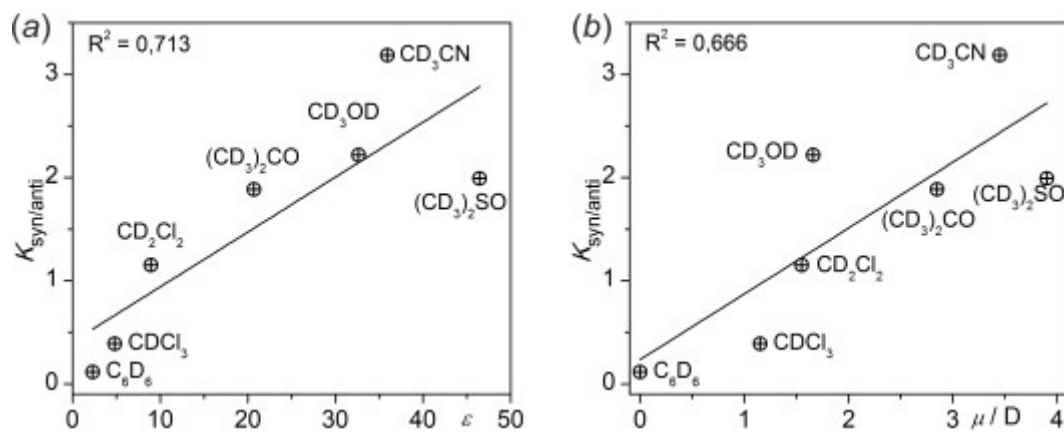


Figure S22. *Syn/anti* equilibrium in **2** as a function of common solvent polarity parameters: (a) dielectric constant; (b) dipole moment.

5.1 NMR spectra of compound 3

Dimethyl 2-biphenylboronate (3) -1H

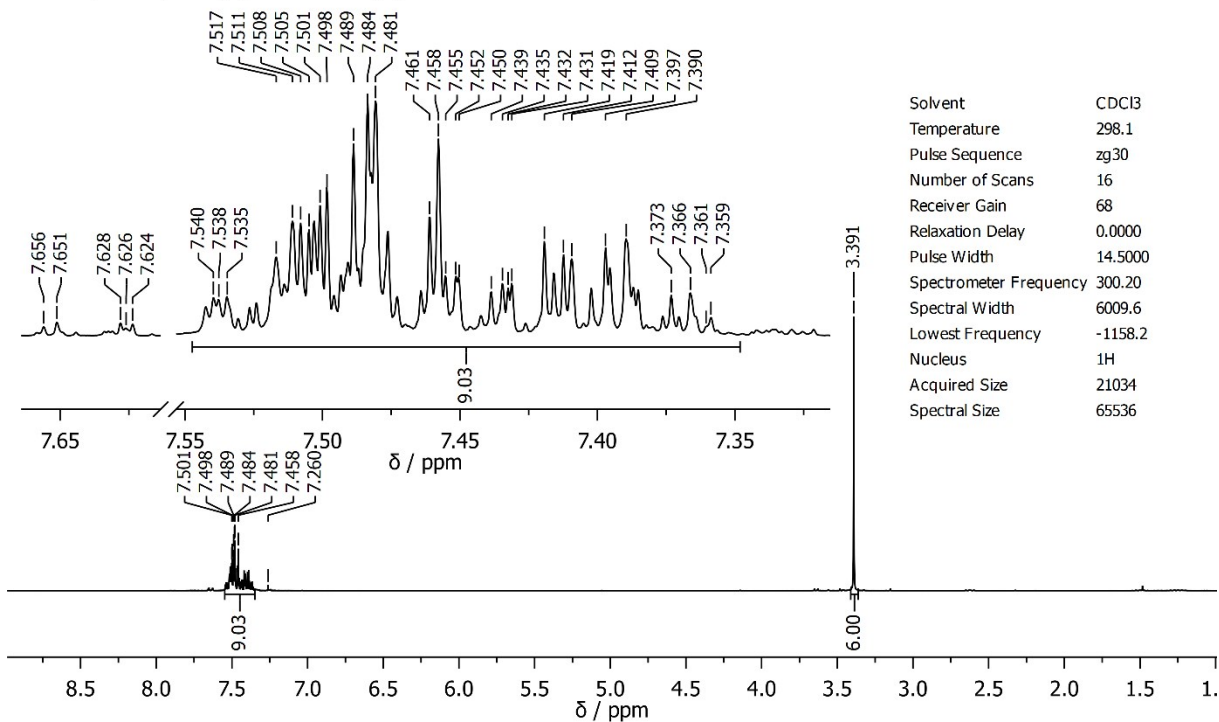


Figure S23. ¹H NMR spectrum of **3** in CDCl₃.

Dimethyl 2-biphenylboronate (3) -13C

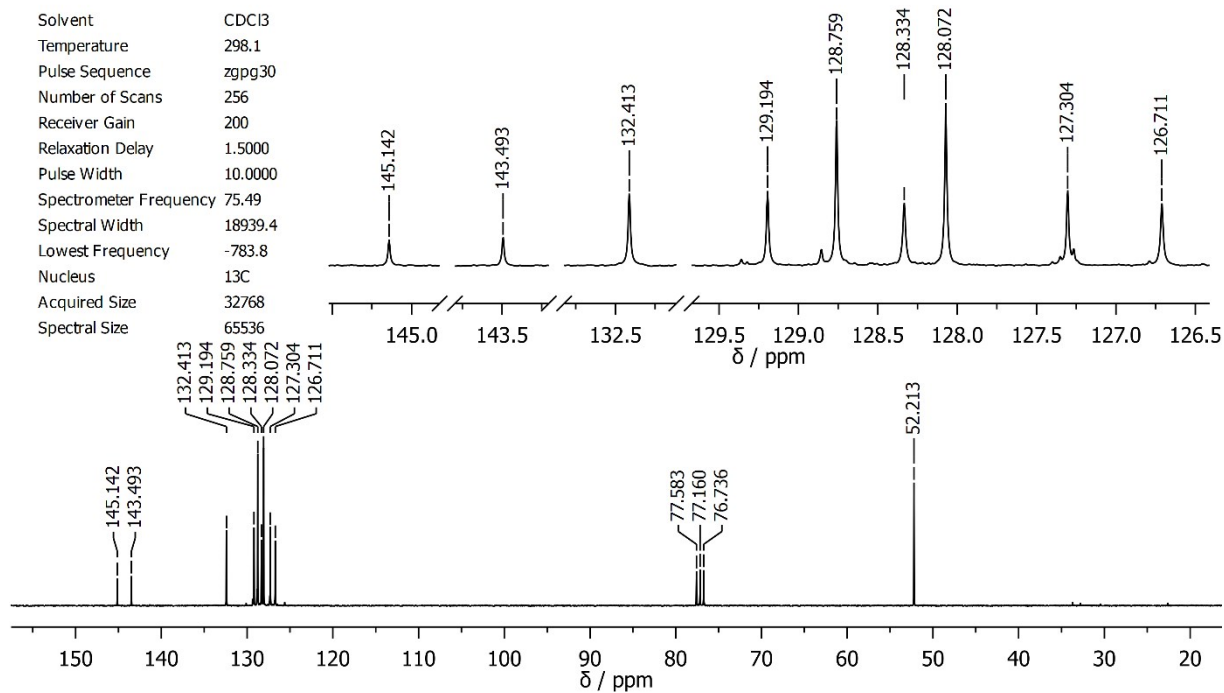


Figure S24. ¹³C{¹H} NMR spectrum of **3** in CDCl₃.

5.2 NMR spectra of complex 1

1 CDCl3 1H@25C

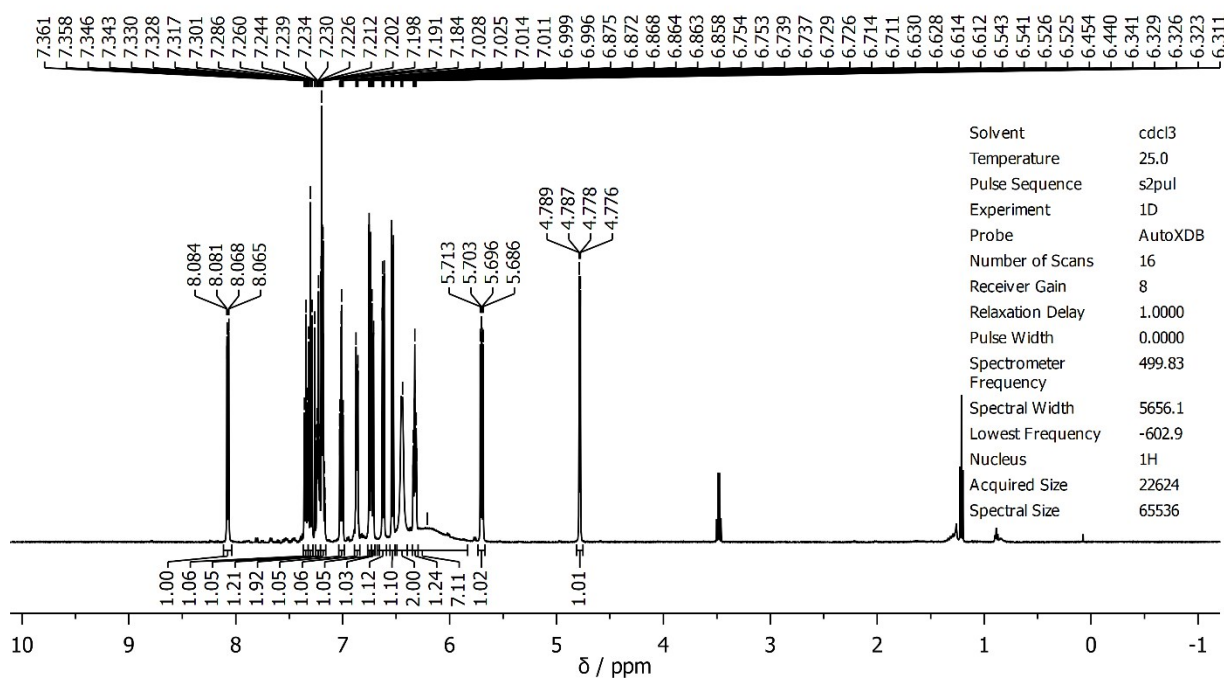


Figure S25. ^1H NMR spectrum of **1** in CDCl_3 at 25°C.

1_CDCI3_1H@25C_expansion_1

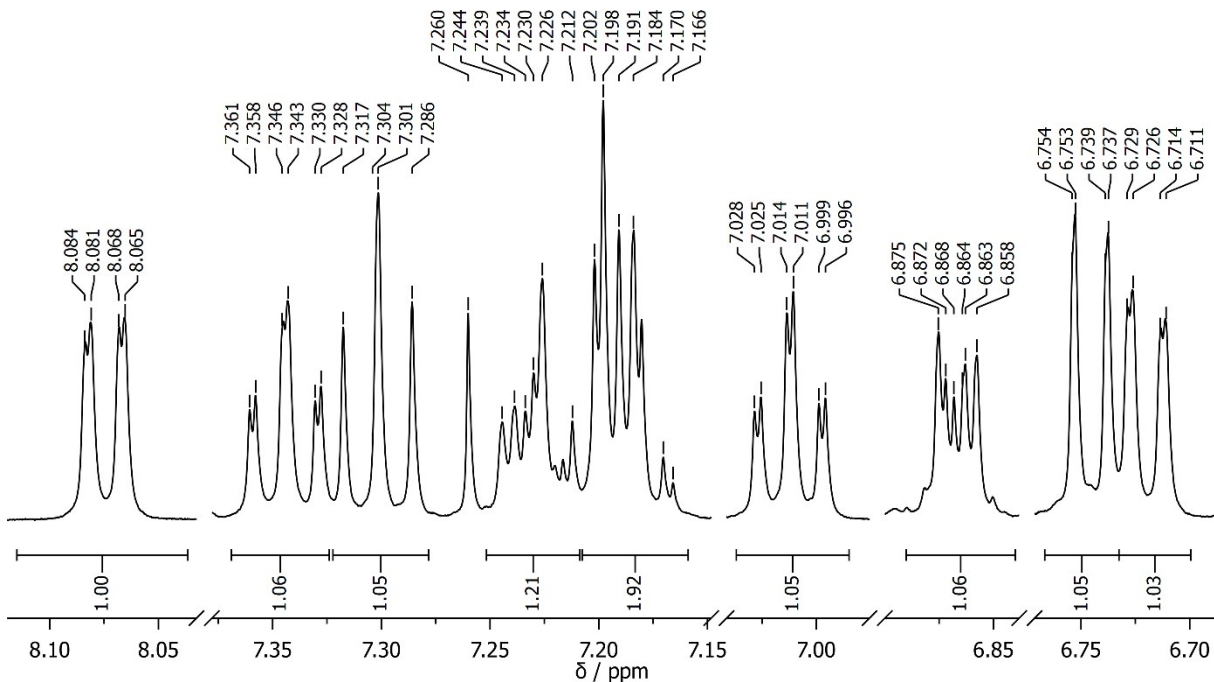


Figure S26. ^1H NMR spectrum of **1** in CDCl_3 at 25°C – expansion part 1.

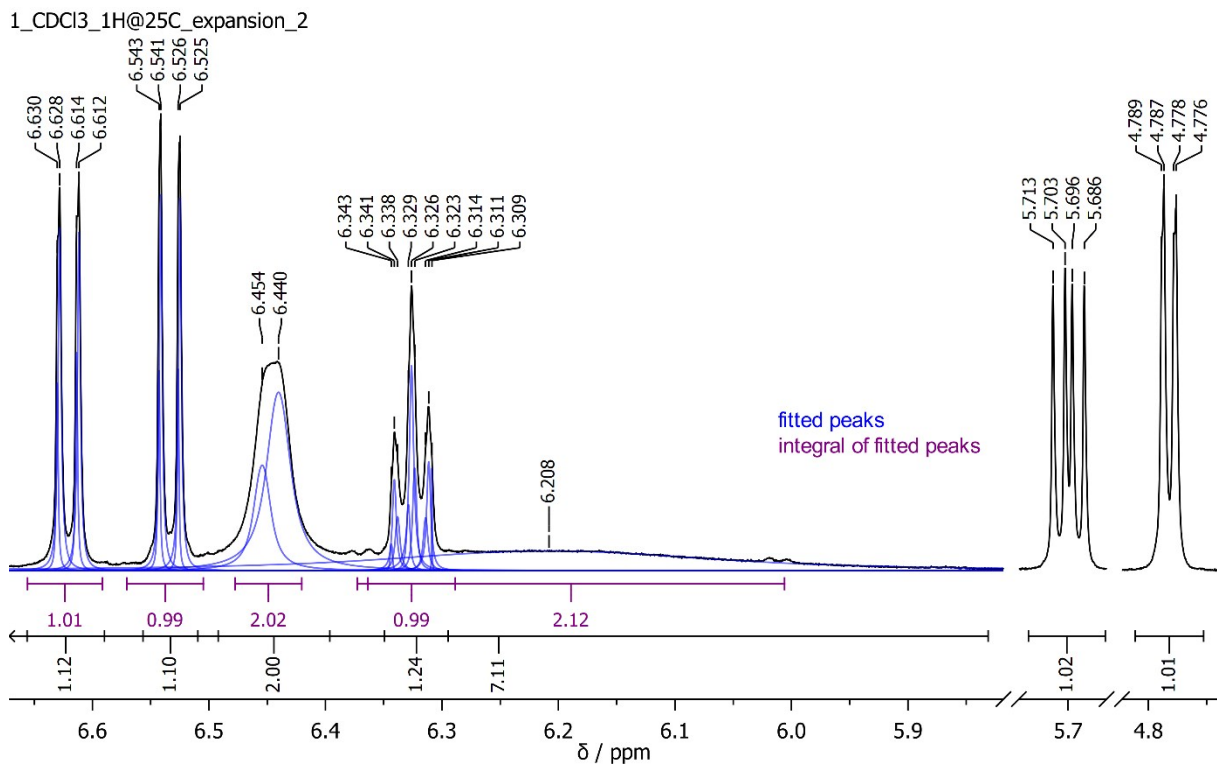


Figure S27. ^1H NMR spectrum of **1** in CDCl_3 at 25°C – expansion part 2.

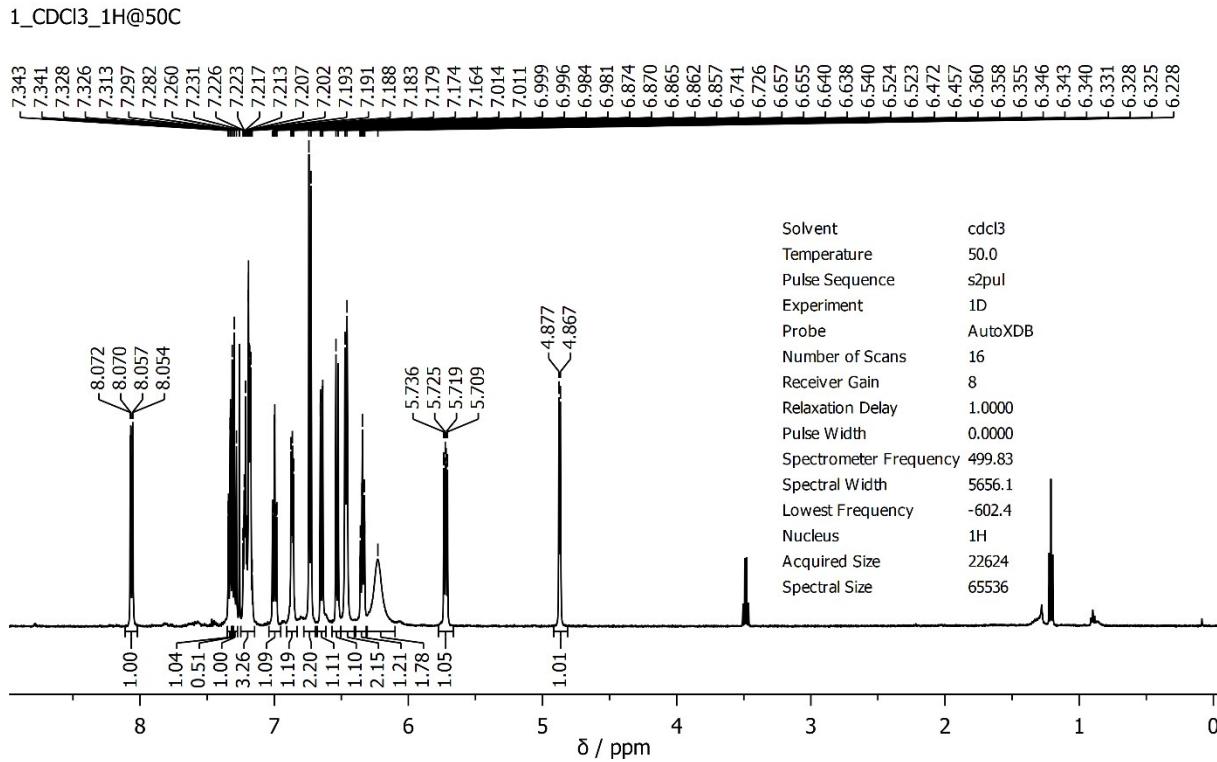


Figure S28. ^1H NMR spectrum of **1** in CDCl_3 at 50°C .

1_CDCl₃_1H@50C_expansion

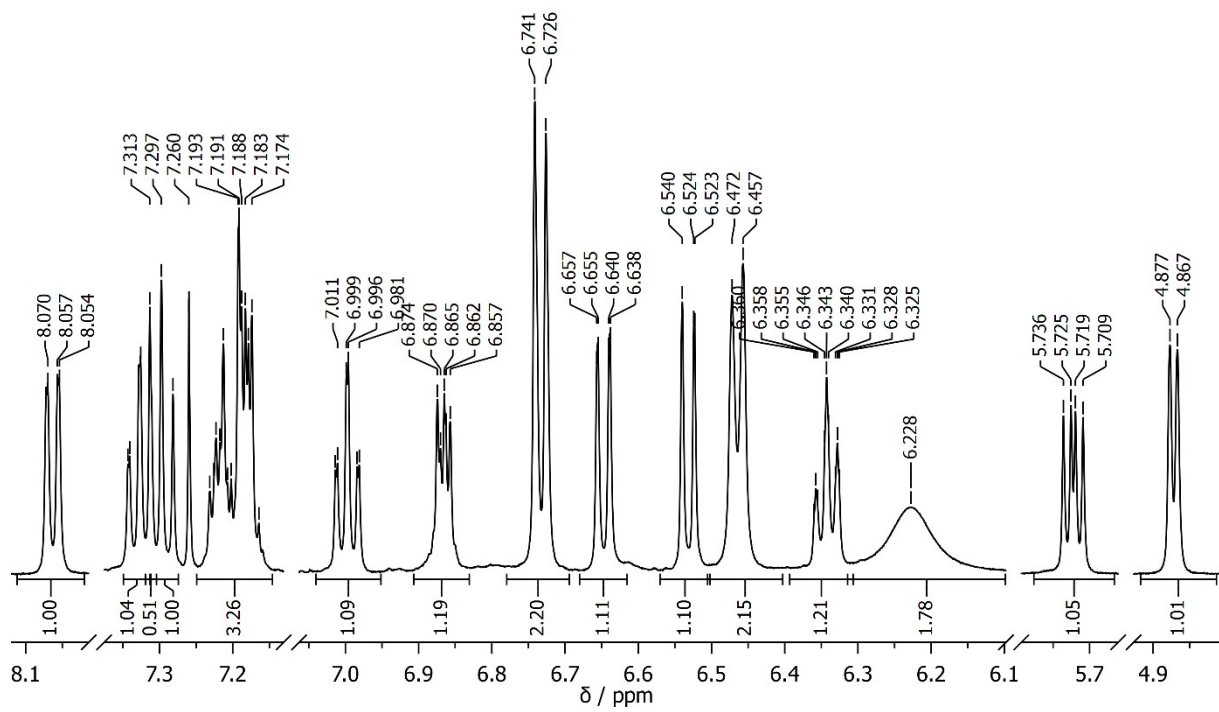


Figure S29. ¹H NMR spectrum of **1** in CDCl₃ at 25°C – expansion.

1_CDCl₃_13C@25C

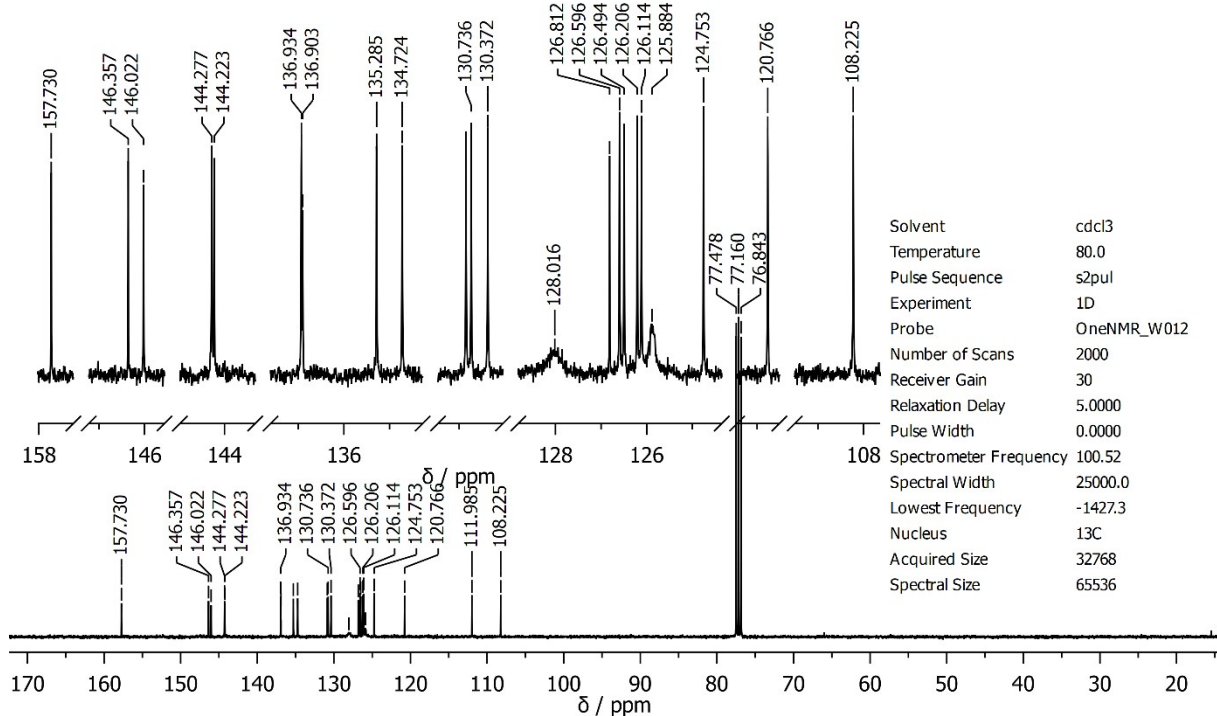


Figure S30. ¹³C{¹H} NMR spectrum of **1** in CDCl₃ at 25°C.

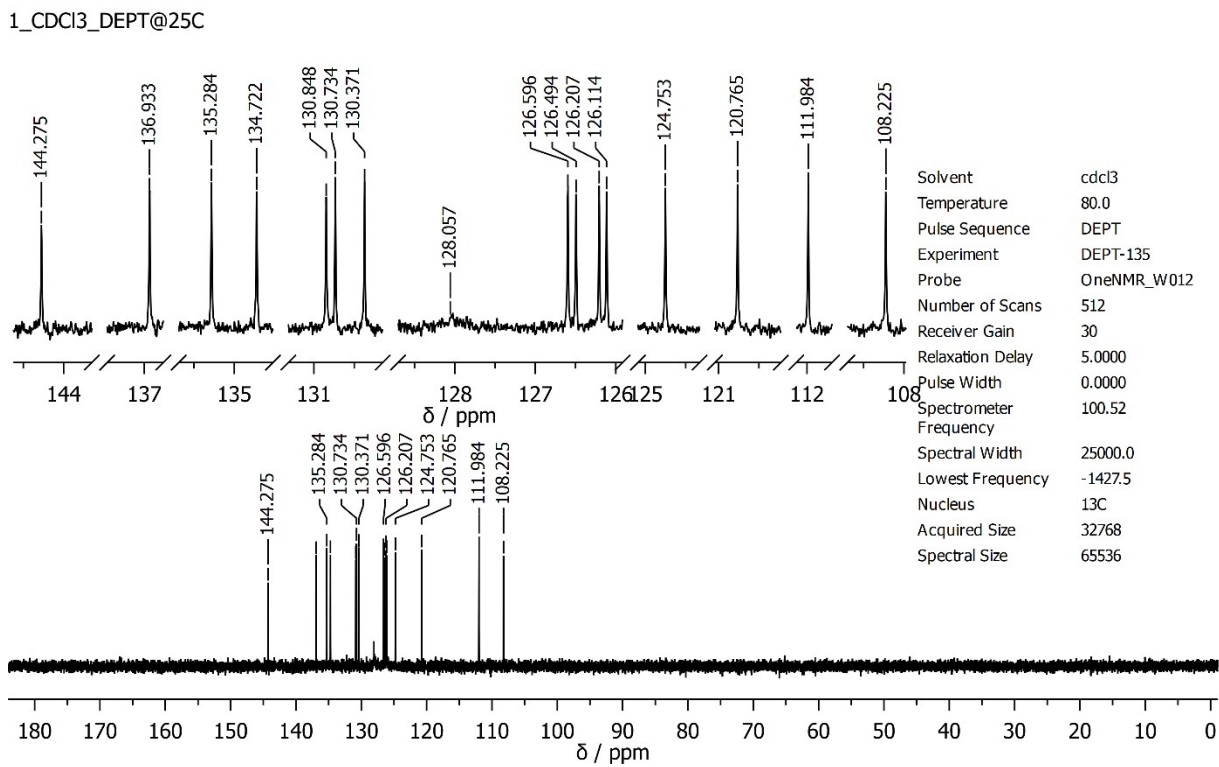


Figure S31. DEPT NMR spectrum of **1** in CDCl_3 at 25°C.

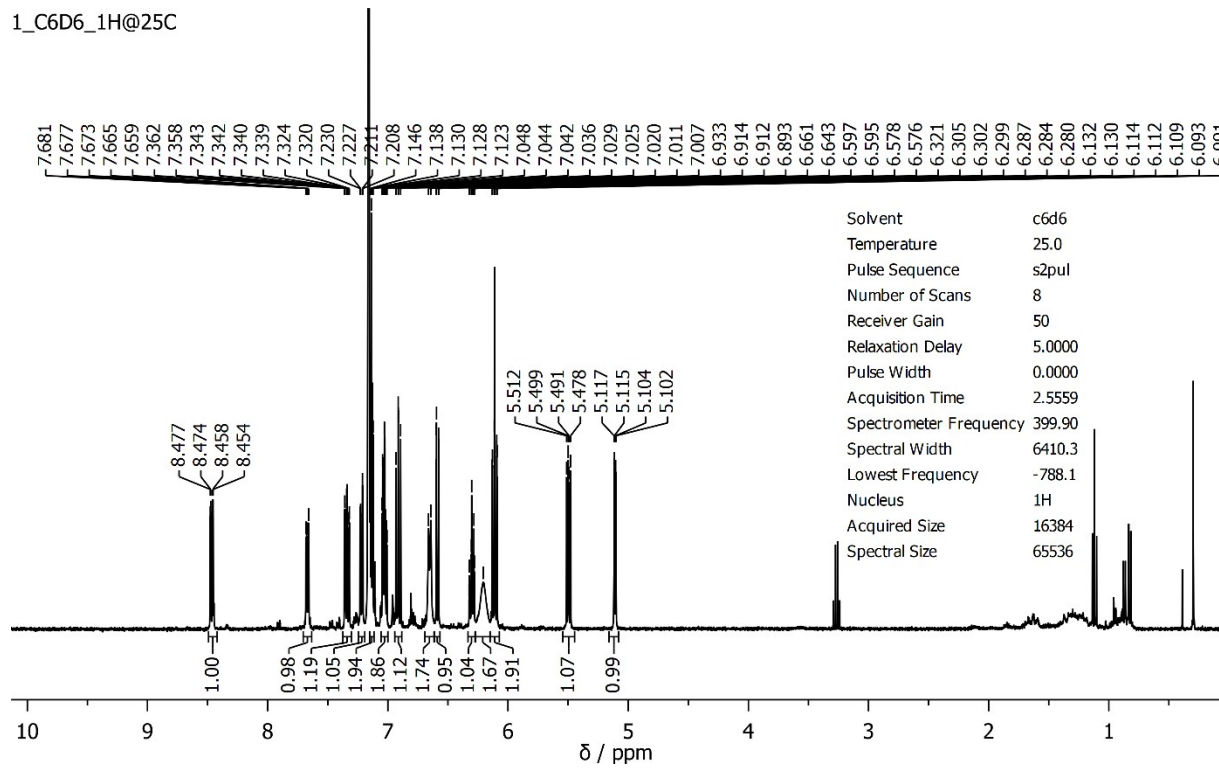


Figure S32. ^1H NMR spectrum of **1** in C_6D_6 at 25°C.

1_C6D6_1H@25C expansion

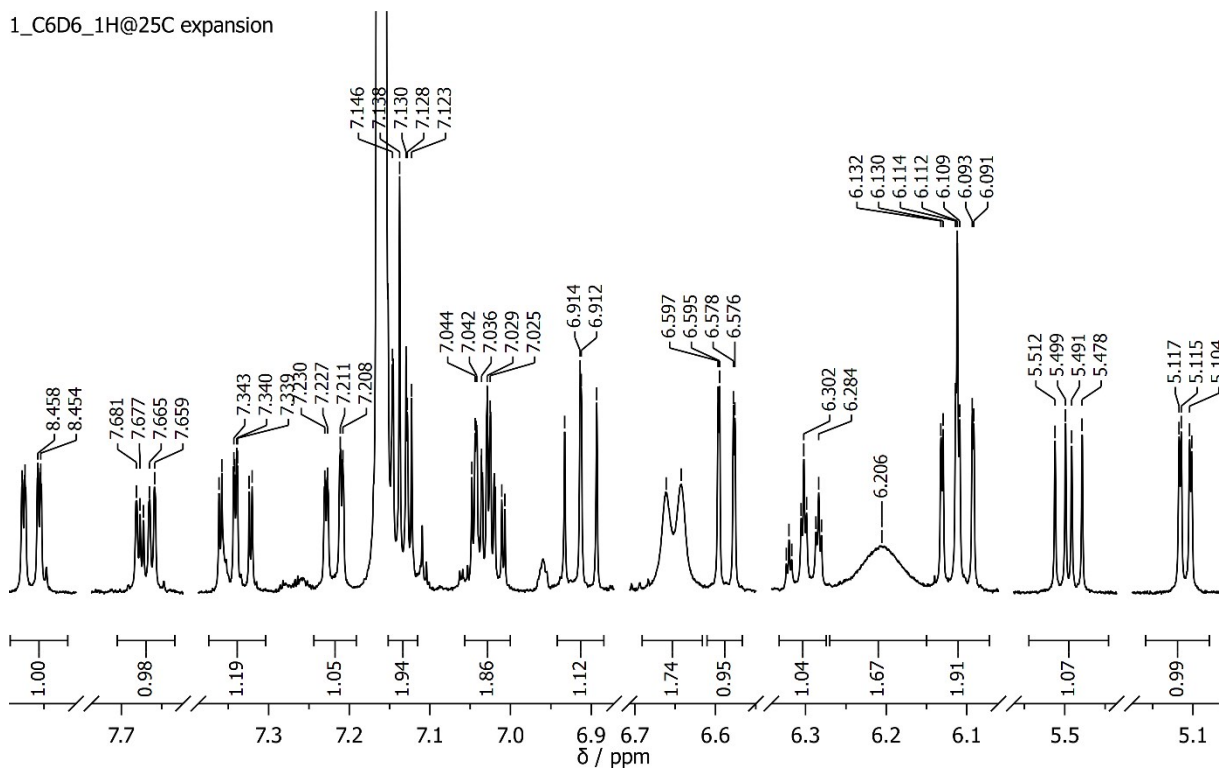


Figure S33. ¹H NMR spectrum of **1** in C₆D₆ at 25°C – expansion.

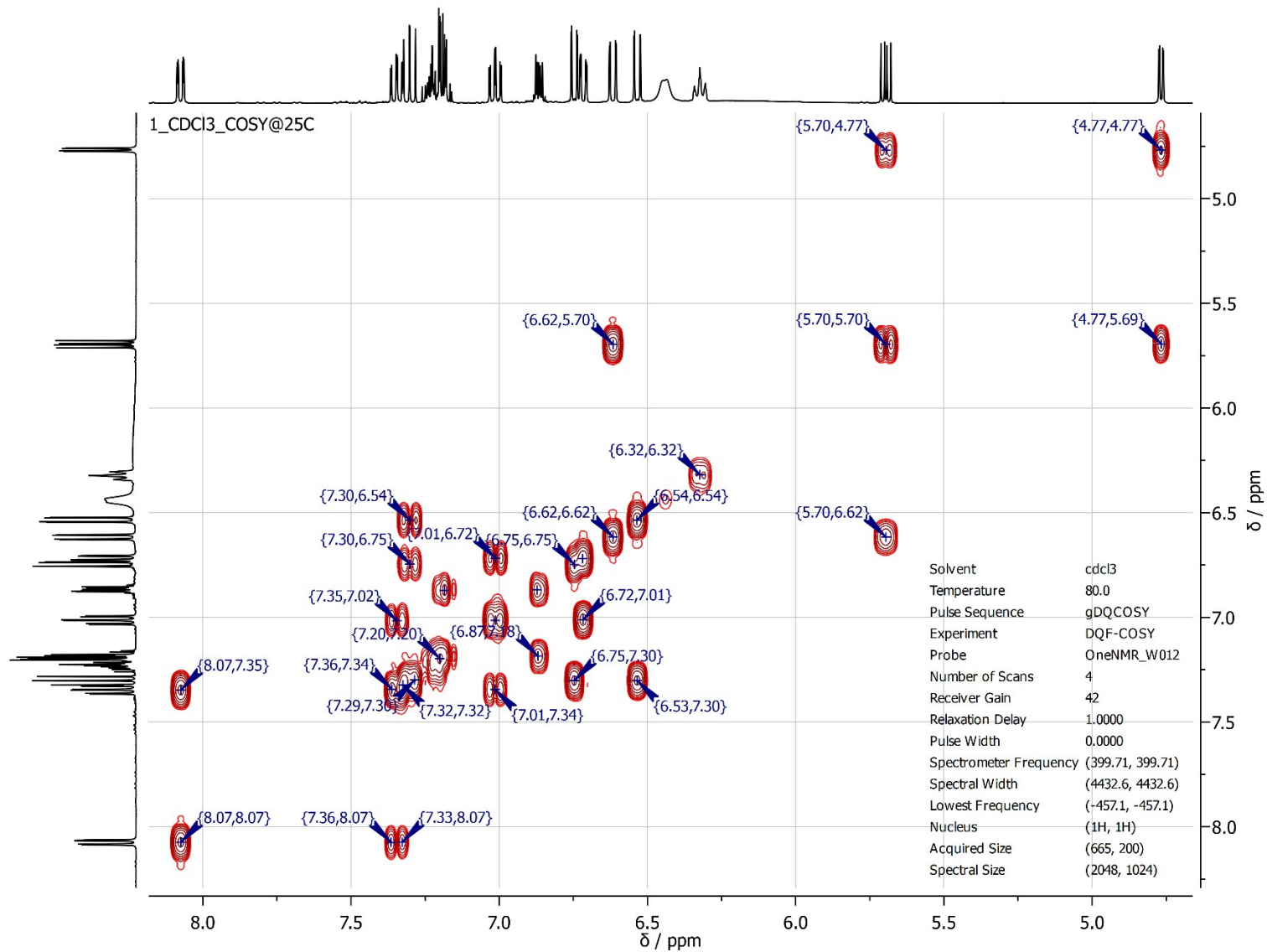


Figure S34. ¹H, ¹H COSY NMR spectrum of **1** in CDCl₃ at 25°C.

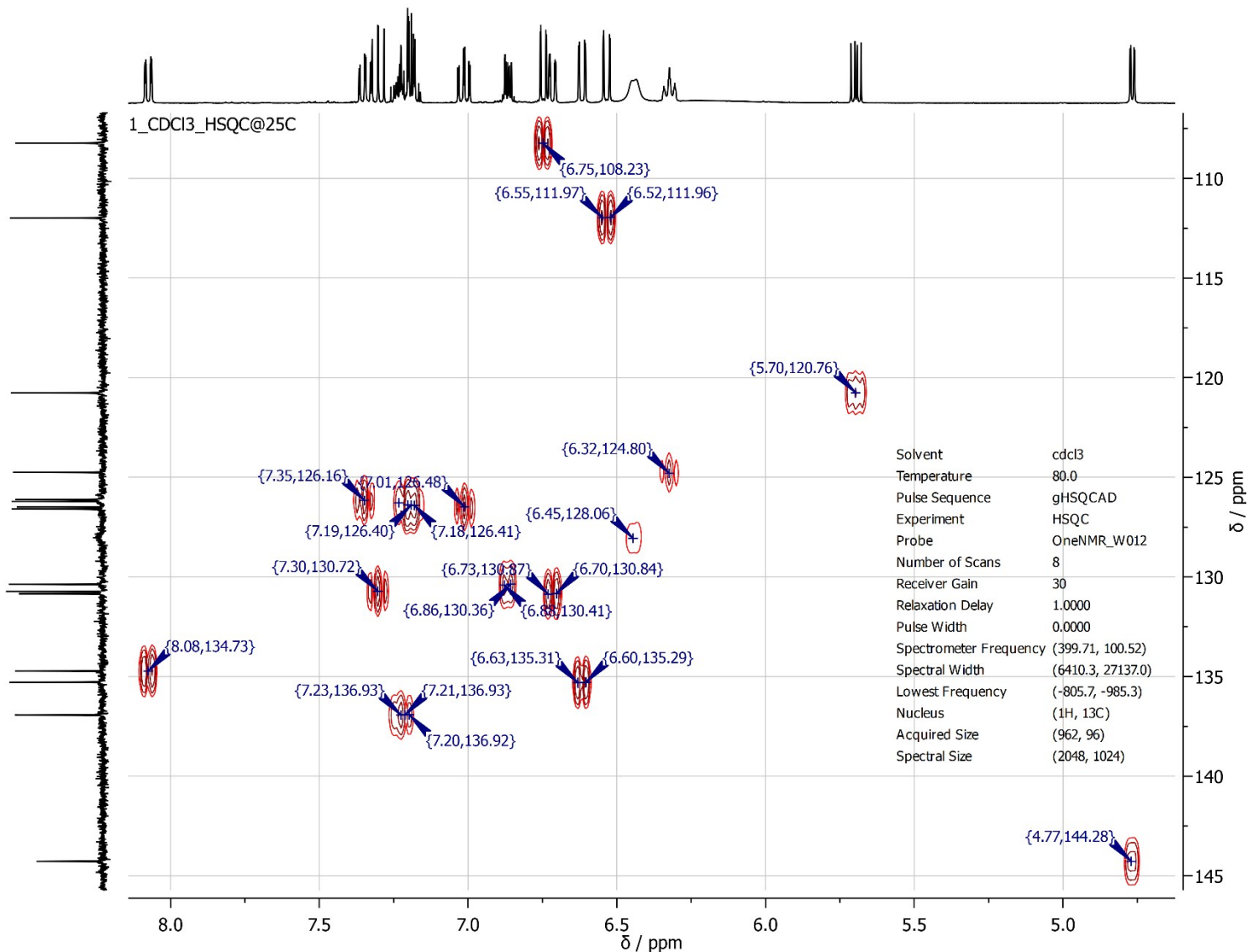


Figure S35. ¹H,¹³C HSQC NMR spectrum of **1** in CDCl₃ at 25°C.

5.3 NMR spectra of complex 2

2_C6D6_1H@25C

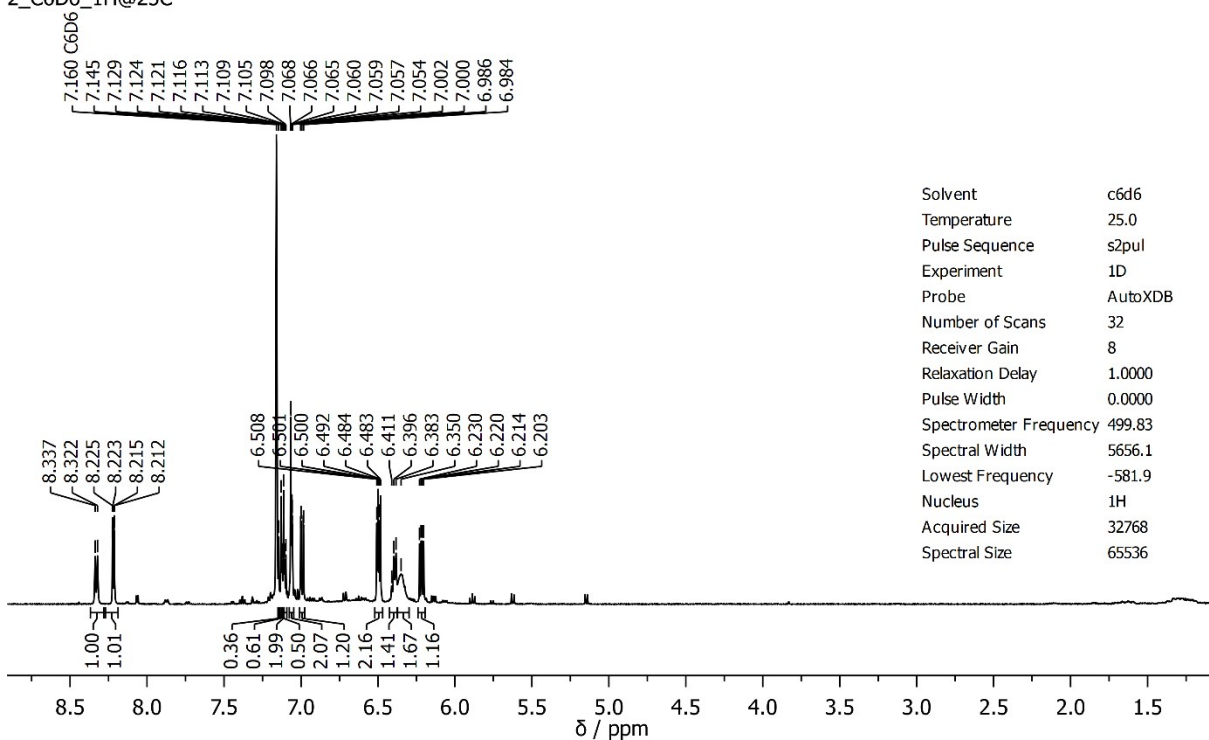


Figure S36. ^1H NMR spectrum of **2** in C_6D_6 at 25°C .

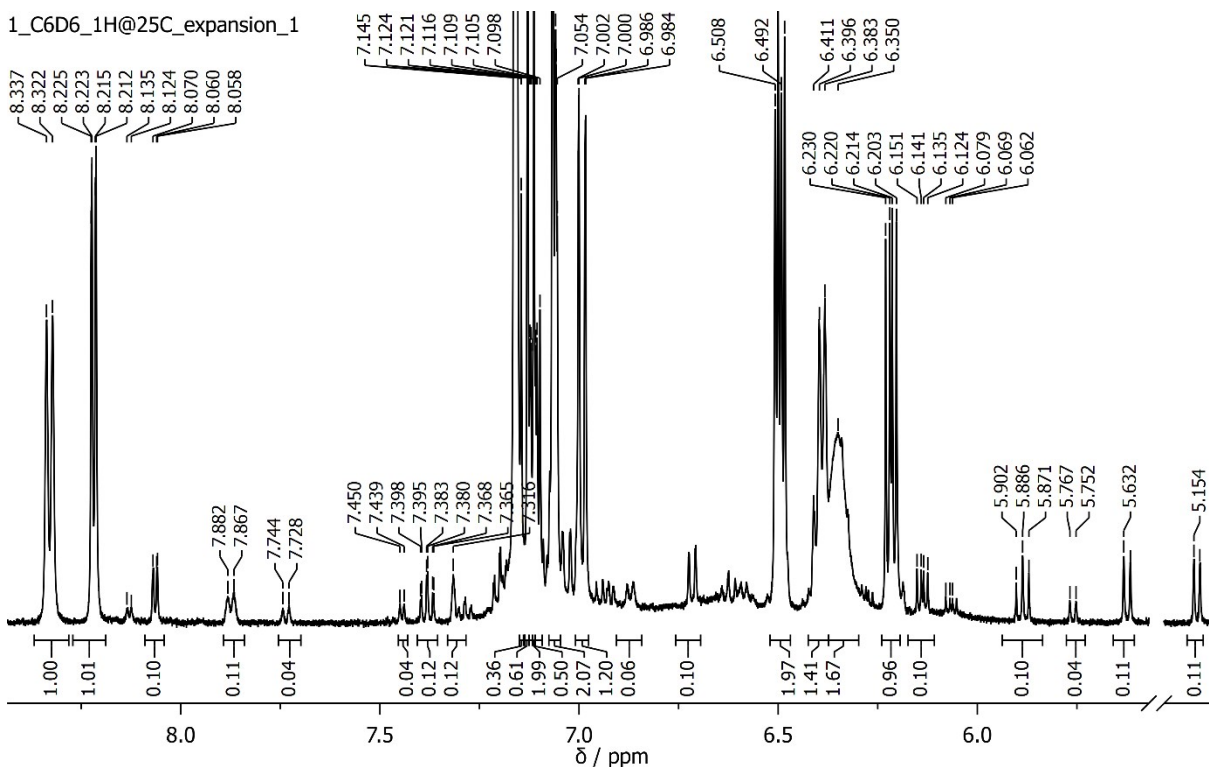


Figure S37. ^1H NMR spectrum of **2** in C_6D_6 at 25°C – expansion part 1.

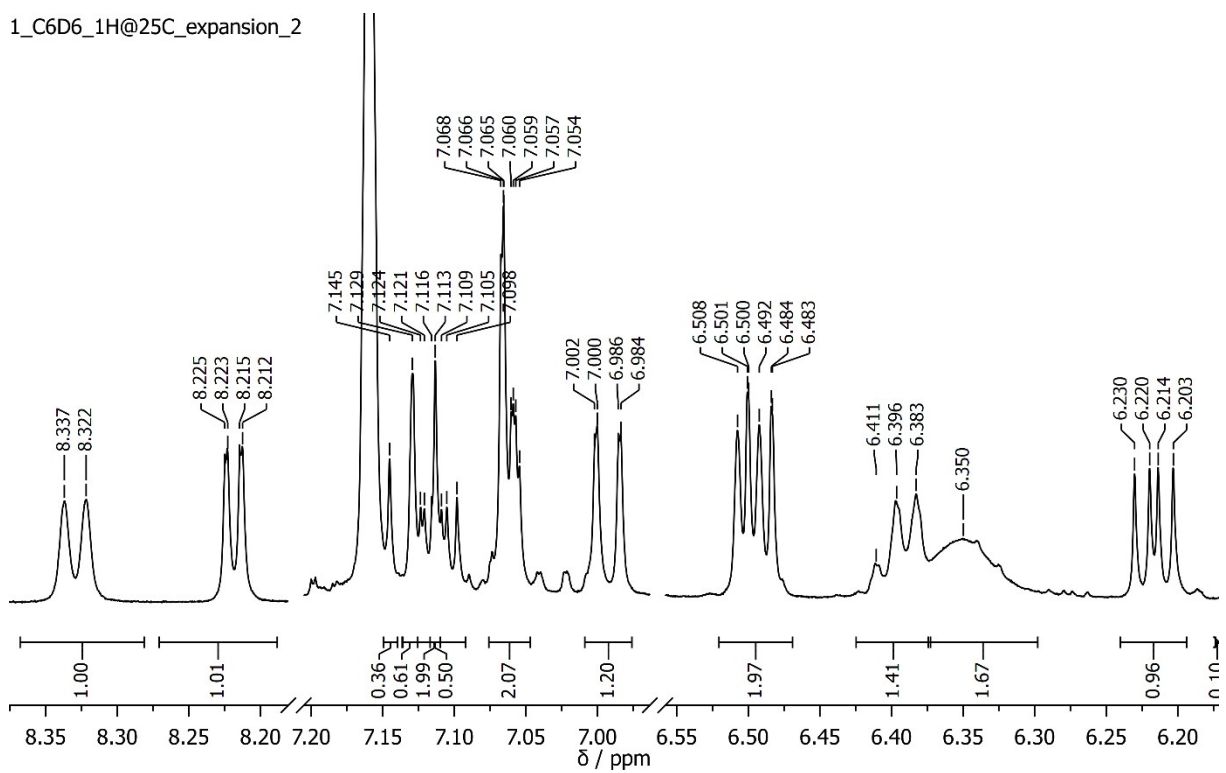


Figure S38. ^1H NMR spectrum of **2** in C_6D_6 at 25°C – expansion part 2.

2_C6H6_19F@25C

Solvent	c6d6
Temperature	25.0
Pulse Sequence	s2pul
Experiment	1D
Probe	AutoXDB
Number of Scans	64
Receiver Gain	42
Relaxation Delay	1.0000
Pulse Width	0.0000
Spectrometer Frequency	470.24
Spectral Width	27777.8
Lowest Frequency	-79557.3
Nucleus	19F
Acquired Size	16384
Spectral Size	32768

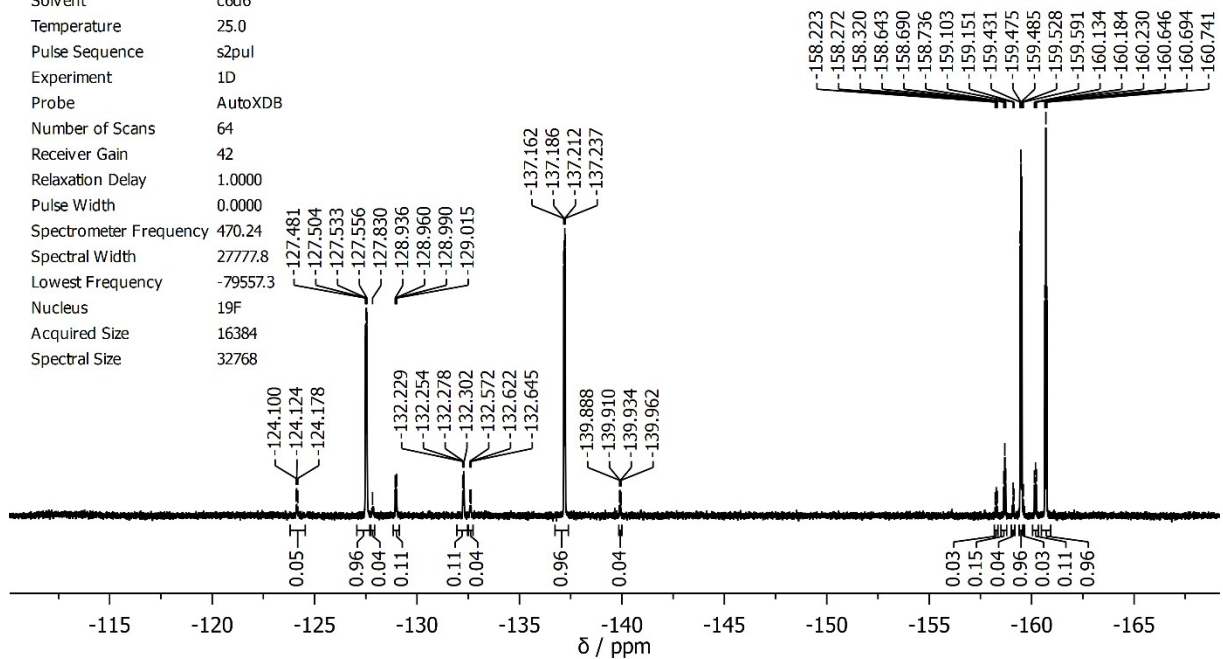


Figure S39. ^{19}F NMR spectrum of **2** in C_6D_6 at 25°C.

2_C6H6_19F@25C_expansion

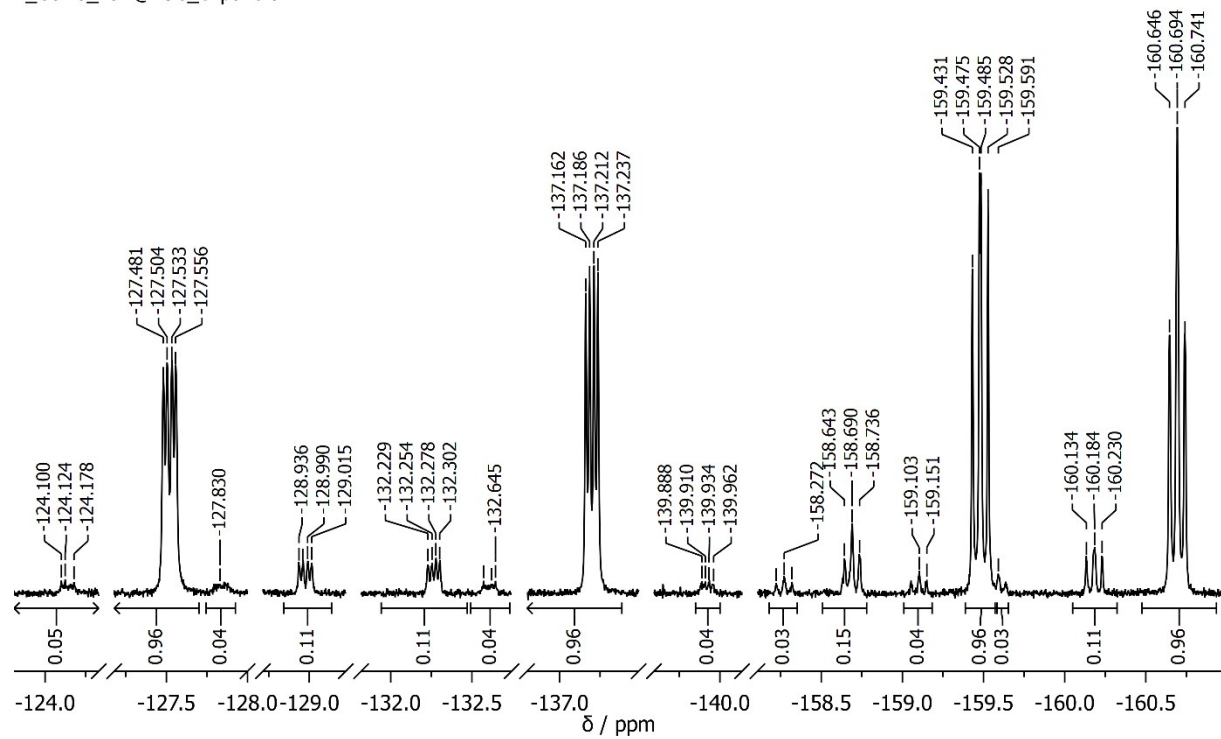


Figure S40. ¹⁹F NMR spectrum of **2** in C_6D_6 at 25°C – expansion.

2_C6D6_13C

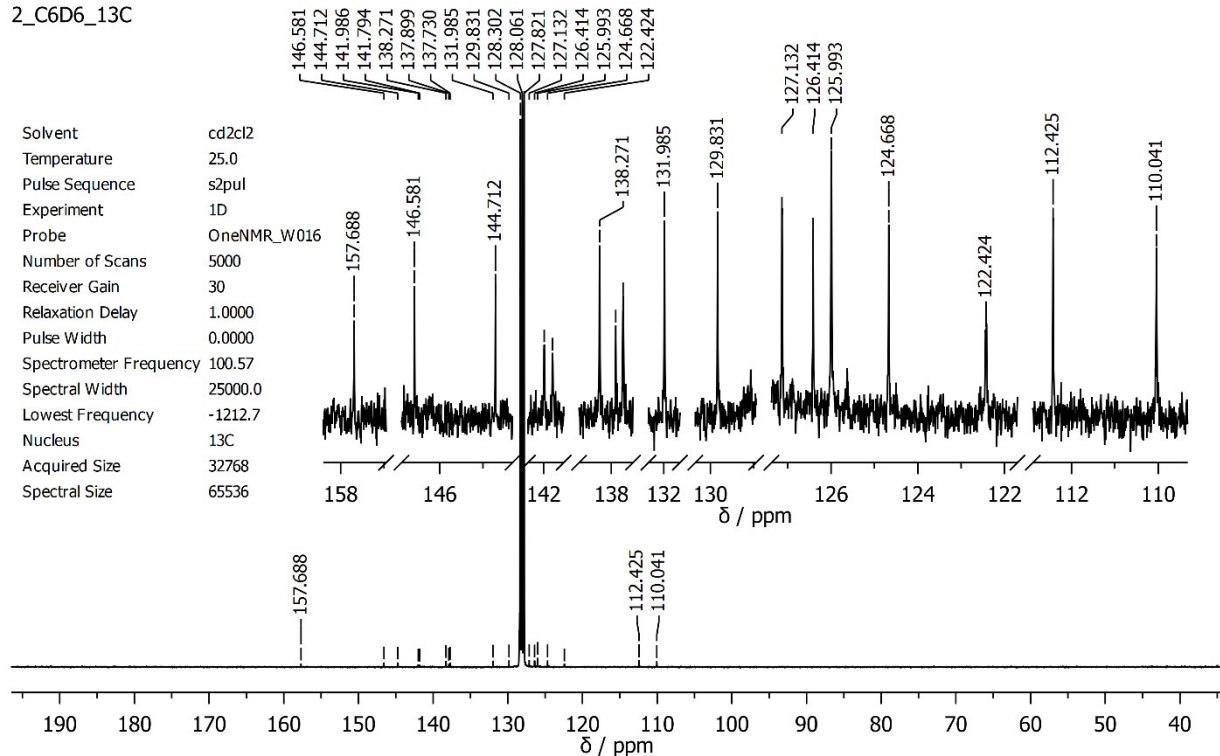


Figure S41. ¹³C{¹H} NMR spectrum of **2** in C_6D_6 at 25°C.

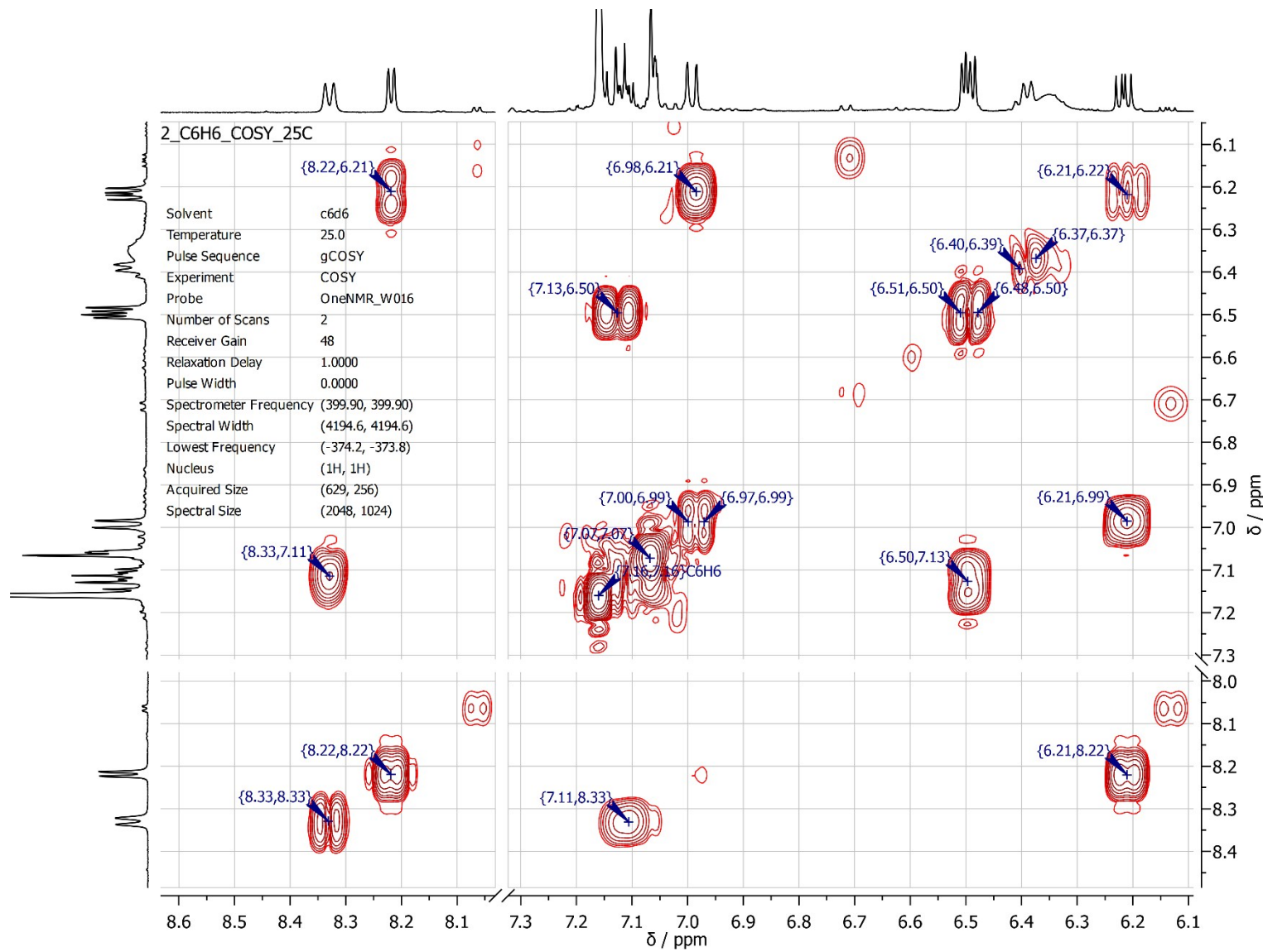


Figure S42. $^1\text{H},^1\text{H}$ COSY NMR spectrum of **2** in C_6D_6 at 25°C .

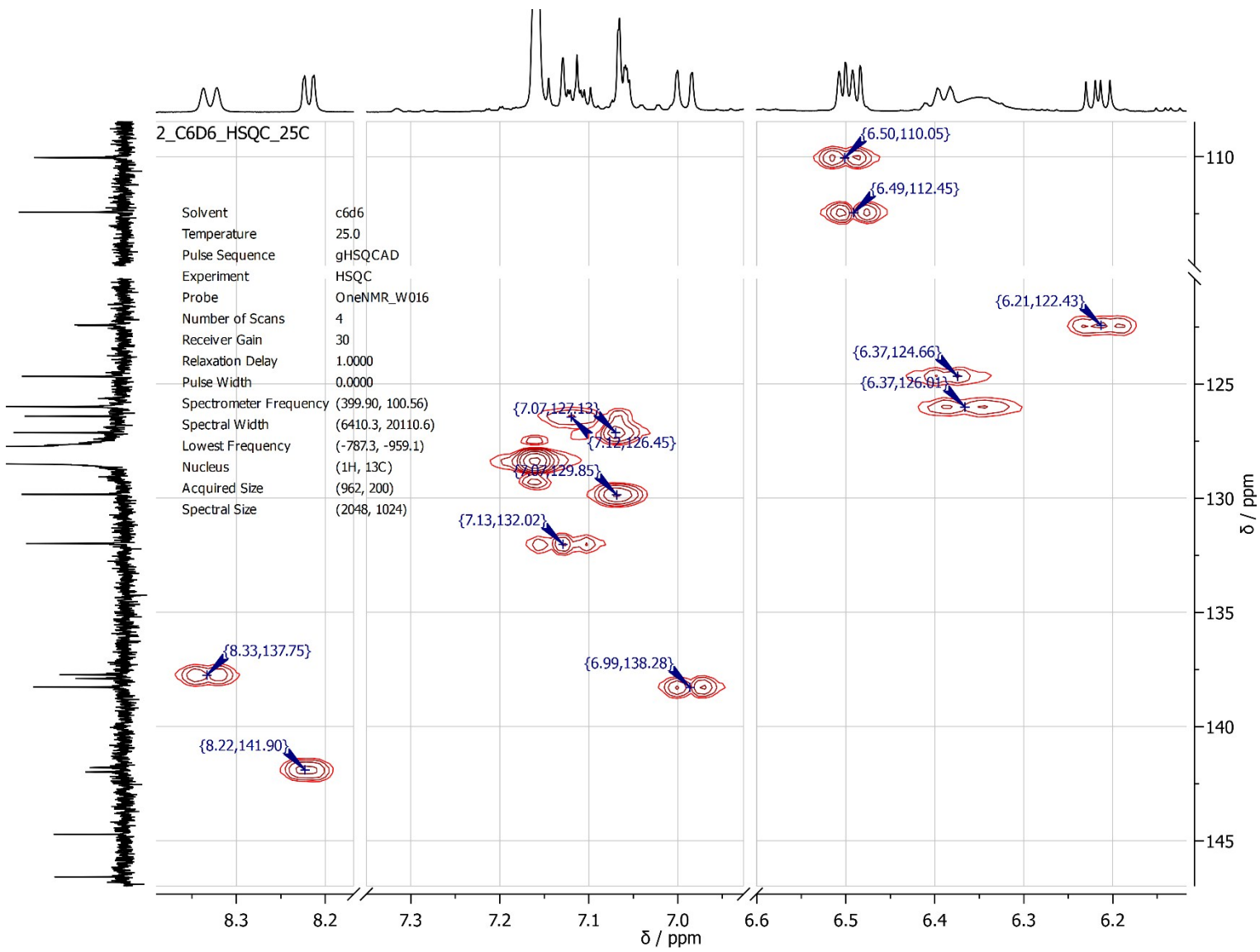


Figure S43. ^1H , ^{13}C HSQC NMR spectrum of **2** in C_6D_6 at 25°C .

2_CDCI3_1H@25C

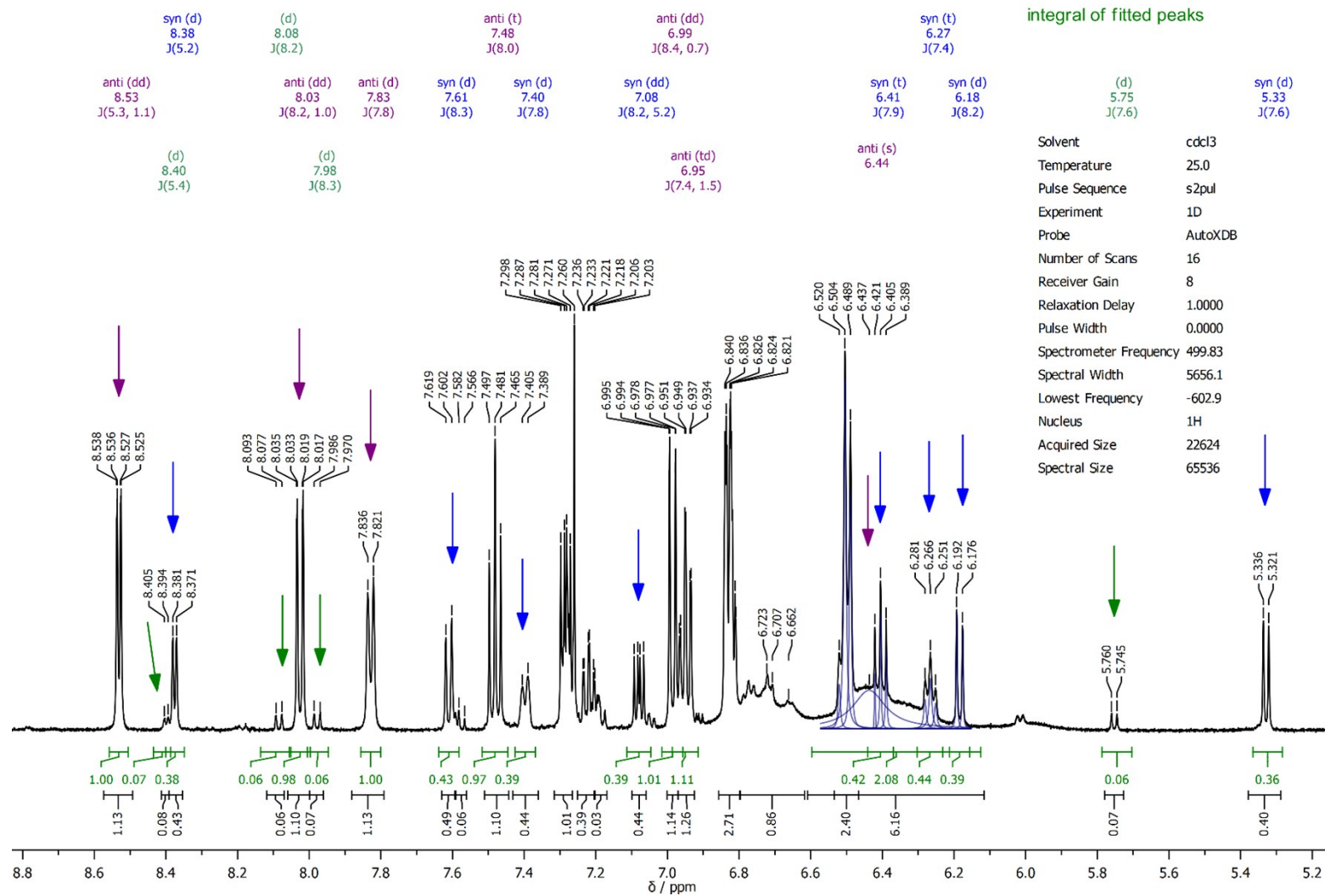


Figure S44. ^1H NMR spectrum of **2** in CDCl_3 at 25°C ; signals marked with purple arrow are derived from **2-anti**, blue arrow - **2-syn** and green arrow - **2-syn-mezo**.

2_CDCl₃_1H@25C

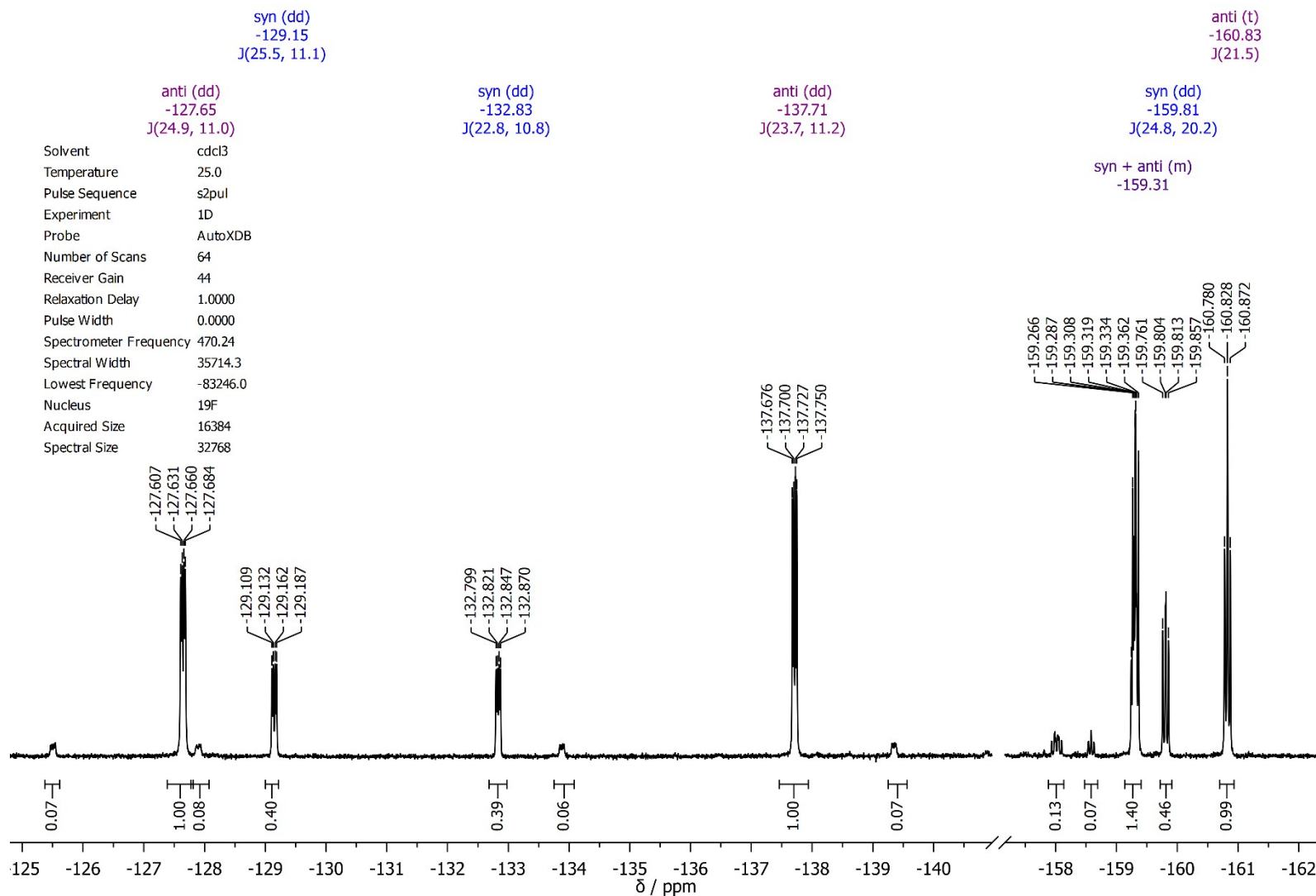


Figure S45. ¹⁹F NMR spectrum of **2** in CDCl₃ at 25°C.

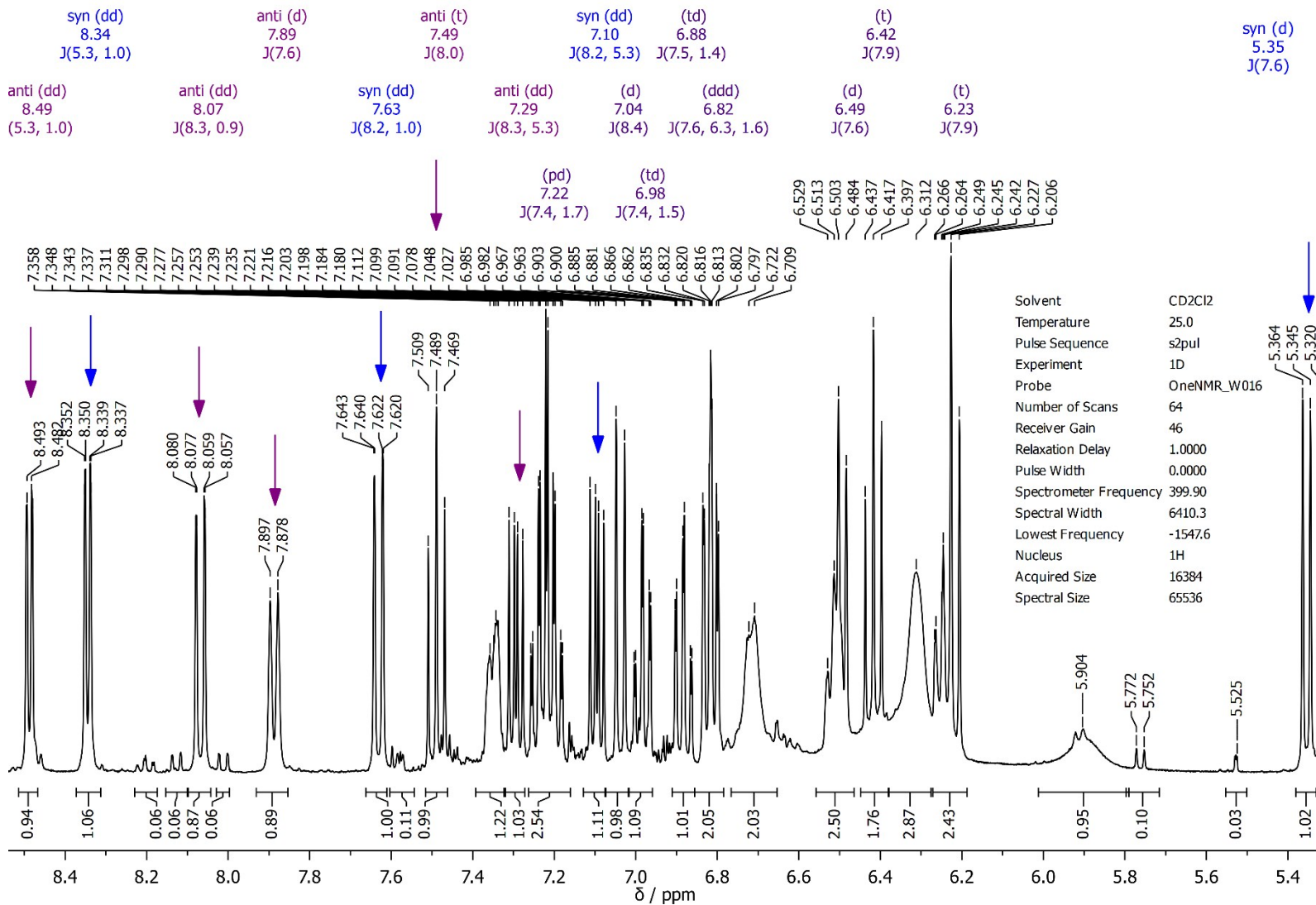
2_CD2Cl₂_1H@25C

Figure S46. ¹H NMR spectrum of **2** in CD₂Cl₂ at 25°C; signals marked with purple arrow are derived from **2**-anti, blue arrow - **2**-syn.

2_DCM_19F@25C

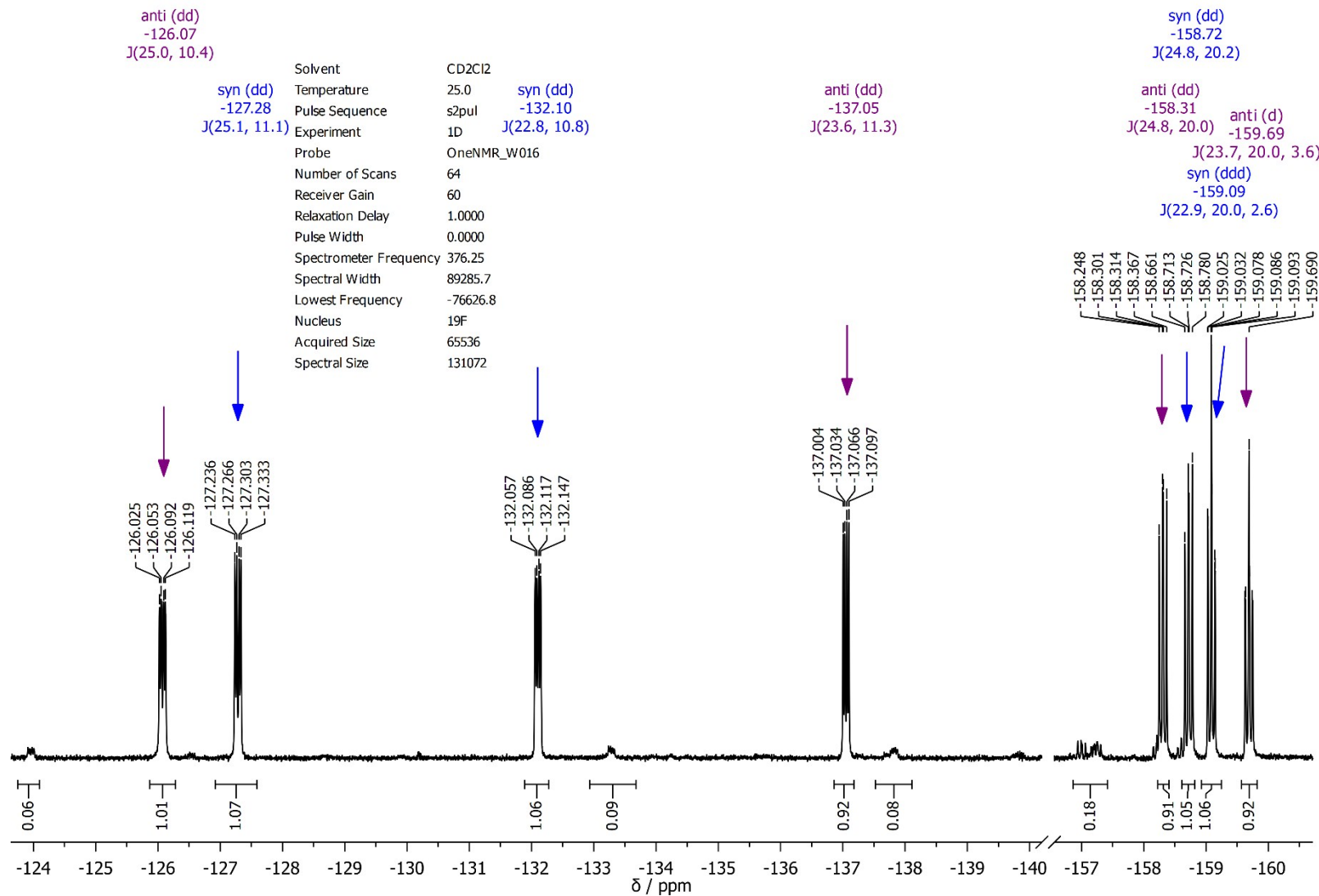


Figure S47. ¹⁹F NMR spectrum of **2** in CD₂Cl₂ at 25°C; signals marked with purple arrow are derived from **2**-anti, blue arrow - **2**-syn.

2_DMSO_1H@25C

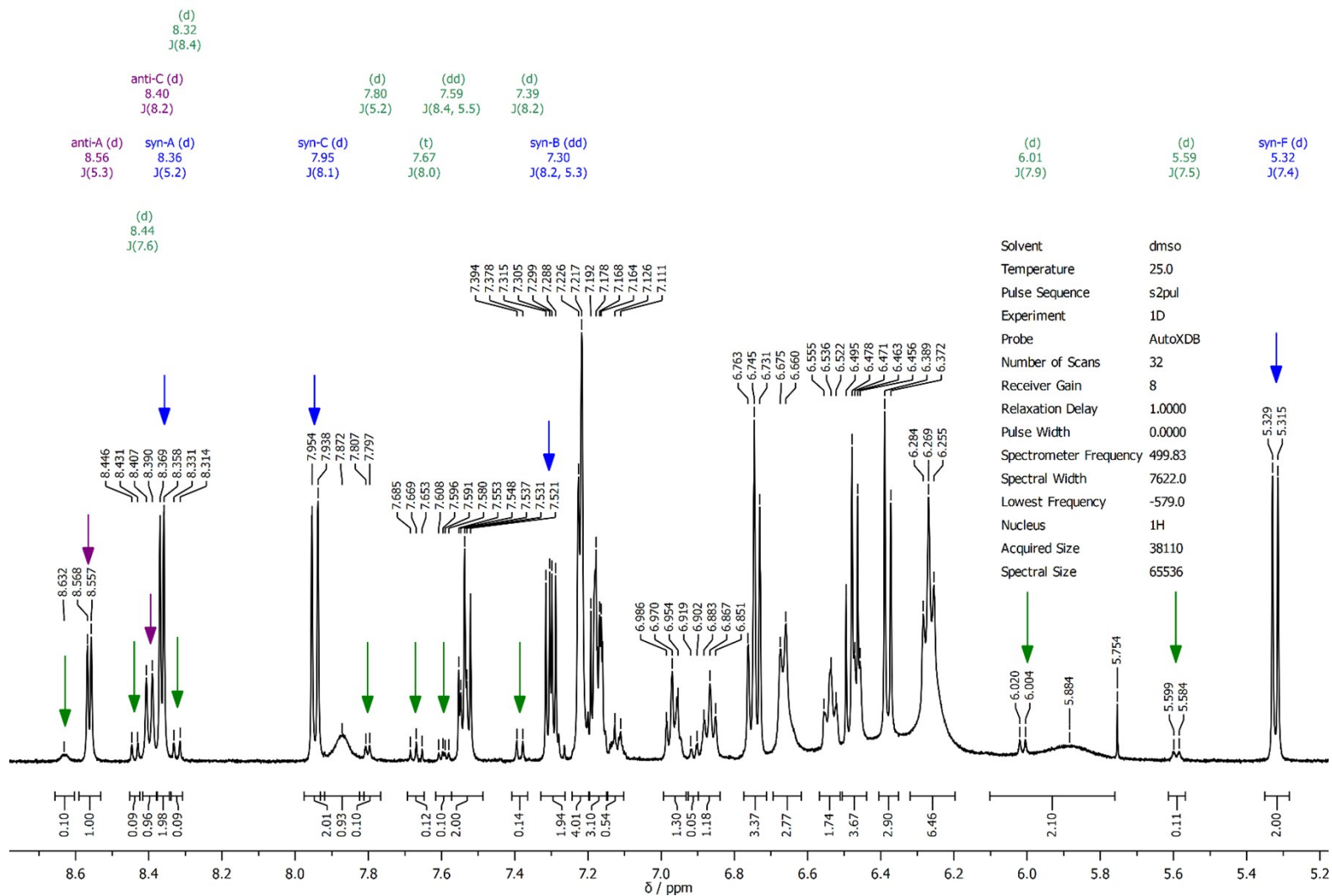


Figure S48. ^1H NMR spectrum of **2** in $\text{DMSO}-d_6$ at 25°C ; signals marked with purple arrow are derived from **2**-*anti*, blue arrow - **2**-*syn* and green arrow - **2**-*syn-mezo*.

2_DMSO_19F_25C

Solvent dmso
Temperature 25.0
Pulse Sequence s2pul
Experiment 1D
Probe AutoXDB
Number of Scans 64
Receiver Gain 44
Relaxation Delay 1.0000
Pulse Width 0.0000
Spectrometer Frequency 470.24
Spectral Width 54347.8
Lowest Frequency -90475.8
Nucleus 19F
Acquired Size 32768
Spectral Size 65536

anti (d) -158.91 J(24.2)
syn (t) -160.90 J(22.8)

syn (dd) -127.24 J(26.5, 11.1)

syn (dd) -133.32 J(24.1, 10.8)

anti (s) -138.77

syn (dd) -159.61 J(26.4, 21.2)

anti (t) -160.57 J(23.0)

-122 -123 -124 -125 -126 -127 -128 -129 -130 -131 -132 -133 -134 -135 -136 -137 -138 -139 -140 -141 -157 -158 -159 -160 -161 -162 -163 -164

δ / ppm

Figure S49. ^{19}F NMR spectrum of **2** in $\text{DMSO}-d_6$ at 25°C ; signals marked with purple arrow are derived from **2-anti**, blue arrow - **2-syn**.

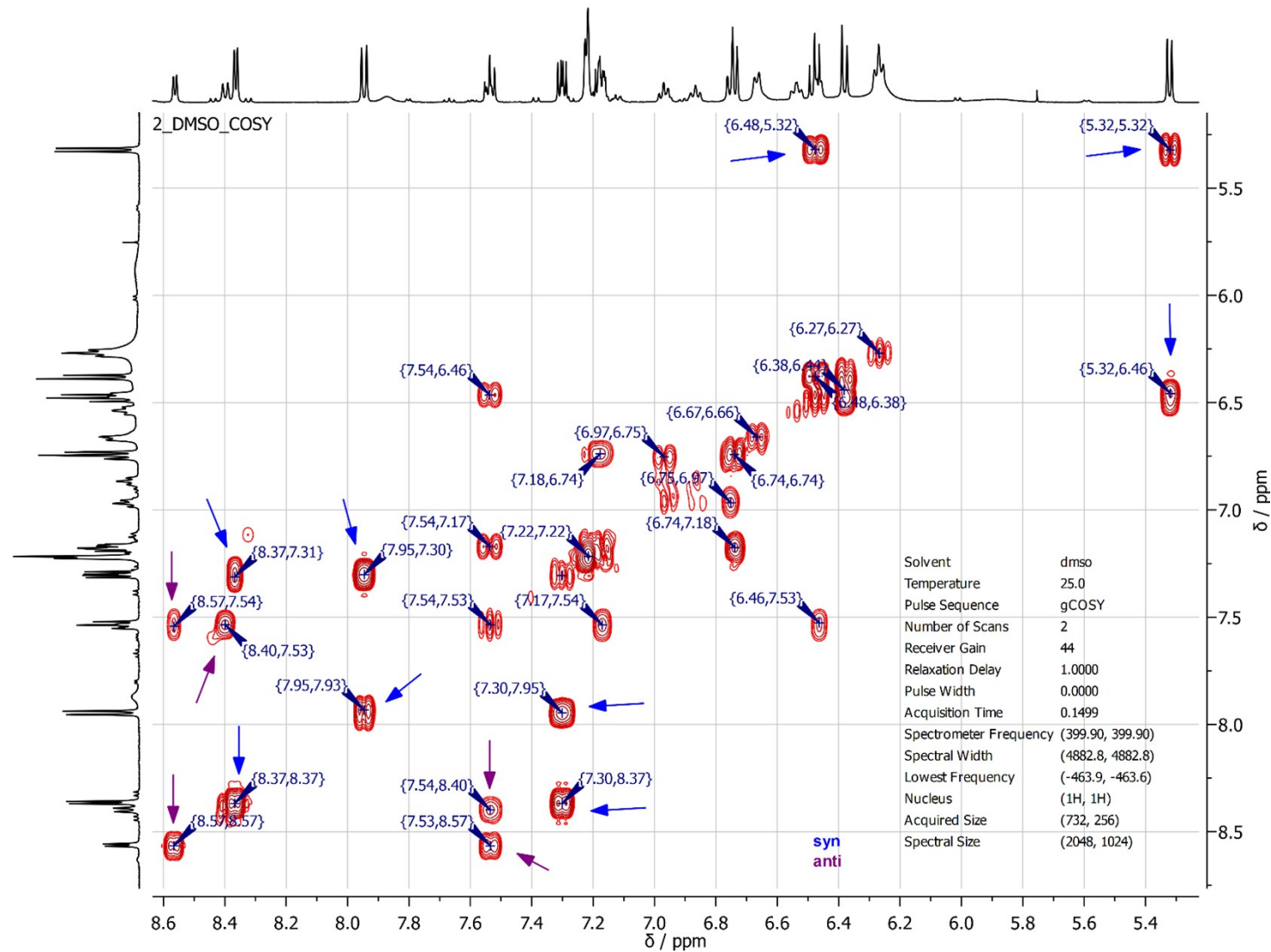


Figure S50. ^1H , ^1H COSY NMR spectrum of **2** in $\text{DMSO}-d_6$ at 25°C ; signals marked with purple arrow are derived from **2-anti**, blue arrow - **2-syn**.

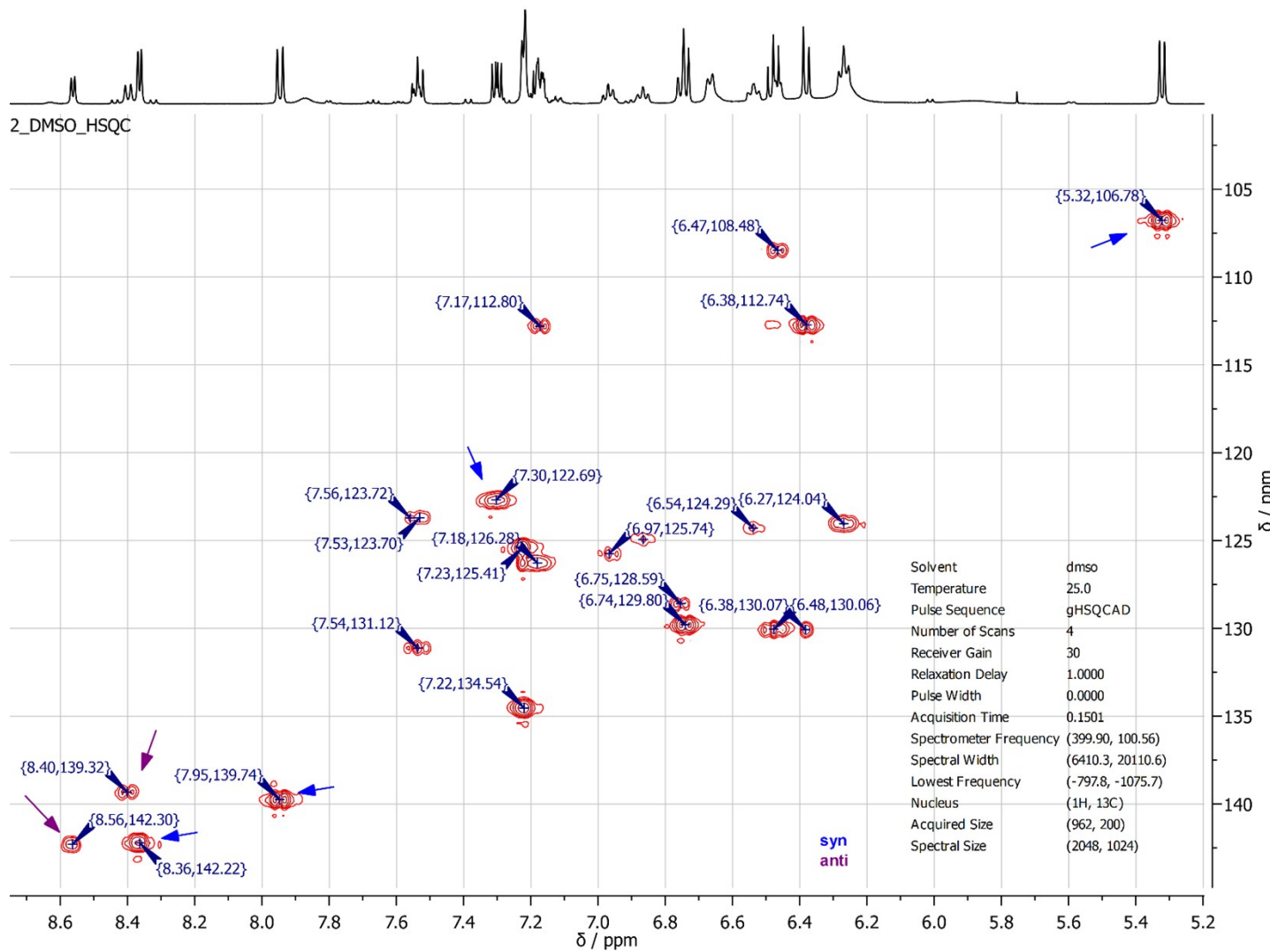


Figure S51. $^1\text{H},^{13}\text{C}$ HSQC NMR spectrum of **2** in $\text{DMSO}-d_6$ at 25°C; signals marked with purple arrow are derived from **2-anti**, blue arrow - **2-syn**.

2_acetone_1H@25C

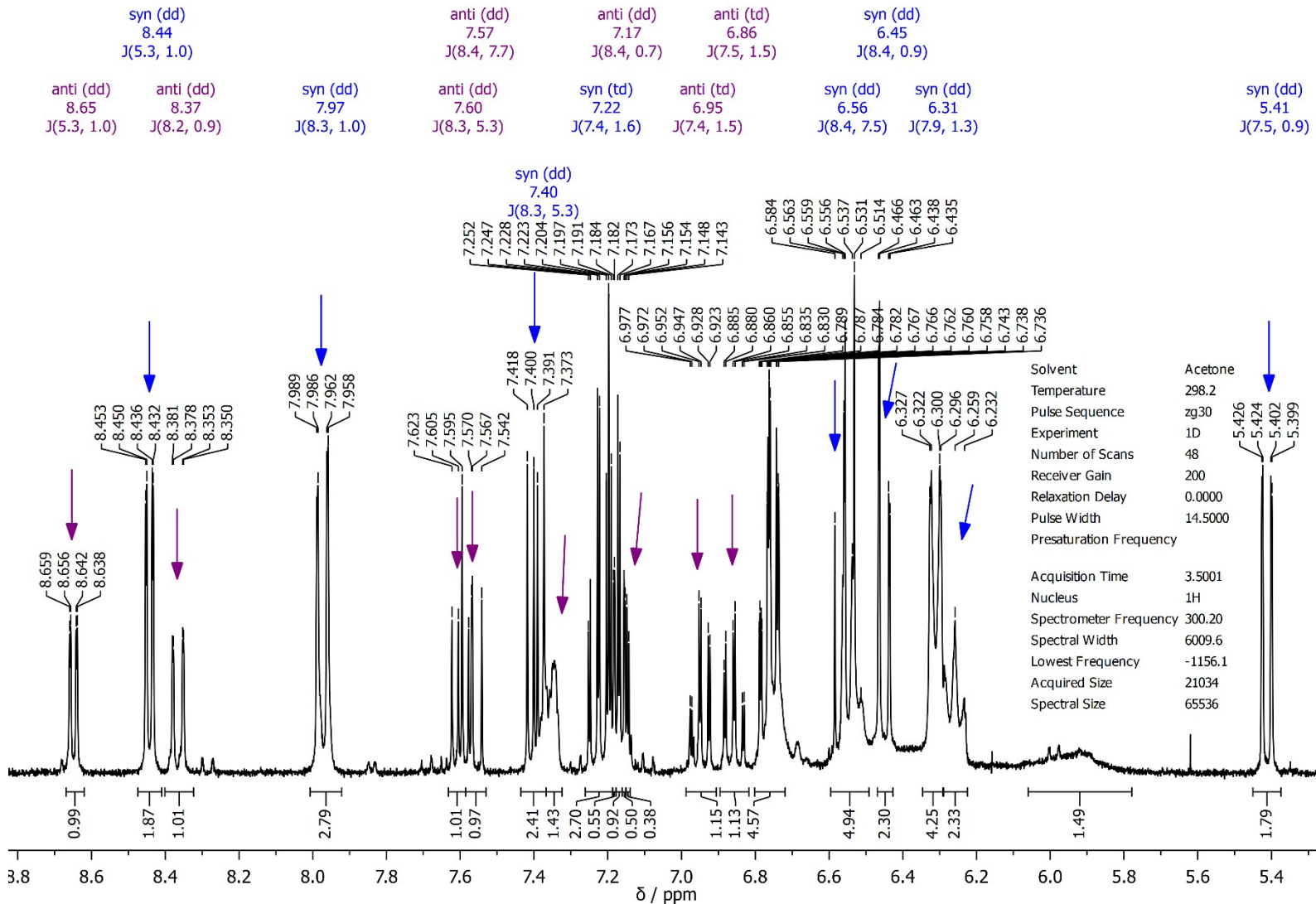


Figure S52. ^1H NMR spectrum of **2** in acetone- d_6 at 25°C; signals marked with purple arrow are derived from **2**-anti, blue arrow - **2**-syn.

2_acetone_19F@25C

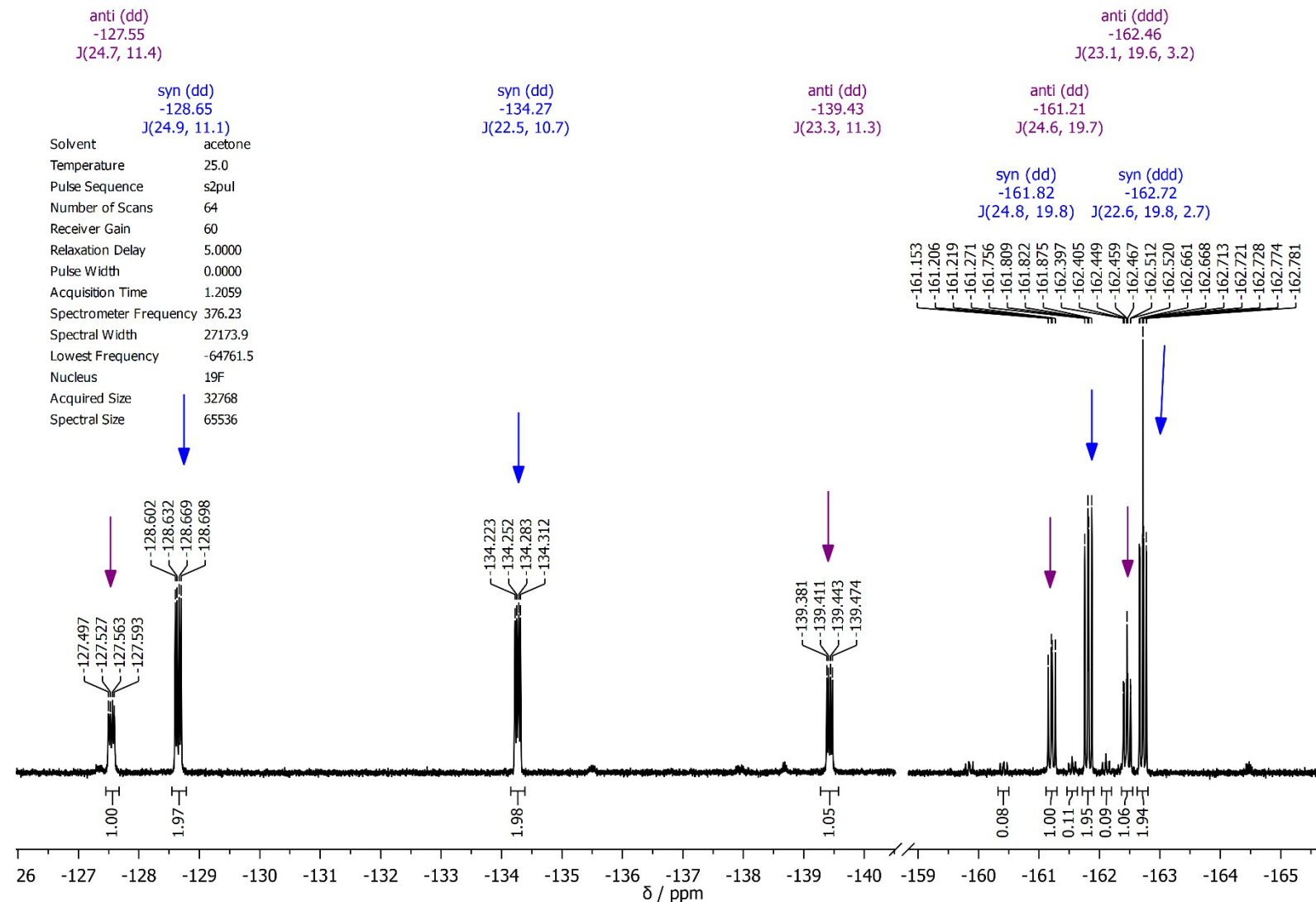


Figure S53. ¹⁹F NMR spectrum of **2** in acetone-*d*₆ at 25°C; signals marked with purple arrow are derived from **2-anti**, blue arrow - **2-syn**.

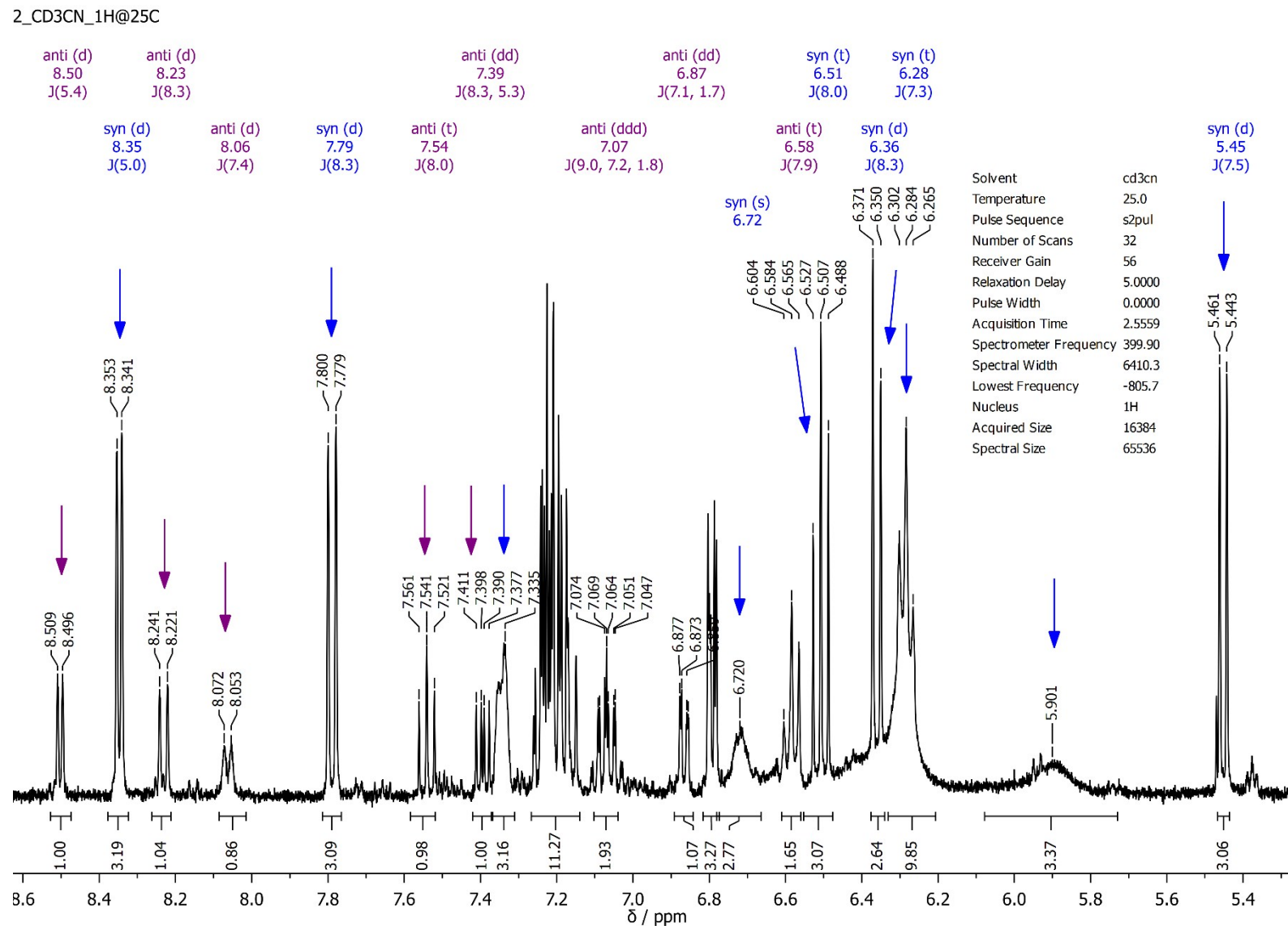


Figure S54. ^1H NMR spectrum of **2** in CD_3CN at 25°C ; signals marked with purple arrow are derived from **2-anti**, blue arrow - **2-syn**.

2_CD3CN_19F@25C

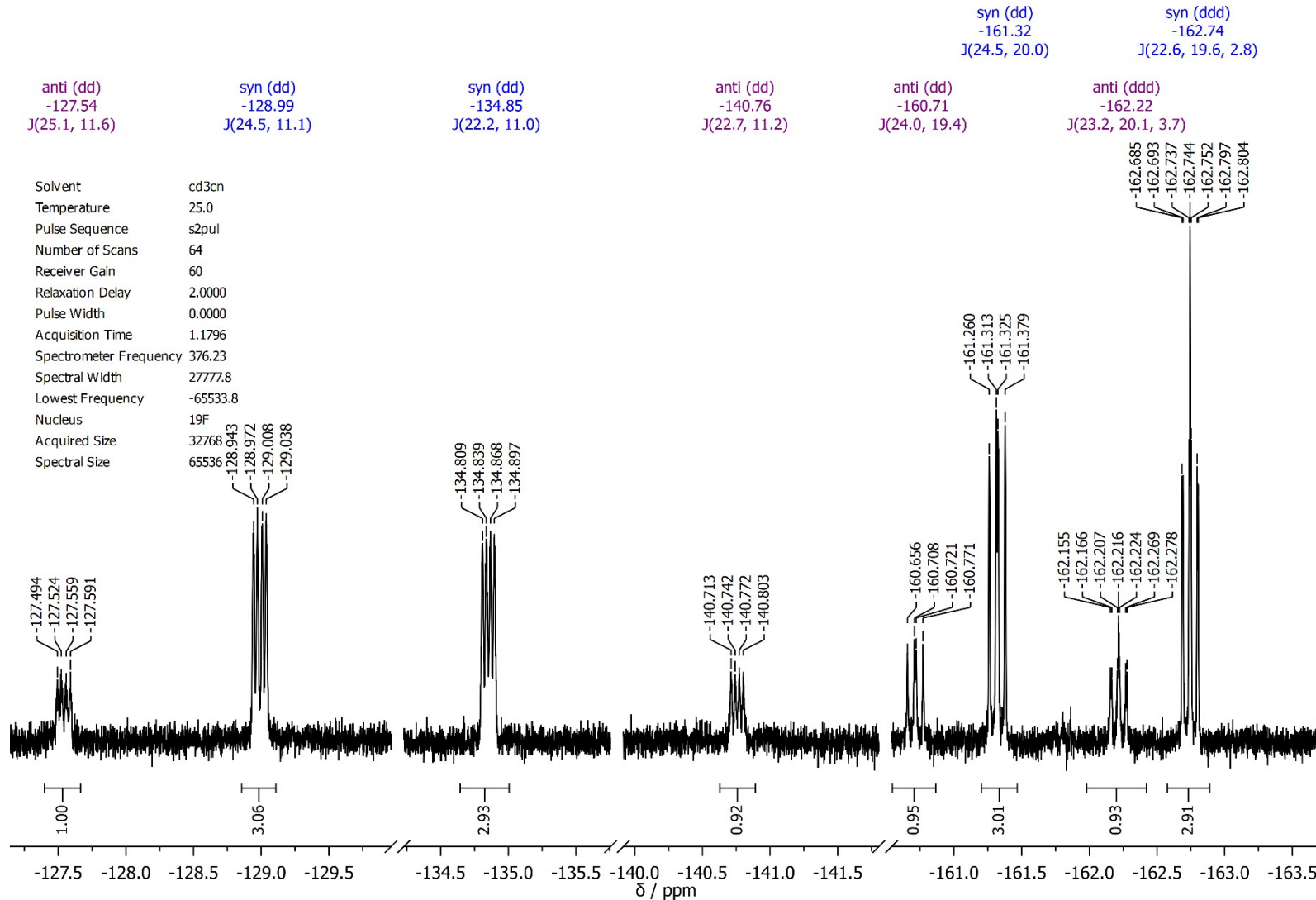


Figure S55. ¹⁹F NMR spectrum of 2 in acetone-*d*₆ at 25°C.

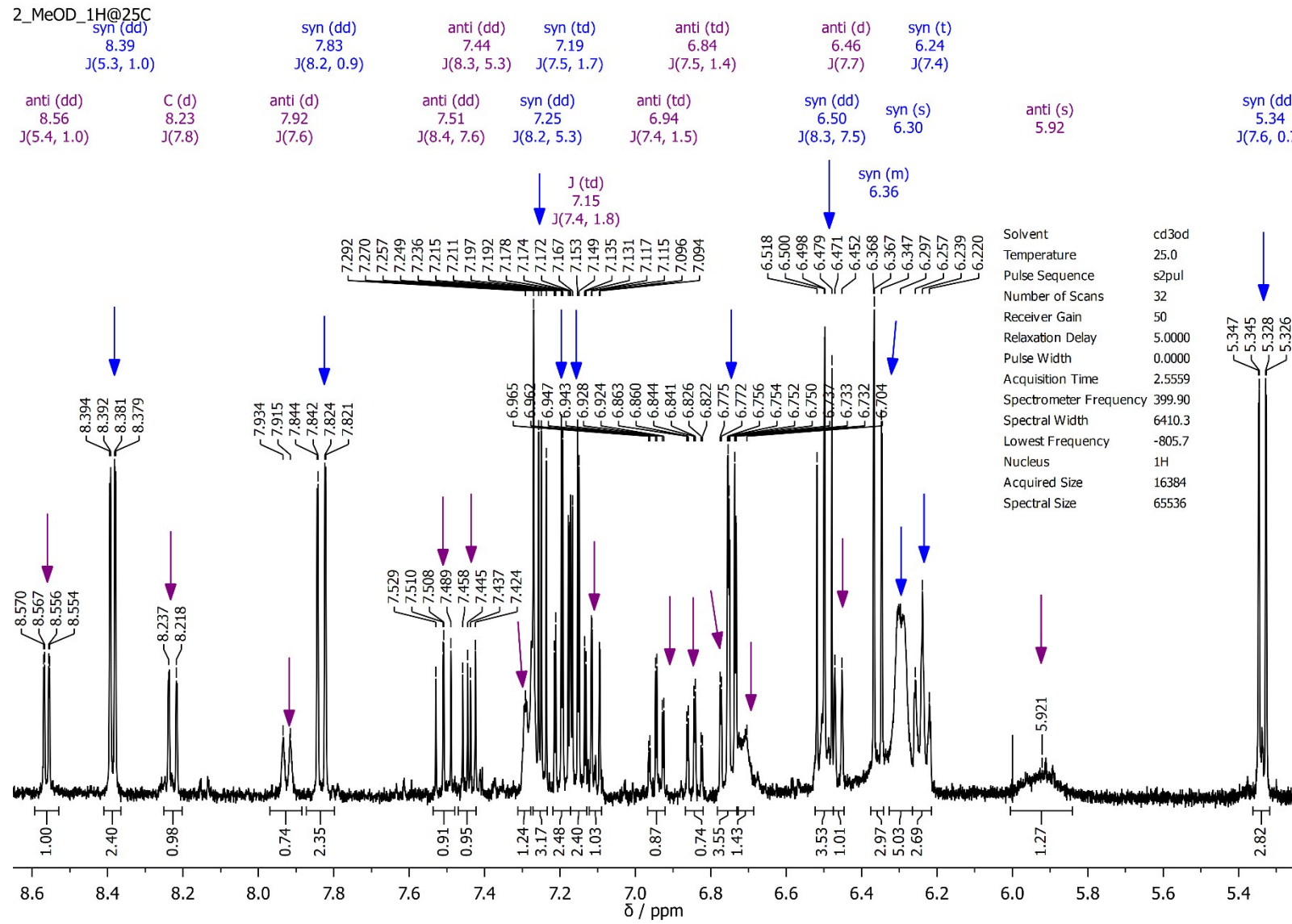


Figure S56. ^1H NMR spectrum of **2** in CD_3OD at 25°C ; signals marked with purple arrow are derived from **2-anti**, blue arrow - **2-syn**.

2_MeOD_19F@25C

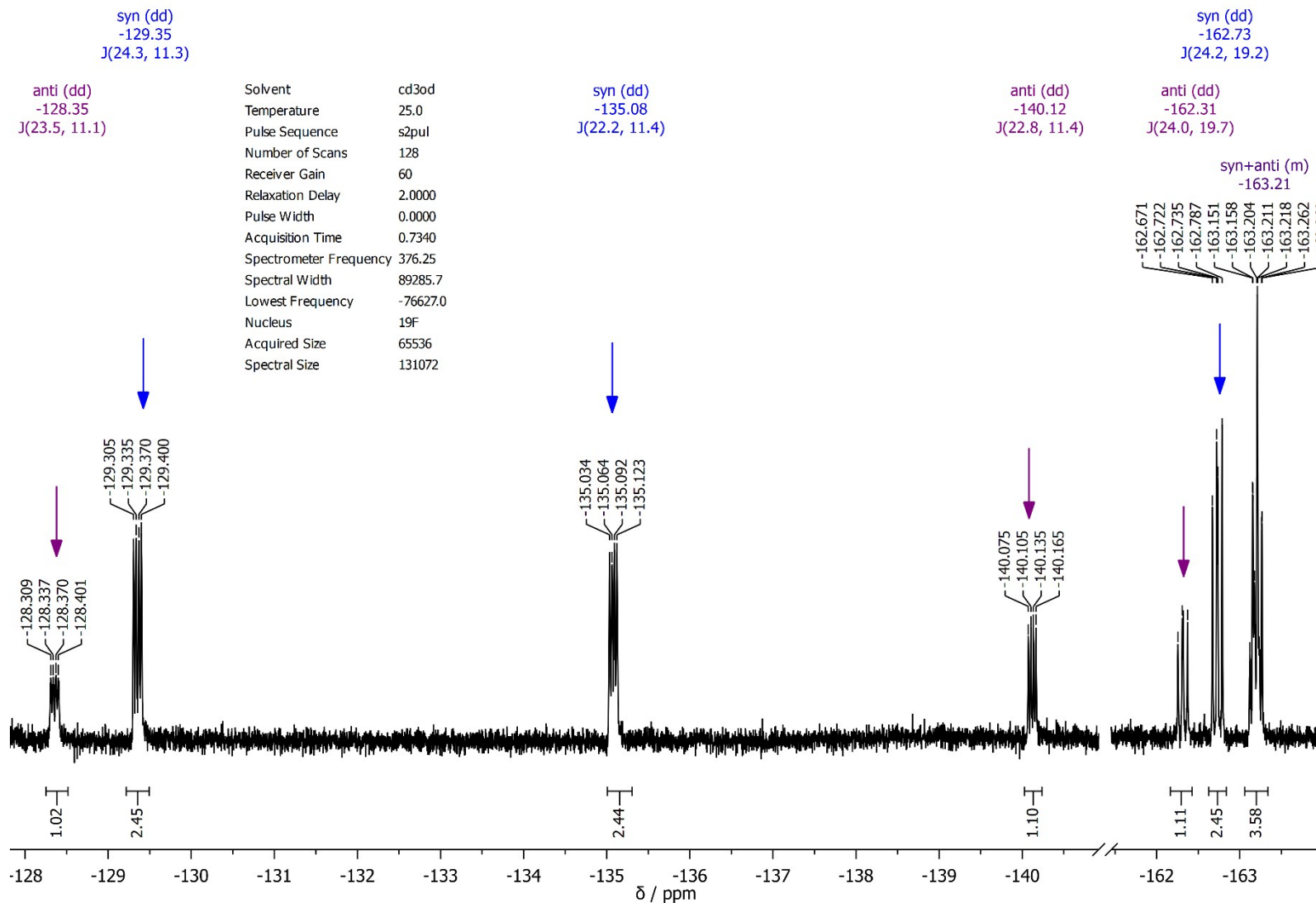


Figure S57. ^{19}F NMR spectrum of **2** in CD_3OD at 25°C ; signals marked with purple arrow are derived from **2**-*anti*, blue arrow - **2**-*syn*.

5.4 NMR of **2** at elevated temperatures:

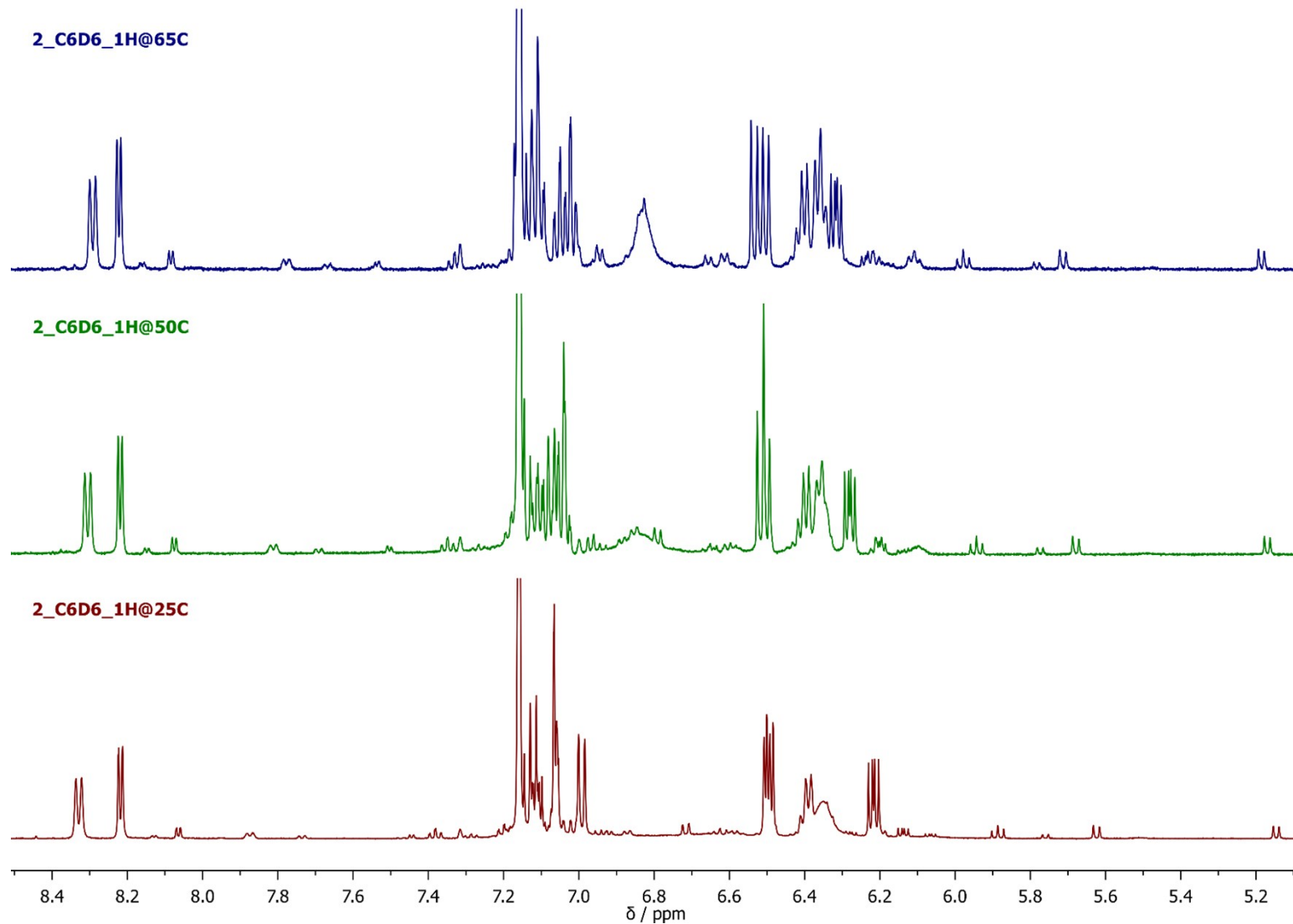


Figure S58. Overlay of ¹H NMR spectra of **2** in C_6D_6 at 25, 50 and 65 °C, marked with red, green and blue lines, respectively.

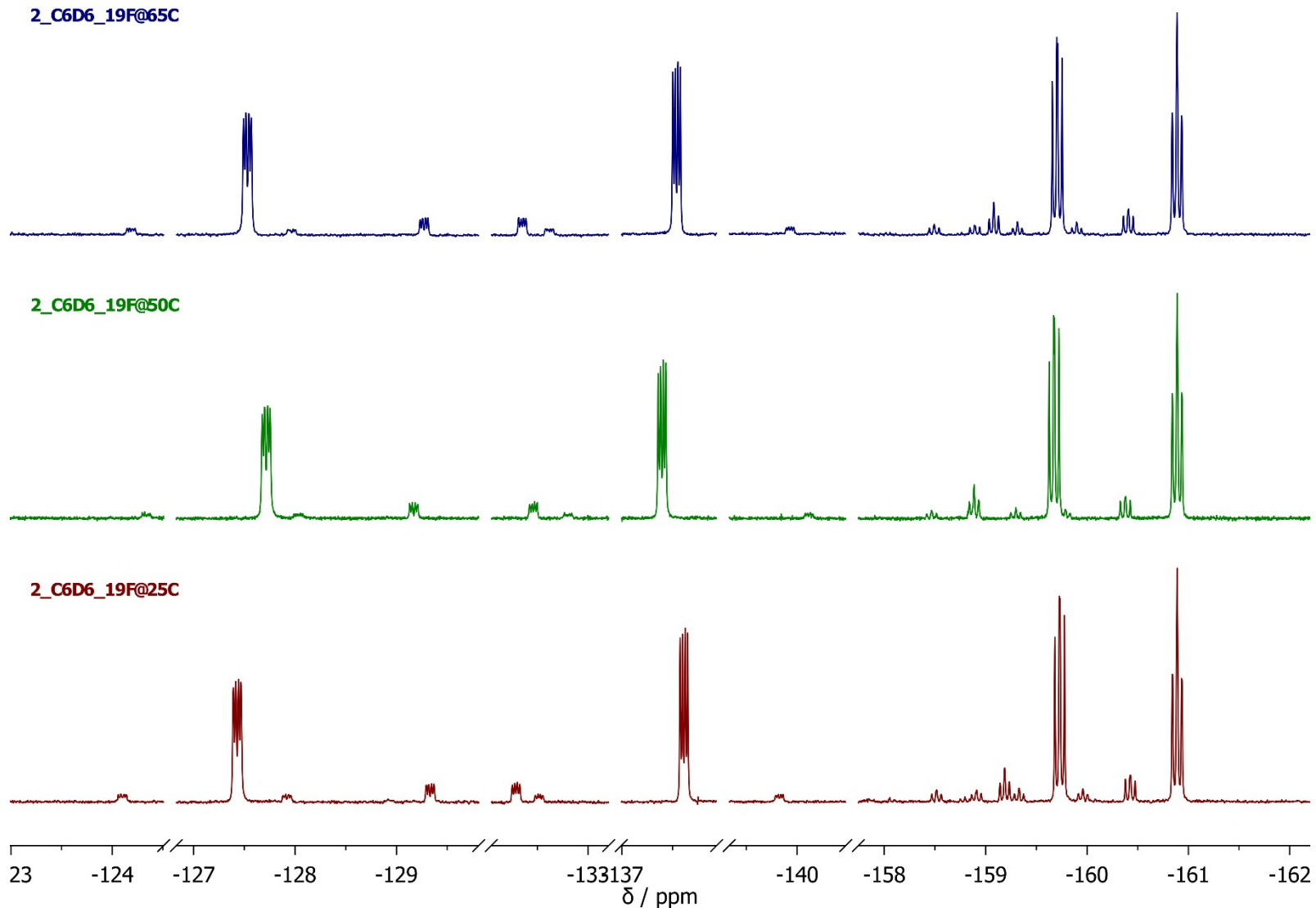


Figure S59. Overlay of ^{19}F NMR spectra of **2** in C_6D_6 at 25, 50 and 65 °C, marked with red, green and blue lines, respectively.

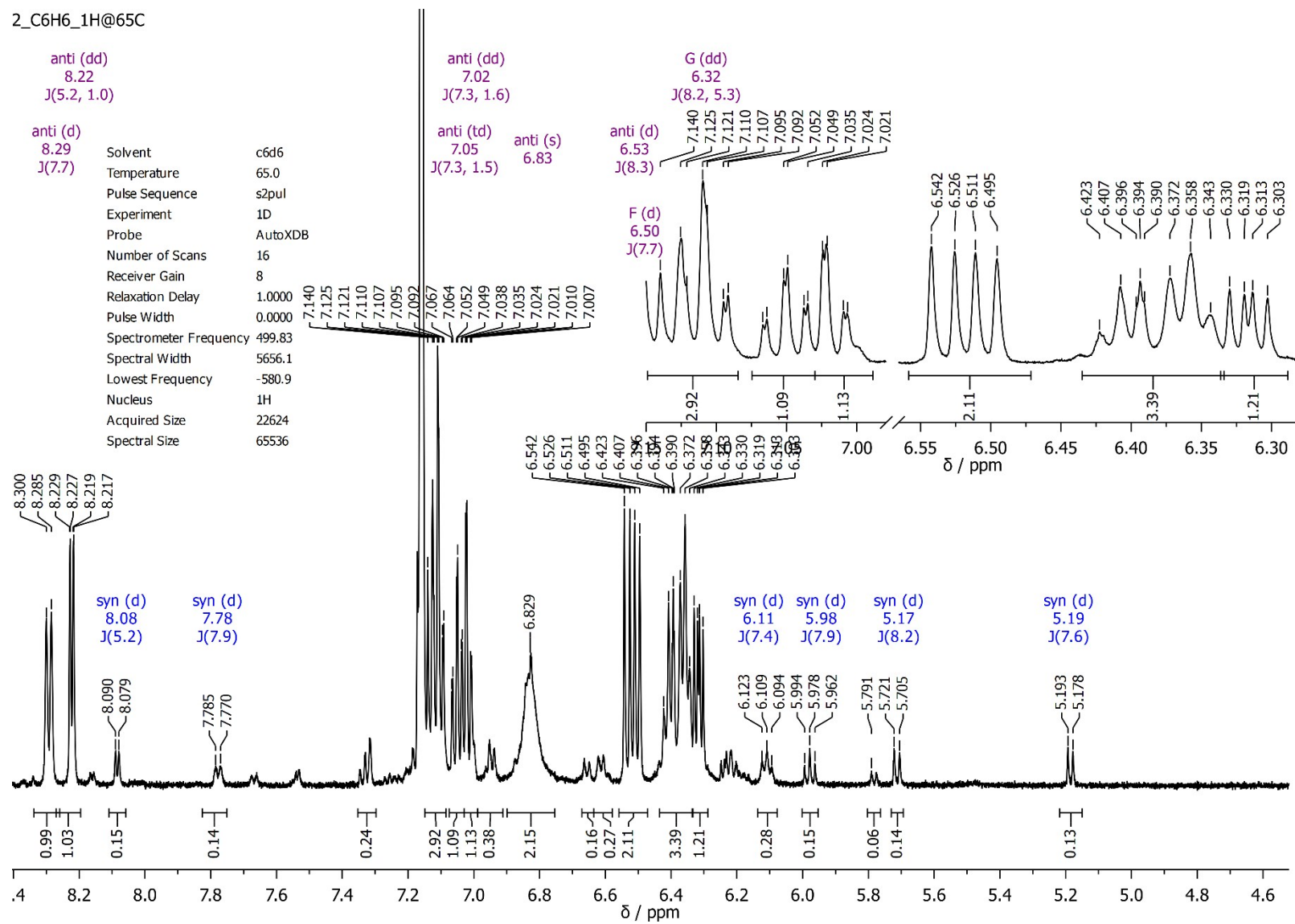


Figure S60. ^1H NMR spectrum of **2** in C_6D_6 at 65°C ; signals marked with purple colour are derived from **2-anti**, blue colour - **2-syn**.

2_C6D6_19F@65C

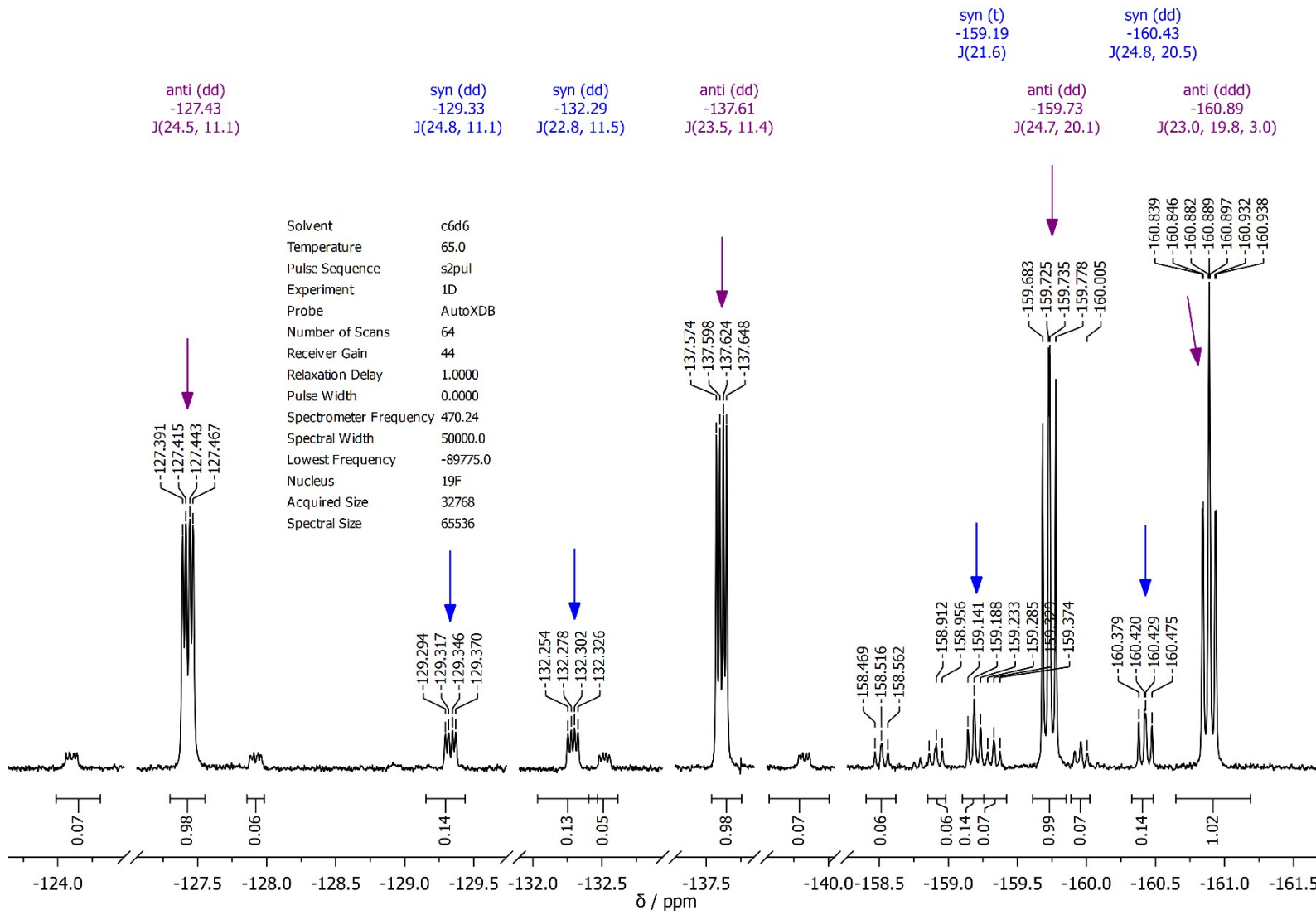


Figure S61. ^{19}F NMR spectrum of **2** in C_6D_6 at 65°C ; signals marked with purple colour are derived from **2-anti**, blue colour - **2-syn**.

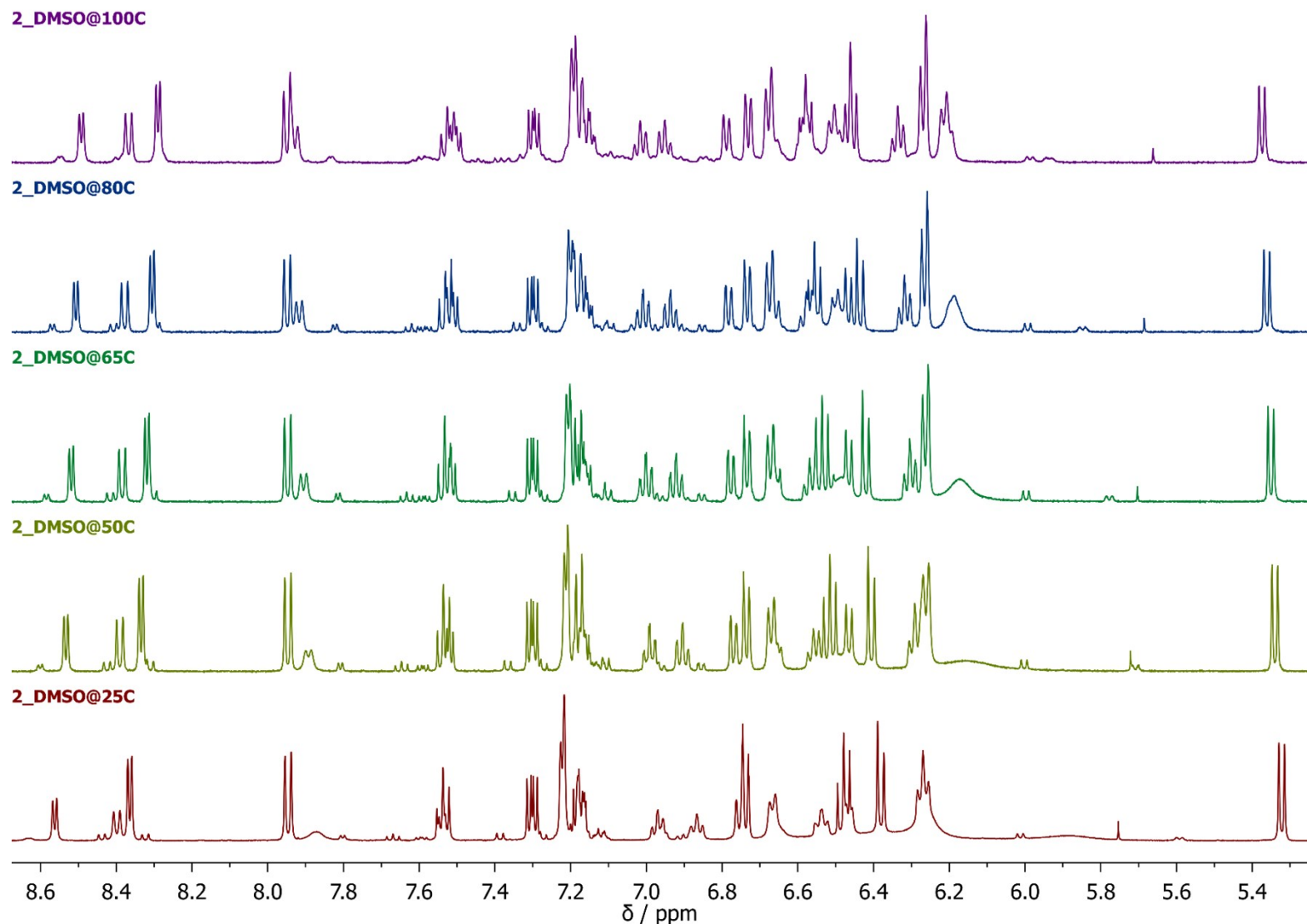


Figure S62. Overlay of ¹H NMR spectra of **2** in *DMSO-d*₆ at 25, 50, 65, 80 and 100 °C, marked with gradient from red (25 °C) to violet (100 °C).

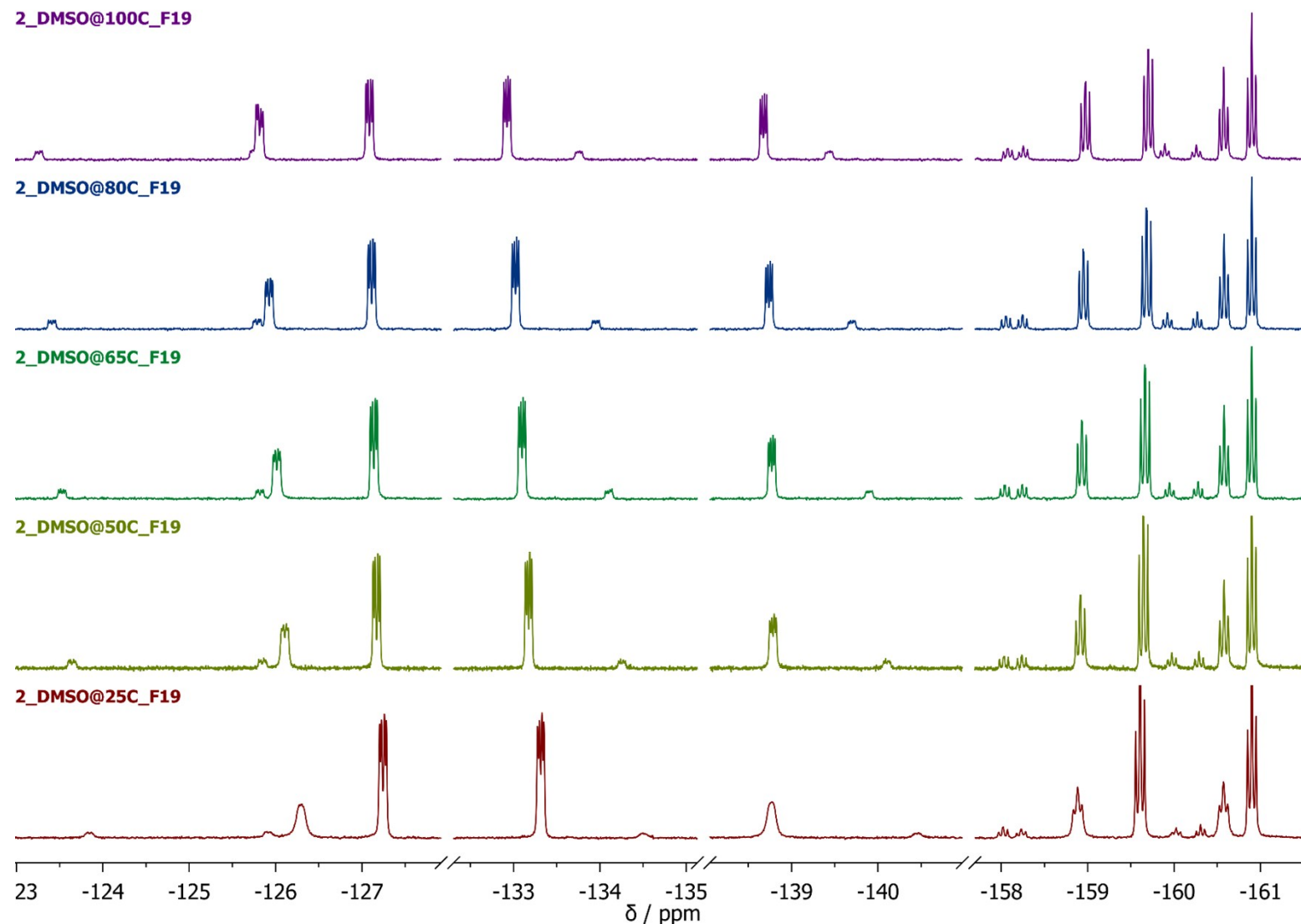


Figure S63. Overlay of ¹⁹F NMR spectra of **2** in $\text{DMSO}-d_6$ at 25, 50, 65, 80 and 100 °C, marked with gradient from red (25 °C) to violet (100 °C).

2_DMSO_1H@100C

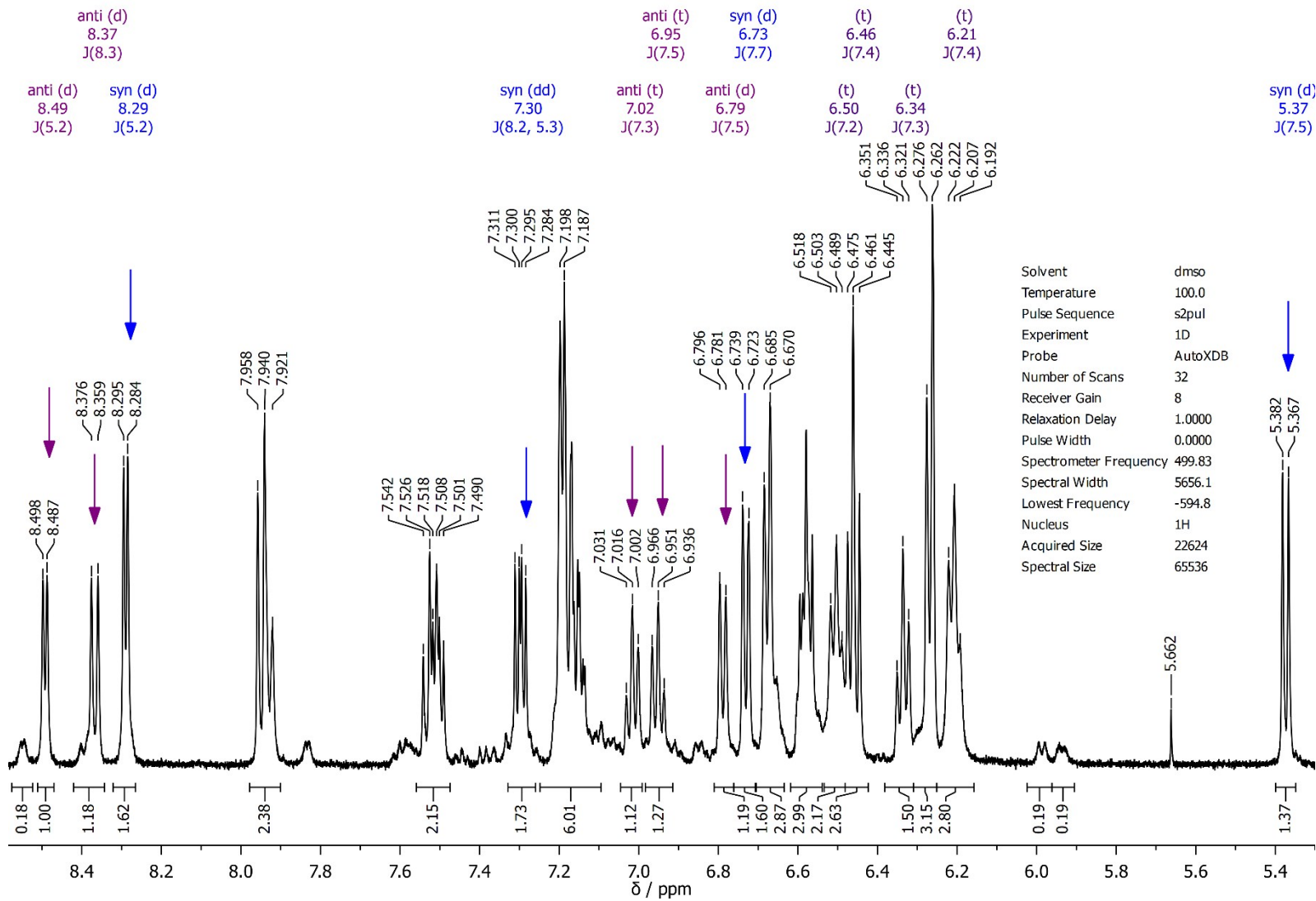


Figure S64. ^1H NMR spectrum of **2** in $\text{DMSO}-d_6$ at 100°C ; signals marked with purple colour are derived from **2-anti**, blue colour - **2-syn**.

2_DMSO_19F@100C

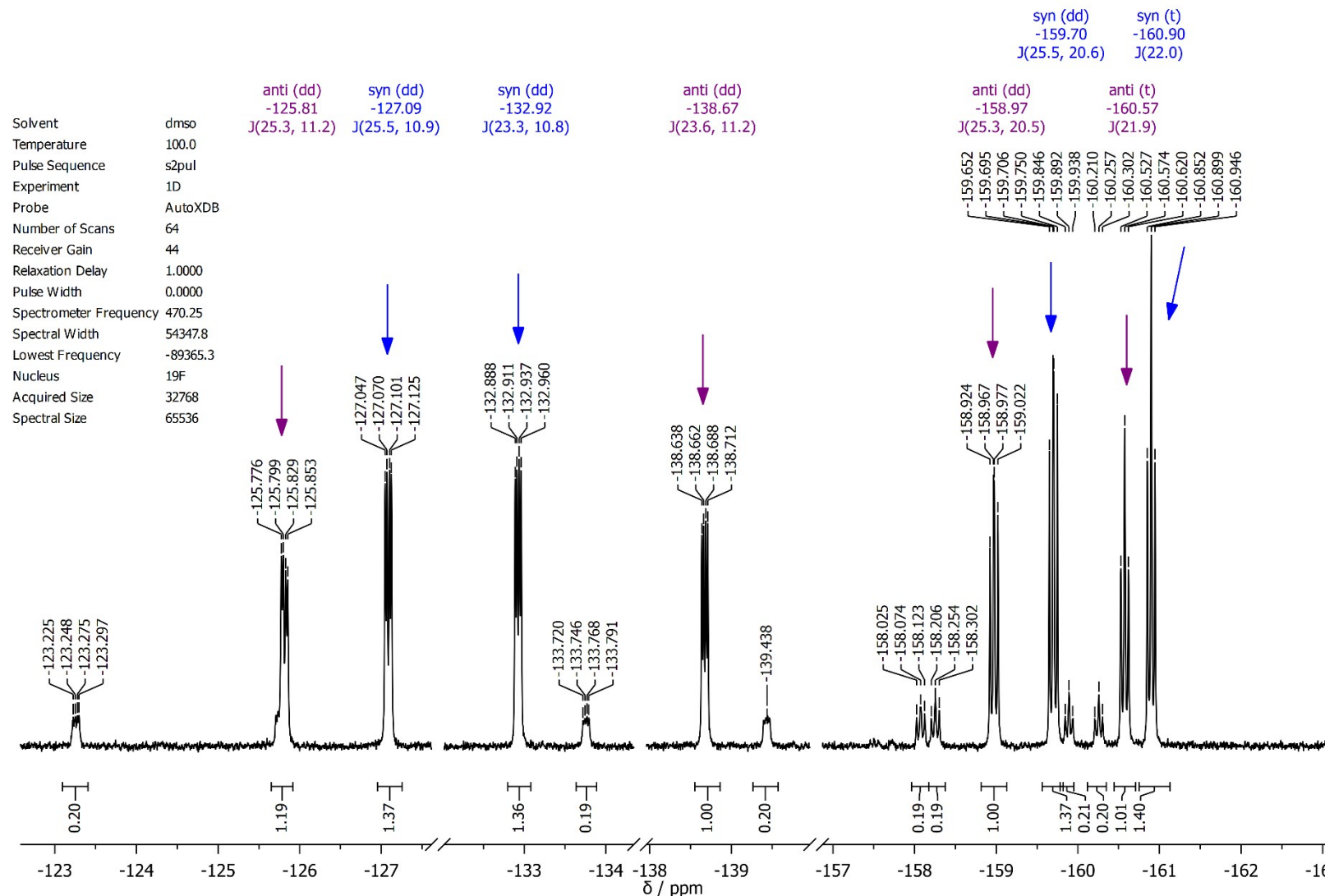


Figure S65. ^1H NMR spectrum of **2** in $\text{DMSO}-d_6$ at 100°C ; signals marked with purple colour are derived from **2-anti**, blue colour - **2-syn**.

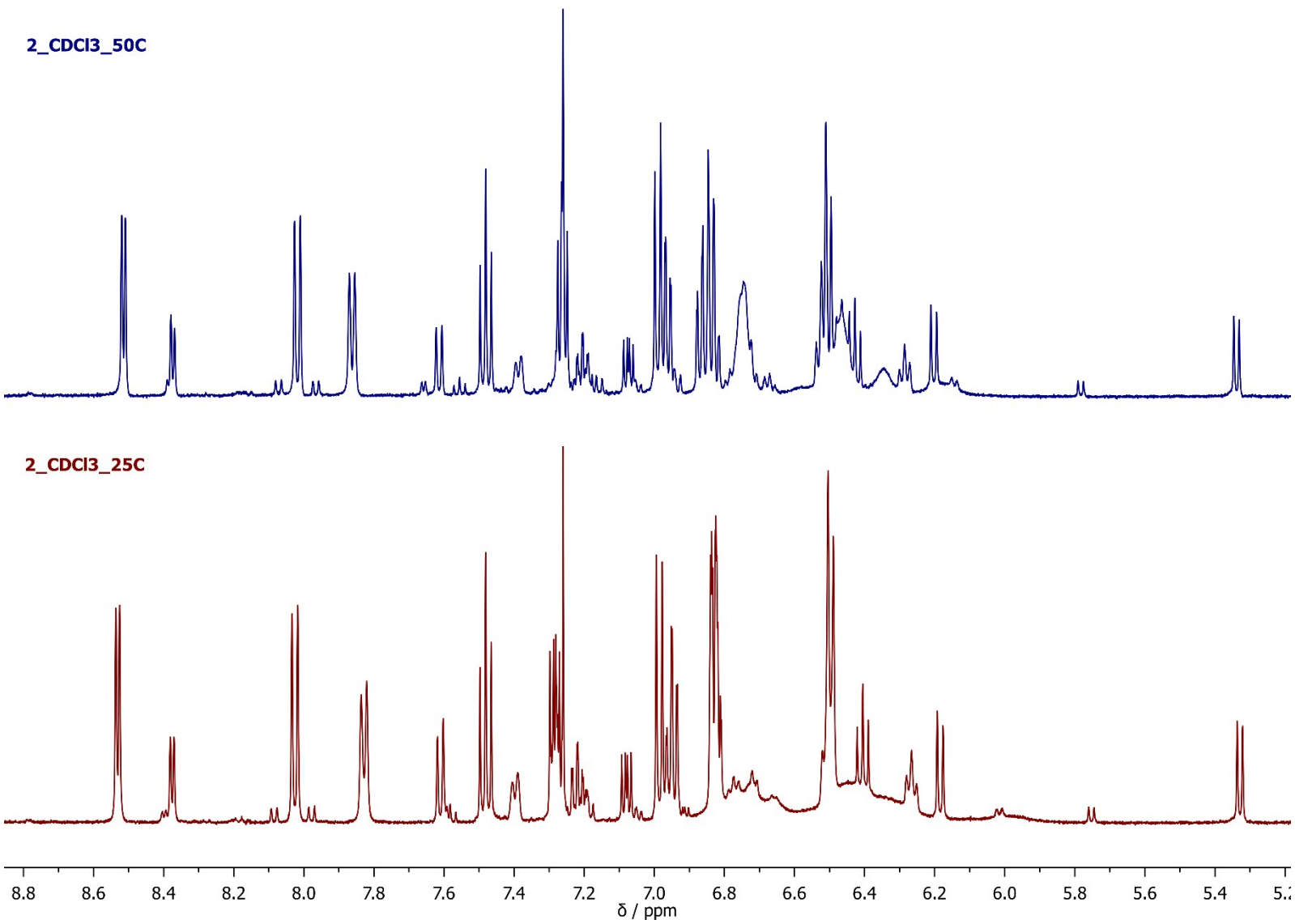


Figure S66. Overlay of ¹H NMR spectra of **2** in CDCl₃ at 25 and 50°C, marked with red and blue lines, respectively.

2_CDCI3_19F@50C

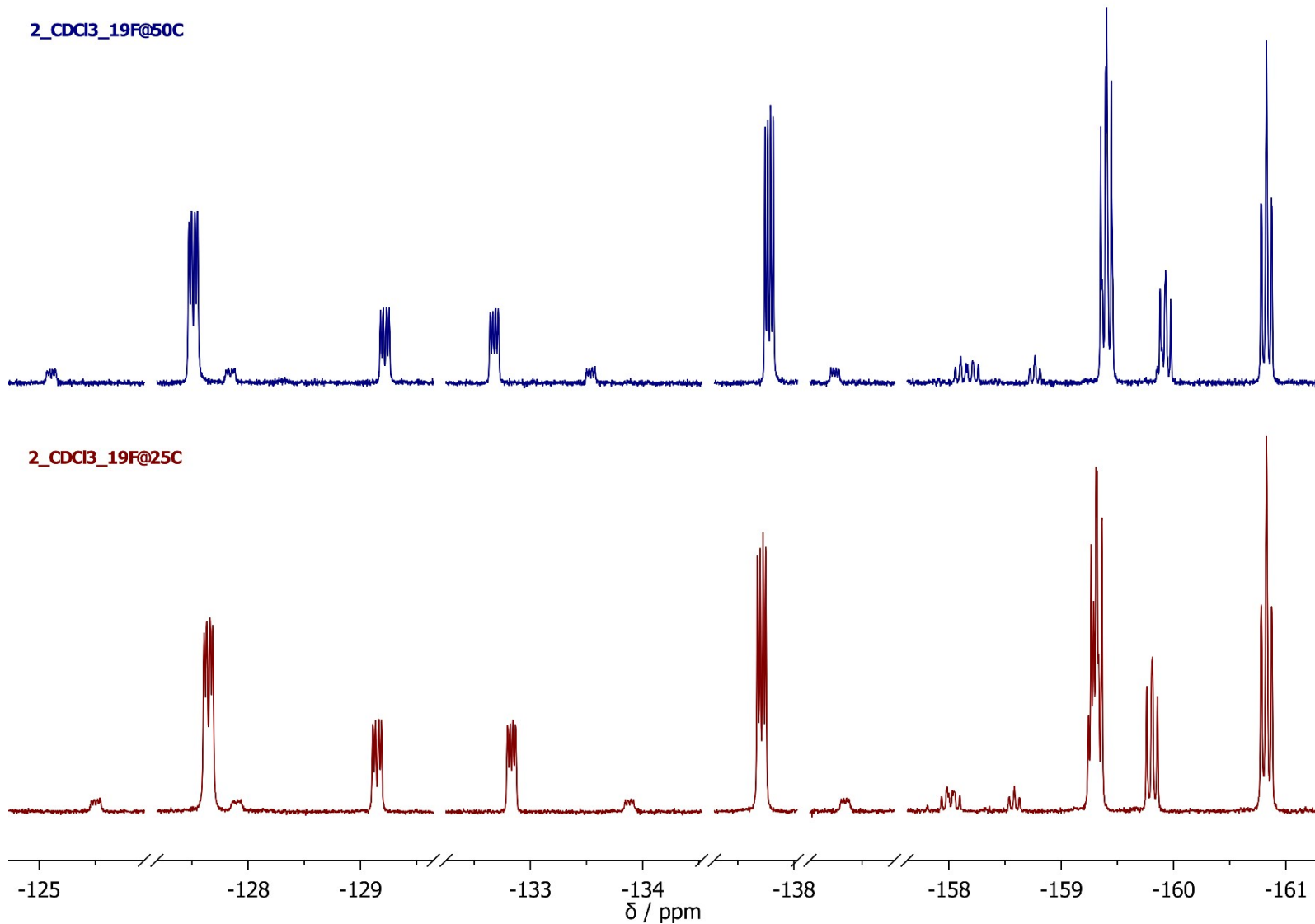
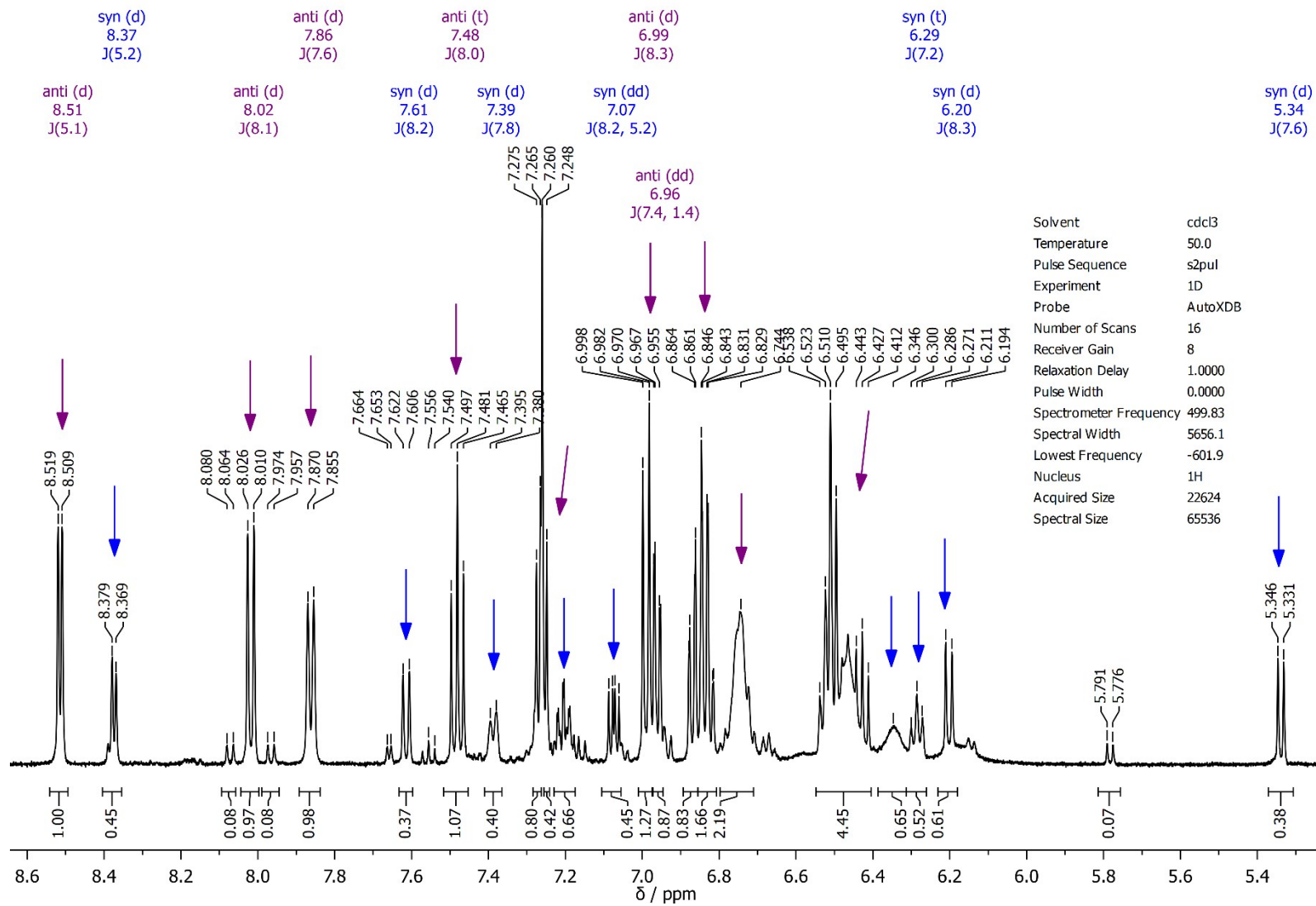


Figure S67. Overlay of ¹⁹F NMR spectra of **2** in CDCl_3 at 25 and 50°C, marked with red and blue lines, respectively.

2_CDCI₃_1H@50C

2_CDCI₃_19F@50C

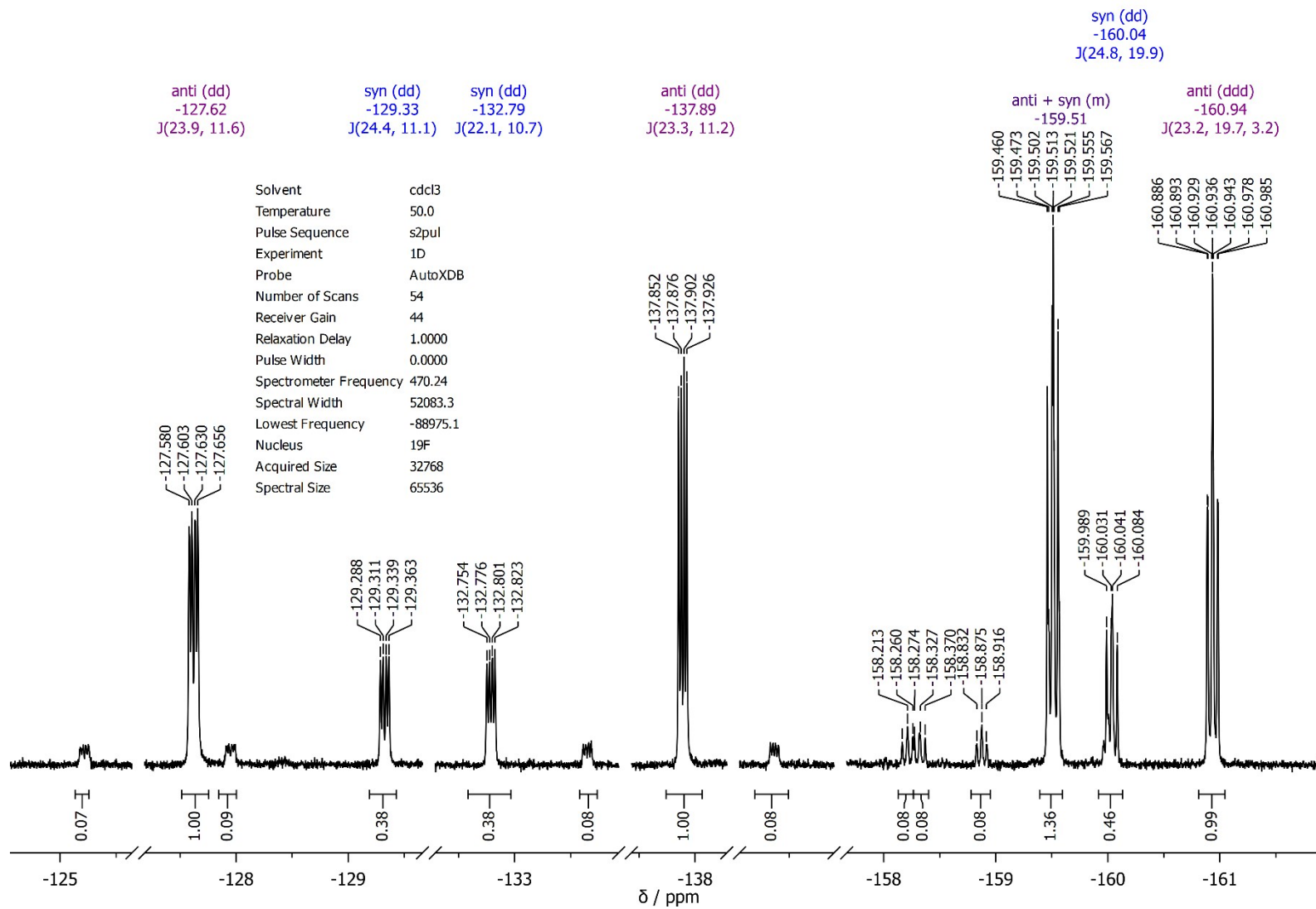


Figure S69. ¹H NMR spectrum of **2** in CDCl₃ at 65°C.